INVESTIGATING HOST-PATHOGEN INTERACTIONS DURING MACROPHAGE INFECTIONS WITH *MYCOBACTERIUM ABSCESSUS*

By

Haleigh Nicole Gilliland

A DISSERTATION

Submitted to
Michigan State University
in partial fulfillment of the requirements
for the degree of

Microbiology and Molecular Genetics – Doctor of Philosophy

2024

ABSTRACT

Mycobacterium abscessus (Mab) is a rapidly growing nontuberculous mycobacterium (NTM) that has been increasing in prevalence in patients with chronic or acquired lung disease for decades. Treatment strategies targeting Mab pulmonary infections largely rely on repurposed antibiotics commonly used for tuberculosis treatment. Unfortunately, Mab is intrinsically resistant to many of these antibiotic therapies, forcing health care professionals to use multiple antibiotics for longer periods of time to effectively treat infection. As such, cost of treatment, acquired antibiotic resistance and patient compliance rates are greatly affected. Notably, Mab pulmonary infections are rarely seen in patients with healthy lung environments, underscoring the requirement of a healthy pulmonary space and intact initial immune responses as key mediators in Mab control.

Central to maintaining healthy lung environments are macrophages, key innate immune cells tasked with preserving healthy tissues, sensing the environment, and mounting initial immune responses upon pathogen exposure. Macrophages are the first immune cell Mab encounters following infection and, as such, represent an important intracellular niche where Mab must persist to survive. Although many elegant studies have begun to define Mab specific pathogenesis factors leveraged at this interface, few studies have investigated global macrophage responses upon Mab exposure. In this dissertation, I sought to address this gap in knowledge by using a combination of iterative genetic approaches and unique macrophage subset models to expand our understanding of macrophage biological responses during Mab infection. We first employ CRISPR-Cas9 genetics on a genome-wide scale to identify novel factors that contribute to Mab uptake by macrophages and pave the way for future genetic approaches to uncover previously undefined uptake mediators leveraged by macrophages following pathogen exposure.

We then explore global transcriptional and cytokine profiles in unique macrophage subsets present in patients most at risk for Mab chronic infection and uncover a tendency for our Mab infected alveolar macrophage model (FLAMs) to remain hypoinflammatory. This study highlights the utility of our macrophage models to uncover key differences in macrophage immune responses that are most likely to impact upregulated immune mechanism during Mab infection.

Combined, these studies explore macrophage immune responses at distinct points during early Mab infection. They underscore the importance of leveraging functional genetic approaches to broaden our current understanding of Mab-host interactions and contribute to the shared goal of improving therapeutic options for at-risk patients in the future.

I dedicate this dissertation to those that hold an unwavering faith in my dreams. This wouldn't have been possible without you.

ACKNOWLEDGEMENTS

First, I would like to thank my PI, Andrew Olive. I can confidently say I would not be the scientist I am today without your patience, guidance, or support. When I first started graduate school, I had no idea what the future entailed. All I knew is I was fascinated with understanding how the immune system responded to infection. I was wide-eyed and excited to learn. Graduate school quickly laughed in my face and showed me the many different faces of impostor syndrome. Yet you consistently pushed me, never wavering in your guidance or mentorship and for that I am eternally grateful.

I would also never have been able to accomplish this PhD without the support and guidance from my committee members. Dr. Rob Abramovitch, Dr. Cheryl Rockwell, Dr. Sean Crosson and Dr. Nina Wale, thank you for always arriving to our meetings with a sense of curiosity and excitement. I often left these meetings with newfound confidence, a long list of ideas to test and reassurance that I was on the right path. Thank for emphasizing the importance of career development as much as research progress. And thank you for making sure this journey was an enjoyable and fulfilling experience.

I next want to thank my lab mates. To Justin and Sean: thank you for teaching me the value of believing in yourself even when others don't. To Kayla: I am so grateful for your bioinformatics expertise as my 2nd data chapter wouldn't be where it is without you, and of course, for introducing Joey and I to Mayfair's Monday Night Bingo. To Reham and Sole: you two are some of the most positive people I have ever met and were a breath of fresh air when you joined the lab in my fourth year. Thank you for reminding this jaded fourth year how impactful a positive outlook can be. To Jared and Elly: Your sarcasm and dry humor never fail to make me laugh. Thank you for oversharing just as much as me and for never blinking an eye at my

outlandish singing. To Chris: I have to say, your weird antics are unmatched. But beyond that you were always willing to listen and provide steadfast reassurance when my fears of failure outweighed my excitement to learn, thank you. To Laurisa: Our TC chats were legendary. Thank you for always making time for them, for creating a space that allowed me to feel my feelings and for never failing to call me out on my BS.

To the Lange and Carone Families: thank you for providing a home away from home. You have made me feel welcomed, loved and supported in so many ways. And although my job is very different than yours, you have always keenly asked about my projects, only to be forced to listen intently as I gush about them. Thank you for being some of my biggest cheerleaders and for celebrating each and every milestone alongside me. I am so incredibly lucky to be marrying into such a loving, supportive and uplifting family.

Growing up, I was surrounded by many hardworking and resilient women. I specifically want to thank three here. To my Aunt Susan, who is the first woman in our family to earn a PhD as a single working mother: thank you for teaching me the value of resilience and persistence. To my flying grandma, who was told in an engineering class at Northwestern University that the subject was too hard for women: thank you for instilling in me a strong, tenacious mindset and for showing me the importance of seeing the world from other peoples' perspective. To my driving grandma, who worked multiple jobs at once to help take care of her three young, rambunctious boys: thank you for showing me the power of hard work, determination and sacrifice. Without realizing it, each of you have shown me just how beautiful, strong and powerful women can be, thank you.

To my family: this achievement, quite simply, would not be possible without you. To my brothers, Jason and Aaron: thank you for never failing to make me laugh, for challenging me and

for never turning down an opportunity to roast me. You two keep me honest in ways only brothers can, and I wouldn't have it any other way. To my parents, Don and Pam: it isn't often that I get to express how much your love, support and annoyingly stubborn belief in my abilities to succeed mean to me. First, thank you for instilling in me the belief that I can do hard things and accomplish anything I set my mind to. This whole journey started when you showed me how cool it is to be a nerd. From Star Wars trivia, to museums, to sitting around the dinner table quizzing each other about random facts, you have always encouraged Jason, Aaron and I to question the world around us and the importance of being a lifelong learner. Dad – thank you for never turning down an opportunity to go down a conversational rabbit hole, and for providing me with some of the best advice, quotes and encouraging one liners I have ever heard. Mom – thank you for instilling in me the power of positive thinking, stubbornness and having a sense of humor through it all. On my worst days, your voice is the first one I hear, telling me to lift my head up, take a deep breath and keep on moving. You both have always been my loudest cheerleaders, thank you.

Lastly, I want to thank my fiancé, Joey. Our journey together started on a blind date our senior year at Indiana University. Unknowingly, this spontaneous decision led me to my best friend. Since then, many highs and lows have hit us, yet we continue to support each other through each and every challenge and achievement. You have never bent in your belief in my ability to earn this degree, but more so than that, you have been a never-ending source of love, reassurance and support. Your outlook on life, ability to see joy in the small things and perseverance is infectious. You never fail to brighten my days when they are hard or make me laugh when I'm stressed. You are simply someone who encourages me to be the best version of

myself. Thank you for agreeing to travel this ever-winding road of life with me, it is an honor to go through it by your side.

TABLE OF CONTENTS

CHAPTER 1: Introduction.

THE RISE OF MAB AS A PUBLIC HEALTH CONCERN

Mycobacteria are an extremely diverse genus that can be categorized as tuberculosis-causing mycobacteria or non-tuberculosis mycobacteria (NTM) [1-3]. Historically, *Mycobacterium tuberculosis* (Mtb) is the most well-known pathogenic mycobacteria responsible for pulmonary and extrapulmonary tuberculosis. On the other hand, NTMs are opportunistic pathogens that cause a broad range of infections in humans [4, 5]. Recently the number of pulmonary infections caused by rapidly growing NTMs are on the rise, increasing more than 400% in prevalence from 1987 to 2015 [6, 7]. Of these, *Mycobacterium abscessus* (Mab) represents 65-80% of NTM lung infections seen in patients with genetic or acquired lung disease [8-10]. Mab remains intrinsically resistant to the common therapies used to treat lung infections [11], making patient compliance, and acquired antibiotic resistance a complicated threat for all at-risk patients.

Highlighting NTM disease complexity, healthy lungs clear Mab efficiently. Yet in patients with cystic fibrosis (CF), chronic obstructive pulmonary disease (COPD), or bronchiectasis, Mab infections can be life threatening [9, 12-14]. The mechanisms for Mab susceptibility in CF patients are exacerbated by hyper inflammation, the presence of a thickened mucus membrane and ciliary dysfunction that primarily result from complications following a mutation in the Cystic Fibrosis Transmembrane Conductance Regulator (CFTR) gene [15, 16]. Loss of CFTR gene function dysregulates alveolar macrophage phagocytosis and efferocytosis function, resulting in the inability of CF patients to successfully clear bacteria, including Mab, and other debris from their pulmonary space [17]. Patients with COPD and bronchiectasis have chronic airway inflammation and buildup of excess mucus lining the pulmonary cavity [12, 18]. The subsequent thickening of their bronchi walls causes insufficient mucociliary clearance and

dysfunctional macrophage immune responses [17, 19]. In addition, research has linked Mab susceptibility to alveolar macrophage dysfunction resulting from silica exposure [20]. A closer look at the lung environments seen in at risk patients implicates macrophage function as a key contributing factor in maintaining healthy lung environments and Mab clearance. In this dissertation, I aim to fill a gap in knowledge concerning macrophage-Mab interactions following pulmonary infection, with particular focus on the underlying lung immune mechanisms that allow healthy airways to clear Mab with relative ease.

HOST-MAB MECHANISTIC INTERACTIONS FOLLOWING INFECTION

Further understanding these critical lung immune responses first requires a deeper understanding of Mab pathogenesis and host-pathogen interactions following infection. The exact transmission routes for Mab pulmonary infections are largely undefined. At-risk patients likely encounter contaminated environmental sources or equipment. Fomites, such as dust, and biofilms found on shower heads or medical equipment in hospitals have been largely implicated in Mab transmission [14, 21-23]. Following exposure, Mab pulmonary infections are recognized by resident alveolar macrophages that engulf the bacteria by phagocytosis or receptor mediated uptake. Initial recognition of pathogens requires effective interactions between the pathogen and macrophages [24-26]. This process is initiated by ligand binding to macrophage surface pattern recognition receptors (PRRs), including Toll-like receptors, Dectin receptors and scavenger receptors [27-30]. For Mab, Dectin-1and TLR2 have been shown to initiate uptake by macrophages during infection [31, 32]. Yet, follow-up studies with Dectin-1 deficient mice saw no defects in Mab control compared to wild-type controls, highlighting parallel mechanisms of Mab uptake in macrophages [33]. TLR2 seems to favor interactions with rough Mab variants to initiate uptake, leading to the upregulation of TNFα responses in macrophages [31]. The

specificity of this mechanism points to Mab's cell wall lipid composition as being a key mediator in both uptake and upregulated antimicrobial responses during infection.

Following adherence, phagocytosis or receptor mediated endocytosis of pathogens enables internalization. Despite the multiplicity of known uptake receptors and unique components within each compartment, the downstream phagosome maturation process remains well conserved. In general, phagosome formation is initiated by ligand binding to macrophage surface receptors [24-26]. This binding is followed by a conserved downstream signaling cascade that leads to the remodeling of actin cytoskeleton, and progressive engagement of additional receptors around the particle [34-36]. After engulfment, membrane fusion leads to the formation of the nascent phagosome [36-38]. Then, the phagosome interacts with various endosomal compartments that result in a highly toxic anti-microbial environment [36, 39]. This maturation process is characterized by compartment acidification by vacuolar-ATPases, production of phagocyte oxidase-mediated reaction oxygen (ROS) and nitrogen species (RNS) and delivery of recruited cathepsins and hydrolases to the maturing phagosome [40-43]. Finally, the matured phagosome fuses with the lysosome, a compartment containing numerous anti-microbial acid-activated hydrolytic enzymes, creating the phagolysosome [44, 45].

Independent of phagosome maturation, nucleotide-binding Oligomerization Domain-containing 2 (NOD2) has been implicated in Mab control by macrophages. Mechanistically, this intracellular pattern receptor is recruited to the pathogen containing phagosome where it directly senses peptidoglycans released from the bacterial cell wall [46-48]. Activation induces a downstream signaling cascade that confers upregulation of antigen presentation pathways and inducible transcription factors, such as NF-κB [49, 50]. Upon induction of NF-κB, many inflammatory cytokines, and antimicrobial defense mechanisms are upregulated, including nitric

oxide synthesis (iNOS) [49, 50]. During Mab infection, IFNγ stimulated BMDMs require NOD2 to produce iNOS [51]. Corroborating this, NOD2 deficient mice saw a lag in Mab clearance, with subsequent studies linking loss of NOD2 to defective NO production and bacterial control in the lung [51, 52]. Combined, these results implicate NOD2 as an important immune modulator that is required when mounting effective antimicrobial defense mechanisms against Mab infection.

Following initial alveolar macrophage responses, chemokines and inflammatory cytokines, including TNFα and IFNγ, are induced by persistent Mab [53, 54]. This leads to the recruitment of neighboring immune cells, such as circulating macrophages, neutrophils, and dendritic cells to the site of infection where they aid in infection control. Presumably, dendritic cells will then travel to nearby lymph nodes to initiate T-cell activation and the recruitment of the adaptive immune response. Recruitment of additional immune cells to the cite of infection eventually leads to granuloma formation [54, 55]. As the granuloma matures, B and T lymphocytes are also recruited, where they aid in infection containment. SCID mice are often used to show the importance of the adaptive immune response in disseminated Mab infection. A study conducted by Byrd and Lyons showed Mab persistence in the lungs of both BALB/c and SCID mice up to 28 days post infection, with SCID mice showing higher disseminated infection in the spleen compared to controls [56]. Similarly, Rottman, et al. showed higher bacterial burden in both the liver and spleen of Rag2 and CD3ε knockout mice, highlighting a particular importance of T-cells in Mab control [53]. Specifically, pulmonary Mab infection shows a preference for Th1 cells in the lungs of infected mice [53, 54]. Both IFNγ and TNFα production are hallmarks of the Th1 response. Notably, an important risk factor of Mab infection includes mutations in the IFN-γ pathway and prolonged use of TNF inhibitors, which are used commonly

during inflammatory disease treatment. [57-59]. Rottman, et al. corroborated the importance of IFNγ and TNFα for Mab control by showing higher disseminated bacterial burden in the liver and spleen of IFNγ receptor 1 knockout and TFNα knockout mice [53]. With that said, IFN-γ and TNFα play a complicated role during Mtb infection. Excessive inflammatory cytokine release results in host cell tissue damage, while mediocre release leads to poor immune activation and unrestricted bacterial growth during Mtb infection [60-62]. During Mab infection, the definitive impact of inflammation as a mediator for infection control remains lacking. Thus, further understanding the complicated role of IFN-γ and TNFα during Mab infection is required to prevent chronic Mab disease, while simultaneously avoiding prolonged pulmonary exasperation.

MAB VIRULENCE FACTORS AND RESISTANCE TO THE HOST

For many people, the previously mentioned immune response is sufficient to control Mab infection. In patients with chronic lung disease, Mab persists past initial host defenses by modulating surface lipid composition, upregulating transmembrane proteins, and expressing specified secretion systems. The role of surface lipids such as phthiocerol dimycocerosates (PDIM) and phenolic glycolipids (PGL) are well known Mtb virulence factors [63-65]. Yet, PDIM and PGL are noticeably absent in Mab. Glycopeptidolipids (GPLs) are the most abundant lipids on smooth Mab and are thought to conceal underlying surface components to facilitate and establish infection [66, 67]. During its pathogenesis, Mab spontaneously transitions from a smooth to rough morphotype. This morphotype shift is characterized by the loss of GPLs on the surface of the Mab membrane. Both smooth and rough Mab variants survive inside macrophages. Rough variants initiate higher rates of phagosomal rupture and type I IFN signaling cascades, resulting in cell death mediated cell-to-cell transmission [9, 55, 68]. To

actively subvert phagosome maturation, Mab can upregulate mycobacterial membrane protein large (MmpL) transporters, such as MmpL8, to induce phagosomal escape [69]. If escape is unsuccessful, Mab leverages a transmembrane P-type ATPase, *mtgC*, to effectively take up Mg^{2+} inside macrophages [70, 71]. However, *mtgC* mutant growth rates remain unaltered during infection, highlighting undefined Mab virulence factors used for essential nutrient uptake [55]. In terms of specified secretion systems, Mab relies on type VII secretions systems to persist. These secretion systems are specific to mycobacteria and limited gram-positive bacteria. The role of five ESX secretions systems (ESX-I – ESX-V), a type of type VII secretion factor, are well studied in Mtb and are widely implemented in bacterial survival, fitness, and virulence during infection [72, 73]. For example, Mtb's ESX-I contains effector proteins EsxA (ESAT-6) and EsxB (CFP-10) [74-76]. Both are required for intracellular invasion and phagosome permeabilization during Mtb infection [72, 76]. In addition, ESX-V promotes Mtb intracellular survival through the secretion of several PPE and PE-PGRS proteins and has been widely considered an essential secretion system when navigating host-pathogen interactions [76-78]. Mab only has two of these secretion systems: ESX-III and ESX-IV. Of these, ESX-IV has been shown to aid in Mab virulence by helping to both acquire essential nutrients being quenched by the phagosome and by trying to subvert phagolysosome toxic defense mechanisms [79]. Transposon mutagenesis studies have shown Mab uses an ATPase gene, *eccB4*, in the ESX-IV secretion system to disrupt phagosome acidification [79]. It has been suggested that Mab's ESX-IV secretion system functions in a similar manner as Mtb's ESX-I secretion system since each is required to subvert phagosome maturation events following infection. Yet, continued research is required to confirm whether this hypothesis holds true or if Mab relies on alternative mechanisms to promote intracellular invasion, nutrient acquisition, and phagosome disruption.

Furthermore, Mab can strategically survive in highly hypoxic conditions. Chronic inflammation and mucus build-up seen in the lungs of at-risk patients, phagosome maturation and granuloma formation all represent oxygen starved host environments where Mab persists. The two-component signaling regulon DosRS is a well-studied virulence factor for Mtb pathogenesis and survival in hypoxic conditions [80-83]. Mab has its own, unique DosRS regulon that is upregulated in hypoxic, carbon monoxide and nitric oxide environments as well [84]. A recent transcriptomics study saw the deletion of $DosRS_{Mab}$ lead to the downregulation of more than 200 genes, attenuated bacterial growth in oxygen starved conditions and a desired shift towards the rough morphotype [84]. Corroborating this, a study using an alveolar organoid model found smooth variants favor traditional biofilm formation to permit Mab survival, while host oxidative stress drove rough Mab variants into a serpentine cording motif [85]. Both states are now considered important Mab virulence factors that allow the bacilli to persist extracellularly while resisting hypoxic lung environments.

Complicating matters further, isolated sputa from Mab infected patients often shows co-infection with more than one microorganism, including *Pseudomonas aeruginosa*, *Staphylococcus aureus* and other NTMs [86-88]. This microbial community exists in an altered lung environment that is characterized by frequent and often unrelenting antibiotic therapy. As a result, recent studies have started looking into the role of co-infections in Mab pathogenesis and virulence. One study has shown *Pseudomonas aeruginosa* inhibits Mab biofilm formation [89, 90]. However, when researchers introduced a common antibiotic, Clarithromycin, used to treat both pathogens, they found treatment selectively decreased *Pseudomonas aeruginosa* biofilm development, thereby increased Mab survival [89, 90]. Furthermore, it has been suggested that Mab degrades a *Pseudomonas aeruginosa* quorum-sensing molecule, *Pseudomonas* quinolone

signal (PQS), to gain a competitive advantage during co-infection [91, 92]. Follow-up experiments examining this antagonistic relationship within liquid cultured biofilms were unsuccessful in determining the specific interbacterial mechanisms at play [91].

THEREAPEUTIC OPTIONS FOLLOWING MAB INFECTION

An FDA approved drug regimen for Mab pulmonary infection does not exist. The lack of a standardized antibiotic treatment for Mab is due, in part, to the variable host environments seen in patients with genetic or acquired lung diseases, including CF and COPD. Oftentimes, these patients face relentless infectious cycles with one or more antibiotic resistant bacterial strain, increasing the possibility of acquired antibiotic resistance. As a result, effective antibiotic therapies are guided by patient isolate antibiotic susceptibility testing. The most common antibiotics used to treat pulmonary Mab infection include two or more intravenous drugs (amikacin, tigecycline, imipenem and/or cefoxitin) with one or two oral antimicrobials (clofazimine, linezolid and/or azithromycin) for 3 months [10, 93]. These treatment timelines are often extended due to Mab's natural recalcitrance to common antibiotic therapies, with under 50% of treatments regimens achieving successful clearance within the first round of therapy [10]. A recent report has shown Mab treatment costs can amount to $50,000 USD, making the financial burden of treatment an important factor to consider as well [94]. Clinical trials to develop more effective therapies are underway, with inhaled liposomal amikacin being a promising candidate [95]. Alternative treatment options, including phage therapy, have also been explored. Phage therapy was recently used in combination with antibiotics to treat a teenager with cystic fibrosis following a bilateral lung transplant [96]. All things considered, as with any prolonged treatment timeline, patient compliance, and antibiotic-related toxic side effects continue to complicate treatment options for many at-risk patients.

MAB RESISTANCE TO ANTIBIOTIC TREATMENT

Mab infections remain incredibly hard to treat due to Mab's intrinsic resistant to most antibiotic classes currently available, including macrolides, aminoglycosides, rifamycins, tetracyclines and β-lactams [11, 97, 98]. One of the intrinsic resistance mechanisms leveraged by Mab is low cell envelope permeability. The high lipid content and thickened mycobacterial cell wall provide effective barriers against hydrophilic and lipophilic antimicrobials and are considered the main factor contributing to low permeability [97, 99]. With that said, porins within the myco-membrane permit diffusion of hydrophilic antibiotics through the cell envelope [100, 101]. In turn, these porins act in synergy with Mab specific antibiotic inducible resistance mechanisms, leading to the upregulation and expression of efflux pumps, antibiotic inactivating enzymes and target-modifying enzymes [100, 101]. Efflux pumps protect bacterium against toxic molecules by exporting toxins and metabolites to the extracellular environment [102, 103]. For example, Mab encodes components of is the ATP-binding cassette (ABC) transporter family efflux pump. These ABC-type multidrug transporters use ATP energy to pump molecules across the myco-membrane to help maintain bacterial homeostasis [104]. The dynamic role of Mab specific ABC efflux mechanisms still needs to be explored to determine the specific role they play following antibiotic treatment during infection. Additionally, Mab encodes mycobacterial membrane protein small and large (MmpS and MmpL) transporter families [69, 105-107]. These efflux pumps are involved in lipid transport of multiple drugs across the myco-membrane, with MmpL protein family playing a well-known role in Mtb intrinsic drug resistance [105, 108-111]. Research has shown mutations in the Mab transcriptional repressor TetR, MAB_2299c, modulate Mab specific MmpS and MmpL efflux pump expression, leading to altered drug efflux levels and increased Mab resistance to clofazimine and bedaquiline [106]. Furthermore, Mab

produces enzymes that directly modify or degrade antimicrobials. For example, Mab hydrolyzes imipenem and cefoxitin, two of the most common antibiotics used to treat Mab pulmonary infections, at a slow rate by expressing a β-lactamase, Bla_{Mab} [112-114]. Mab also upregulates WhiB7, a multidrug-inducible transcriptional activator that modulates a large set of Mab genes during infection, including *eis2* and *erm41* [115-117]. Indel mutations in either of these genes or in the WhiB7 promoter region increase Mab susceptibility to clarithromycin and amikacin, while also decreasing Mab intracellular survival during infection [115, 118]. Antibiotic resistance studies have confirmed a single nucleotide exchange in *erm41* is responsible for abrogating macrolide-resistance [119, 120]. This polymorphism is present in 15-20% of clinical isolates, permitting macrolide susceptibility and highlighting the continued requirement for antibiotic susceptibility testing for all clinical isolates prior to treatment [121, 122].

EXPLORING THE IMPORTANCE OF THE HOST-MAB-ANTIBIOTIC INTERFACE

Antibiotics interfere with the immune system either indirectly by disrupting the body's natural microbiota, or directly by modulating host immune cell function [123, 124]. These interactions impact treatment efficacy and general host susceptibility to infection. Adverse side effects of antibiotic treatment following Mab infections are well known, with almost 78.8% of patients reporting ototoxicity, gastrointestinal distress, and myelosuppression [94]. As a result, nearly half (48.3%) of patients require treatment plan modifications prior to treatment completion [10, 94]. The majority of reported adverse side effects are associated with tigecycline, linezolid and amikacin treatment [94]. Coincidentally, these three antibiotics are correlated with the highest treatment success rates compared to other, better tolerated antibiotics. Therefore, research focused on understanding the host impact of antibiotic treatment is of critical importance to develop more tolerable treatment strategies. Host impact of traditional antibiotics

used during Mtb infection are well studied [125-128]. For example, Isoniazid treatment in Mtb infected mice have been found to induce apoptosis in activated CD4+ T cells; and Pyrazinamide treatment reduced pro-inflammatory cytokine and chemokine release in Mtb-infected human monocytes and mice [129, 130]. Such research has since expanded to focus on leveraging host-directed therapies to improve appropriate host immune responses following pathogen exposure. For example, metformin, an approved drug that reduces high blood glucose levels in diabetic patients, has been shown to promote phagosome-lysosome fusion events and boost mitochondrial ROS (mtROS) production to control Mtb infection in mice [131-133]. Combined, these research areas highlight the importance of understanding the complex interactions at play at all points of infection and antibiotic treatment. For Mab infection, research focused on how drug treatment impact host immune regulation remains unexplored. Thus, future research should focus on understanding this host-Mab-antibiotic interface, with particular focus on identifying immune-boosting mechanisms that can be exploited to improve therapeutic treatment options.

MODELS EMPLOYED FOR STUDYING MAB INFECTION

Interactions between the host and a pathogen significantly impact disease outcome. Mab preferentially infects host immune cells, such as macrophages, which contribute to its pathogenesis. Research focused on host-Mab interactions is critical in defining immune responses involved in Mab restriction while giving insight into mechanisms permitting persistence. In general, a variety of immunocompetent murine models, such as C57BL/6 and leptin-deficient (Ob/Ob) mice, have been used to try and understand chronic Mab infection, yet these murine models' cleared infection quickly [134-136]. As a result, researchers turned to immunodeficient mice to glean key insights into immune responses. Beige (dominant T_H2 immunity), $iNOS^{-/-}$, $Cybb^{-/-}$ (devoid of super-oxide generating enzyme), $TNF\alpha R^{-/-}$ and $MyD88^{-/-}$

mice all cleared Mab infection quickly [53, 135]. Yet, SCID, IFNγ$^{-/-}$ and GM-CSF$^{-/-}$ mice infected intravenously saw progressive Mab burden [53, 135]. These studies revealed the importance of functional T and B lymphocytes and GM-CSF reliant cell phenotypes in establishing protective immunity against Mab. In addition, researchers have leveraged Zebrafish (*Danio rerio*) models to understand more intricate immune responses following acute infection [17, 137, 138]. It is through these studies that rough Mab variants were shown to favor extracellular cording motifs to subvert phagocytosis by macrophages and neutrophils, accelerate abscess formation and promote disseminated infection [54, 55]. Zebrafish embryo studies were also used to highlight the importance of host TNF signaling and IL8-mediated neutrophil recruitment in immune cell recruitment prior to granuloma formation [54]. Lastly, free-living amoebae, an intracellular niche for environmental NTMs, have been used alongside *ex vivo* macrophage models to delineated Mab virulence factors within intracellular environments [71, 139, 140].

In macrophage studies, bone-marrow derived macrophages (BMDMs) are often leveraged. BMDMs are well characterized due to ease of access to high quantities of primary cells from bone-marrow, and the existence of many immortalized BMDM (iBMDM) models [141-144]. Such iBMDM models recapitulate BMDM biology, while allowing replication of large-scale *in vitro* experiments [142, 145, 146]. These strategies significantly improve the ability of researchers to define BMDM immune responses following infection. Recently, our lab has employed large scale CRISPR-Cas9-mediated genetic knockout studies to further understand iBMDM immune regulation [147]. With that said, the first immune cell Mab encounters following pulmonary infection is the alveolar macrophage. Therefore, it has become increasingly necessary to define mechanistic interactions occurring at this interface. Historically, alveolar

macrophages are much harder to study, with the most pressing concerns being low cell count yield ($5x10^4$ – $2x10^5$ cells/mouse) and unreliable alveolar macrophage-like properties seen when cultured *ex vivo* [148-150]. In response to this gap in research, our group developed an alveolar macrophage-like model called fetal-liver derived alveolar-like macrophages (FLAMs) [151]. FLAMs are products of fetal-liver derived macrophages that are maintained in traditional cell culture media, GM-CSF and TGFβ [151]. Initial studies confirmed FLAMs maintained alveolar macrophage-like characteristics *ex vivo* for prolonged periods of time [151]. We have since leveraged the FLAM model to conduct large scale CRISPR-Cas9-mediated genetic knockout studies to further define alveolar macrophage immune regulation [151]. Thus, positioning our group in an optimal position to dissect mechanistic interactions occurring between distinct macrophage populations and Mab during infection.

DISSERTATION DIRECTION AND OVERVIEW

Since Mab was recognized as an independent species in 1992, researchers have made huge strides in understanding its pathogenesis [152, 153]. Yet, we still do not fully understand why healthy lung environments clear Mab pulmonary infection with ease. In this dissertation, I seek to fill a gap in knowledge regarding the intricate host-macrophage responses at play during the early stages of infection, so that we may glean insight into, and eventually prevent, host environments that allow Mab infections to thrive.

To begin this work, I leverage our previously optimized CRISPR-Cas9 loss-of-function (LOF) macrophage library and conduct a forward genetic screen to identify novel genetic pathways required for macrophage uptake of Mab during early infection. In addition to known uptake regulators, such as ITGB2 and ITGAM, I discover a unique requirement for sulfated glycosaminoglycan (sGAG) synthesis in Mab uptake by macrophages. Downstream mechanistic

analysis studies suggest that these sGAGs are required to maintain the expression of known phagocytic receptors on the macrophage membrane and highlight a previously undescribed requirement for sGAGs in initializing Mab uptake.

I then sought to understand how unique macrophage subsets respond to Mab. In the lungs, both resident alveolar macrophages and recruited macrophages play important roles in upregulating antimicrobial responses, disease progression and lung homeostasis following infection. We use resting and IFNγ activated BMDMs and FLAMs to differences seen in these two macrophage subsets following Mab infection. Although results show few differences in Mab intracellular levels or macrophage cell death over the first few days of infection, global analysis of upregulated transcriptional and cytokine profiles highlight significant differences in both FLAMs and BMDMs responses during Mab infection in both resting and IFNγ-activated states. Notably, we find both Nrf2 and NF-κB, two global transcriptional regulators that widely impact inflammatory responses during infection, are not robustly activated in Mab infected FLAMs. We also observed low levels of inducible nitric oxide synthase (Nos2) in IFNγ-activated FLAMs relative to BMDMs, with this phenotype reversed following activation of HIF1α. Together, these data uncover key differences in unique macrophage subset responses following Mab infection and emphasizes the continued need to better define the unique immune mechanisms regulating macrophage responses to improve pulmonary infection control.

To finish, I delve into the complex relationships occurring at the macrophage-Mab-antibiotic interface. Here we choose to dissect these interactions during Linezolid treatment, an antibiotic with known off-target effects on the host that is commonly used to treat Mab pulmonary infection. In this chapter, we complete a genome-wide loss-of-function macrophage screen in the presence of Linezolid treatment to identify host genes required for macrophage

control of Mab in the presence of Linezolid. Pathway analysis of screen results identify known modulators required for pathogen control, including genes modulating phagosome maturation and upregulation of NF-κB. Interestingly, pathway analysis also identified the requirement of oxidative phosphorylation regulating genes in macrophage mediated control of Mab. However, validation studies show top screen hits are required for baseline Mab restriction, independent of antibiotic treatment. Combined, this study identifies novel restriction mechanisms leveraged following Mab uptake, while highlighting the continued need for research on cell-autonomous mechanisms of Mab control in the future.

REFERENCES

1. Tortoli, E., *Microbiological features and clinical relevance of new species of the genus Mycobacterium.* Clin Microbiol Rev, 2014. **27**(4): p. 727-52.

2. Tortoli, E., et al., *The new phylogeny of the genus Mycobacterium: The old and the news.* Infect Genet Evol, 2017. **56**: p. 19-25.

3. Turenne, C.Y., *Nontuberculous mycobacteria: Insights on taxonomy and evolution.* Infect Genet Evol, 2019. **72**: p. 159-168.

4. Runyon, E.H., *Anonymous mycobacteria in pulmonary disease.* Med Clin North Am, 1959. **43**(1): p. 273-90.

5. Wolinsky, E., *Mycobacterial Diseases Other Than Tuberculosis.* Clinical Infectious Diseases, 1992. **15**(1): p. 1-12.

6. Sharma, S.K. and V. Upadhyay, *Epidemiology, diagnosis & treatment of non-tuberculous mycobacterial diseases.* Indian J Med Res, 2020. **152**(3): p. 185-226.

7. Prevots, D.R., et al., *Nontuberculous mycobacterial lung disease prevalence at four integrated health care delivery systems.* Am J Respir Crit Care Med, 2010. **182**(7): p. 970-6.

8. Harris, K.A. and D.T.D. Kenna, *Mycobacterium abscessus infection in cystic fibrosis: molecular typing and clinical outcomes.* J Med Microbiol, 2014. **63**(Pt 10): p. 1241-1246.

9. Roux, A.L., et al., *Multicenter study of prevalence of nontuberculous mycobacteria in patients with cystic fibrosis in france.* J Clin Microbiol, 2009. **47**(12): p. 4124-8.

10. Daley, C.L., et al., *Treatment of Nontuberculous Mycobacterial Pulmonary Disease: An Official ATS/ERS/ESCMID/IDSA Clinical Practice Guideline.* Clin Infect Dis, 2020. **71**(4): p. 905-913.

11. Nessar, R., et al., *Mycobacterium abscessus: a new antibiotic nightmare.* J Antimicrob Chemother, 2012. **67**(4): p. 810-8.

12. Olivier, K.N., et al., *Nontuberculous mycobacteria. I: multicenter prevalence study in cystic fibrosis.* Am J Respir Crit Care Med, 2003. **167**(6): p. 828-34.

13. Taiwo, B. and J. Glassroth, *Nontuberculous mycobacterial lung diseases.* Infect Dis Clin North Am, 2010. **24**(3): p. 769-89.

14. Bryant, J.M., et al., *Whole-genome sequencing to identify transmission of Mycobacterium abscessus between patients with cystic fibrosis: a retrospective cohort study.* Lancet, 2013. **381**(9877): p. 1551-60.

15. Kreda, S.M., C.W. Davis, and M.C. Rose, *CFTR, mucins, and mucus obstruction in cystic fibrosis.* Cold Spring Harb Perspect Med, 2012. **2**(9): p. a009589.

16. Moni, S.S. and A. Al Basheer, *Molecular targets for cystic fibrosis and therapeutic potential of monoclonal antibodies.* Saudi Pharm J, 2022. **30**(12): p. 1736-1747.

17. Bernut, A., et al., *CFTR Protects against Mycobacterium abscessus Infection by Fine-Tuning Host Oxidative Defenses.* Cell Rep, 2019. **26**(7): p. 1828-1840 e4.

18. Fahy, J.V. and B.F. Dickey, *Airway mucus function and dysfunction.* N Engl J Med, 2010. **363**(23): p. 2233-47.

19. De Rose, V., et al., *Airway Epithelium Dysfunction in Cystic Fibrosis and COPD.* Mediators Inflamm, 2018. **2018**: p. 1309746.

20. Abdelaal, H.F.M., et al., *Mycobacterium abscessus: It's Complex.* Microorganisms, 2022. **10**(7).

21. Malcolm, K.C., et al., *Mycobacterium abscessus Displays Fitness for Fomite Transmission.* Appl Environ Microbiol, 2017. **83**(19).

22. Leah M. Feazela, L.K.B., Kristen L. Petersona, Daniel N. Franka, J. Kirk Harrisb, and Norman R. Pacea, *Opportunistic pathogens enriched in showerhead biofilms.* The Preceedings of the National Academy of Sciences, 2009. **106**(38): p. 16393-16399.

23. Josephine M. Bryant, D.M.G., Daniela Rodriguez-Rincon, Isobel Everall, et al., *Emergence and Spread of a human-transmissible multidrug-resistance nontuberculous mycobacterium.* Science, 2016. **354**(6313): p. 751-757.

24. Frank M. Griffin, J.A.G., Judith E. Leider and Samuel C. Silverstein, *Studies of the mechanisms of phagocytosis. I. Requirements for circumferential attachment of particle-bound ligands to specific receptors on the macrophage plasma membrane.* Journal of Experimental Medicine, 1975. **142**(5): p. 1263-1282.

25. Kheir, W.A., et al., *A WAVE2-Abi1 complex mediates CSF-1-induced F-actin-rich membrane protrusions and migration in macrophages.* J Cell Sci, 2005. **118**(Pt 22): p. 5369-79.

26. Scott, C.C., et al., *Phosphatidylinositol-4,5-bisphosphate hydrolysis directs actin remodeling during phagocytosis.* J Cell Biol, 2005. **169**(1): p. 139-49.

27. Kang, P.B., et al., *The human macrophage mannose receptor directs Mycobacterium tuberculosis lipoarabinomannan-mediated phagosome biogenesis.* J Exp Med, 2005. **202**(7): p. 987-99.

28. Sever-Chroneos, Z., et al., *Prolonged survival of scavenger receptor class A-deficient mice from pulmonary Mycobacterium tuberculosis infection.* Tuberculosis (Edinb), 2011. **91 Suppl 1**(Suppl 1): p. S69-74.

29. Means, T.K., et al., *Differential effects of a Toll-like receptor antagonist on Mycobacterium tuberculosis-induced macrophage responses.* J Immunol, 2001. **166**(6): p. 4074-82.

30. Taban, Q., et al., *Scavenger receptors in host defense: from functional aspects to mode of action.* Cell Commun Signal, 2022. **20**(1): p. 2.

31. Rhoades, E.R., et al., *Mycobacterium abscessus Glycopeptidolipids mask underlying cell wall phosphatidyl-myo-inositol mannosides blocking induction of human macrophage TNF-alpha by preventing interaction with TLR2.* J Immunol, 2009. **183**(3): p. 1997-2007.

32. Shin, D.M., et al., *Mycobacterium abscessus activates the macrophage innate immune response via a physical and functional interaction between TLR2 and dectin-1.* Cell Microbiol, 2008. **10**(8): p. 1608-21.

33. Ochoa, A.E., et al., *Dectin-1-Independent Macrophage Phagocytosis of Mycobacterium abscessus.* Int J Mol Sci, 2023. **24**(13).

34. Rougerie, P., V. Miskolci, and D. Cox, *Generation of membrane structures during phagocytosis and chemotaxis of macrophages: role and regulation of the actin cytoskeleton.* Immunol Rev, 2013. **256**(1): p. 222-39.

35. Rosales, C. and E. Uribe-Querol, *Phagocytosis: A Fundamental Process in Immunity.* Biomed Res Int, 2017. **2017**: p. 9042851.

36. Lee, H.J., et al., *Formation and Maturation of the Phagosome: A Key Mechanism in Innate Immunity against Intracellular Bacterial Infection.* Microorganisms, 2020. **8**(9).

37. Marie-Anais, F., et al., *Dynamin-Actin Cross Talk Contributes to Phagosome Formation and Closure.* Traffic, 2016. **17**(5): p. 487-99.

38. Fratti, R.A., et al., *Role of phosphatidylinositol 3-kinase and Rab5 effectors in phagosomal biogenesis and mycobacterial phagosome maturation arrest.* J Cell Biol, 2001. **154**(3): p. 631-44.

39. Poteryaev, D., et al., *Identification of the switch in early-to-late endosome transition.* Cell, 2010. **141**(3): p. 497-508.

40. Hackam, D.J., et al., *Regulation of phagosomal acidification. Differential targeting of Na+/H+ exchangers, Na+/K+-ATPases, and vacuolar-type H+-atpases.* J Biol Chem, 1997. **272**(47): p. 29810-20.

41. Roberts, E.A., et al., *Higher order Rab programming in phagolysosome biogenesis.* J Cell Biol, 2006. **174**(7): p. 923-9.

42. Lukacs, G.L., O.D. Rotstein, and S. Grinstein, *Phagosomal acidification is mediated by a vacuolar-type H(+)-ATPase in murine macrophages.* Journal of Biological Chemistry, 1990. **265**(34): p. 21099-21107.

43. Minakami, R. and H. Sumimotoa, *Phagocytosis-coupled activation of the superoxide-producing phagocyte oxidase, a member of the NADPH oxidase (nox) family.* Int J Hematol, 2006. **84**(3): p. 193-8.

44. Marshansky, V. and M. Futai, *The V-type H+-ATPase in vesicular trafficking: targeting, regulation and function.* Curr Opin Cell Biol, 2008. **20**(4): p. 415-26.

45. Nauseef, W.M., *Myeloperoxidase in human neutrophil host defence.* Cell Microbiol, 2014. **16**(8): p. 1146-55.

46. Wang, Q., et al., *Synthesis of characteristic Mycobacterium peptidoglycan (PGN) fragments utilizing with chemoenzymatic preparation of meso-diaminopimelic acid (DAP), and their modulation of innate immune responses.* Org Biomol Chem, 2016. **14**(3): p. 1013-23.

47. Girardin, S.E., et al., *Nod2 is a general sensor of peptidoglycan through muramyl dipeptide (MDP) detection.* J Biol Chem, 2003. **278**(11): p. 8869-72.

48. Davis, K.M., S. Nakamura, and J.N. Weiser, *Nod2 sensing of lysozyme-digested peptidoglycan promotes macrophage recruitment and clearance of S. pneumoniae colonization in mice.* J Clin Invest, 2011. **121**(9): p. 3666-76.

49. Dube, J.Y. and M.A. Behr, *A nod to the bond between NOD2 and mycobacteria.* PLoS Pathog, 2023. **19**(6): p. e1011389.

50. Trindade, B.C. and G.Y. Chen, *NOD1 and NOD2 in inflammatory and infectious diseases.* Immunol Rev, 2020. **297**(1): p. 139-161.

51. Ahn, J.H., et al., *Type I Interferons Are Involved in the Intracellular Growth Control of Mycobacterium abscessus by Mediating NOD2-Induced Production of Nitric Oxide in Macrophages.* Front Immunol, 2021. **12**: p. 738070.

52. Lee, J.Y., et al., *Nucleotide-Binding Oligomerization Domain 2 Contributes to Limiting Growth of Mycobacterium abscessus in the Lung of Mice by Regulating Cytokines and Nitric Oxide Production.* Front Immunol, 2017. **8**: p. 1477.

53. Rottman, M., et al., *Importance of T cells, gamma interferon, and tumor necrosis factor in immune control of the rapid grower Mycobacterium abscessus in C57BL/6 mice.* Infect Immun, 2007. **75**(12): p. 5898-907.

54. Bernut, A., et al., *Mycobacterium abscessus-Induced Granuloma Formation Is Strictly Dependent on TNF Signaling and Neutrophil Trafficking.* PLoS Pathog, 2016. **12**(11): p. e1005986.

55. Bernut, A., et al., *Mycobacterium abscessus cording prevents phagocytosis and promotes abscess formation.* Proc Natl Acad Sci U S A, 2014. **111**(10): p. E943-52.

56. Lyons, T.F.B.a.C.R., *Preliminary Characterization of a Mycobacterium abscessus Mutant in Human and Murine Models of Infection.* Infection and Immunity, 1999. **67**(9): p. 4700-4707.

57. Areeja H Mufti, B.W.T., Robert R K Mckendry, Jonathan B Angel, *Mycobacterium abscessus infection after use of tumer necrosis factor alpha inhibitor therapy: case report and review of infectious complications associated with tumor necrosis factor alpha inhibitor use.* Diagnostic Microbiology and Infectious Disease, 2005. **53**(3): p. 233-238.

58. Rosain, J., et al., *Mendelian susceptibility to mycobacterial disease: 2014-2018 update.* Immunol Cell Biol, 2019. **97**(4): p. 360-367.

59. Abel, J.-L.C.a.L., *Genetic Dissection of Immunity to Mycobacteria: The Human Model.* Annual Review of Immunology, 2002. **20**: p. 581-620.

60. Andersen, P., *Host responses and antigens involved in protective immunity to Mycobacterium tuberculosis.* Scand J Immunol, 1997. **45**(2): p. 115-31.

61. Andrea M. Cooper, D.K.D., Timothy A. Stewart, John P. Griffin, David G. Russel, and Ian M. Orme, *Disseminated Tuberculosis in Interferon γ Gene-disrupted Mice.* Journal of Experimental Medicine, 1993. **178**(6): p. 2243-2247.

62. Karki, R., et al., *Synergism of TNF-alpha and IFN-gamma Triggers Inflammatory Cell Death, Tissue Damage, and Mortality in SARS-CoV-2 Infection and Cytokine Shock Syndromes.* Cell, 2021. **184**(1): p. 149-168 e17.

63. Jankute, M., et al., *The role of hydrophobicity in tuberculosis evolution and pathogenicity.* Sci Rep, 2017. **7**(1): p. 1315.

64. Astarie-Dequeker, C., et al., *Phthiocerol dimycocerosates of M. tuberculosis participate in macrophage invasion by inducing changes in the organization of plasma membrane lipids.* PLoS Pathog, 2009. **5**(2): p. e1000289.

65. Cambier, C.J., et al., *Phenolic Glycolipid Facilitates Mycobacterial Escape from Microbicidal Tissue-Resident Macrophages.* Immunity, 2017. **47**(3): p. 552-565 e4.

66. Gutierrez, A.V., et al., *Glycopeptidolipids, a Double-Edged Sword of the Mycobacterium abscessus Complex.* Front Microbiol, 2018. **9**: p. 1145.

67. Ripoll, F., et al., *Genomics of glycopeptidolipid biosynthesis in Mycobacterium abscessus and M. chelonae.* BMC Genomics, 2007. **8**: p. 114.

68. Kim, B.R., et al., *Phagosome Escape of Rough Mycobacterium abscessus Strains in Murine Macrophage via Phagosomal Rupture Can Lead to Type I Interferon Production and Their Cell-To-Cell Spread.* Front Immunol, 2019. **10**: p. 125.

69. Dubois, V., et al., *MmpL8(MAB) controls Mycobacterium abscessus virulence and production of a previously unknown glycolipid family.* Proc Natl Acad Sci U S A, 2018. **115**(43): p. E10147-E10156.

70. Vincent Le Moigne, M.R., Celine Goulard, Benoit Barteanu, Isabelle Poncin, Nathalie Soismier, Stephane Canaan, Bruno Pitard, Jean-Louis Gaillard, Jean-Louis Herrmann, *Bacterial phospholipases C as vaccine candidate antigens against cystic fibrosis respiratory pathogens: the Mycobacterium abscessus model.* Vaccine, 2015. **33**(18): p. 2118-2124.

71. Le Moigne, V., et al., *MgtC as a Host-Induced Factor and Vaccine Candidate against Mycobacterium abscessus Infection.* Infect Immun, 2016. **84**(10): p. 2895-903.

72. Vaziri, F. and R. Brosch, *ESX/Type VII Secretion Systems-An Important Way Out for Mycobacterial Proteins.* Microbiol Spectr, 2019. **7**(4).

73. Abdalla M. Abdallah, N.C.G.v.P., Patricia A. DiGiuseppe Champion, Jeffery Cox, Joen Luirink, Christina M. J. E. Vandenbroucke-Grauls, Ben J. Appelmelk and Wilbert Bitter, *Type VII secretion - mycobacteria show the way.* Nature Reviews Microbiology, 2007. **5**: p. 883-891.

74. Simeone, R., et al., *Phagosomal rupture by Mycobacterium tuberculosis results in toxicity and host cell death.* PLoS Pathog, 2012. **8**(2): p. e1002507.

75. Guinn, K.M., et al., *Individual RD1-region genes are required for export of ESAT-6/CFP-10 and for virulence of Mycobacterium tuberculosis.* Mol Microbiol, 2004. **51**(2): p. 359-70.

76. Roy, S., et al., *ESX secretion system: The gatekeepers of mycobacterial survivability and pathogenesis.* Eur J Microbiol Immunol (Bp), 2020. **10**(4): p. 202-209.

77. Guo, F., et al., *Immunological effects of the PE/PPE family proteins of Mycobacterium tuberculosis and related vaccines.* Front Immunol, 2023. **14**: p. 1255920.

78. Garcia-Bengoa, M., et al., *Mycobacterium tuberculosis PE/PPE proteins enhance the production of reactive oxygen species and formation of neutrophil extracellular traps.* Front Immunol, 2023. **14**: p. 1206529.

79. Laencina, L., et al., *Identification of genes required for Mycobacterium abscessus growth in vivo with a prominent role of the ESX-4 locus.* Proc Natl Acad Sci U S A, 2018. **115**(5): p. E1002-E1011.

80. Heui-Dong Park, K.M.G., Maria I. Harrell, Reiling Liao, Martin I. Voskuil, Martin Tompa, Gary K. Schoolnik, and David R. Sherman, *Rv3133c/dosR is a trascription factor that mediates the hypoxic response of Mycobacterium tuberculosis.* Molecular Microbiology, 2003. **48**(3): p. 833-843.

81. Leistikow, R.L., et al., *The Mycobacterium tuberculosis DosR regulon assists in metabolic homeostasis and enables rapid recovery from nonrespiring dormancy.* J Bacteriol, 2010. **192**(6): p. 1662-70.

82. Cunningham-Bussel, A., T. Zhang, and C.F. Nathan, *Nitrite produced by Mycobacterium tuberculosis in human macrophages in physiologic oxygen impacts bacterial ATP consumption and gene expression.* Proc Natl Acad Sci U S A, 2013. **110**(45): p. E4256-65.

83. Peterson, E.J.R., et al., *Intricate Genetic Programs Controlling Dormancy in Mycobacterium tuberculosis.* Cell Rep, 2020. **31**(4): p. 107577.

84. Simcox, B.S., et al., *Mycobacterium abscessus DosRS two-component system controls a species-specific regulon required for adaptation to hypoxia.* Front Cell Infect Microbiol, 2023. **13**: p. 1144210.

85. Iakobachvili, N., et al., *Mycobacteria-host interactions in human bronchiolar airway organoids.* Mol Microbiol, 2022. **117**(3): p. 682-692.

86. Takano, K., et al., *Severe Pulmonary Mycobacterium abscessus Cases Due to Co-Infection with Other Microorganisms Well Treated by Clarithromycin and Sitafloxacin in Japan.* Int Med Case Rep J, 2021. **14**: p. 465-470.

87. Whittier, S., Olivier, K., Gilligan, P., Knowles, M., and Della-Latta, P, *Proficiency Testing of Clinical Microbiology Laboratories Using Modified Decontaminated Procedures for Detection of Nontuberculous Mycobacteria in Sputum Samples from Cystic Fibrosis Patients.* Journal of Clinical Microbiology, 1997. **35**: p. 2706-2708.

88. Antonio Oliver, L.M., Rafael Canton, Hector Escobar, Fernando Baquero, and Enrique Gomez-Mampaso, *Nontuberculous Mycobacteria in Patients with Cystic Fibrosis.* Clin Infect Dis, 2001. **32**(9): p. 1298-1303.

89. Rodriguez-Sevilla, G., et al., *Influence of three-dimensional lung epithelial cells and interspecies interactions on antibiotic efficacy against Mycobacterium abscessus and Pseudomonas aeruginosa.* Pathog Dis, 2018. **76**(4).

90. Rodriguez-Sevilla, G., et al., *Antimicrobial Treatment Provides a Competitive Advantage to Mycobacterium abscessus in a Dual-Species Biofilm with Pseudomonas aeruginosa.* Antimicrob Agents Chemother, 2019. **63**(11).

91. Ayantu W. Idosa, D.J.W., Luanne Hall-Stoodley, *Surface Dependent Inhibition of Mycobacteirum abscessus by Diverse Pseudomonas aeruginosa Strains.* Microbiol Spectrum, 2022. **10**(6): p. e02471-22.

92. Birmes, F.S., et al., *Mycobacterium abscessus subsp. abscessus Is Capable of Degrading Pseudomonas aeruginosa Quinolone Signals.* Front Microbiol, 2017. **8**: p. 339.

93. Griffith, D.E. and C.L. Daley, *Treatment of Mycobacterium abscessus Pulmonary Disease.* Chest, 2022. **161**(1): p. 64-75.

94. Haworth, C.S., et al., *British Thoracic Society guidelines for the management of non-tuberculous mycobacterial pulmonary disease (NTM-PD).* Thorax, 2017. **72**(Suppl 2): p. ii1-ii64.

95. Griffith, D.E., et al., *Amikacin Liposome Inhalation Suspension for Treatment-Refractory Lung Disease Caused by Mycobacterium avium Complex (CONVERT). A Prospective, Open-Label, Randomized Study.* Am J Respir Crit Care Med, 2018. **198**(12): p. 1559-1569.

96. Dedrick, R.M., et al., *Engineered bacteriophages for treatment of a patient with a disseminated drug-resistant Mycobacterium abscessus.* Nat Med, 2019. **25**(5): p. 730-733.

97. Luthra, S., A. Rominski, and P. Sander, *The Role of Antibiotic-Target-Modifying and Antibiotic-Modifying Enzymes in Mycobacterium abscessus Drug Resistance.* Front Microbiol, 2018. **9**: p. 2179.

98. Johansen, M.D., J.L. Herrmann, and L. Kremer, *Non-tuberculous mycobacteria and the rise of Mycobacterium abscessus.* Nat Rev Microbiol, 2020. **18**(7): p. 392-407.

99. Joaquim Trias, V.J., and Roland Benz, *Porins in the Cell Wall of Mycobacteria.* Science, 1992. **258**(5087): p. 1479-1481.

100. de Moura, V.C.N., et al., *Increased Virulence of Outer Membrane Porin Mutants of Mycobacterium abscessus.* Front Microbiol, 2021. **12**: p. 706207.

101. Lewin, A., et al., *Genetic diversification of persistent Mycobacterium abscessus within cystic fibrosis patients.* Virulence, 2021. **12**(1): p. 2415-2429.

102. Kerr, I.D., *Structure and associate of ATP-binding cassette transporter nucleotide-binding domains.* Biochim Biophys Acta, 2002. **1561**(1): p. 47-64.

103. I D Kerr, E.D.R., J H Cove, *ABC proteins and antibiotic drug resistance: is it all about transport?* Biochem Soc Trans, 2005. **33**: p. 1000-2.

104. Ripoll, F., et al., *Non mycobacterial virulence genes in the genome of the emerging pathogen Mycobacterium abscessus.* PLoS One, 2009. **4**(6): p. e5660.

105. Viljoen, A., et al., *The diverse family of MmpL transporters in mycobacteria: from regulation to antimicrobial developments.* Mol Microbiol, 2017. **104**(6): p. 889-904.

106. Ana Victoria Gutiérrez, M.R., Françoise Roquet-Banères, Albertus Viljoen, Laurent Kremer, *The TetR Family Transcription Factor MAB_2299c Regulates the Expression of Two Distinct MmpS-MmpL Efflux pumps Involved in Cross-Resistance to Clofazimine and Bedaquiline in Mycobacterium abscessus.* Antimicrobial Agents and Chemotherapy, 2019. **63**(10): p. e01000-10.

107. Halloum, I., et al., *Resistance to Thiacetazone Derivatives Active against Mycobacterium abscessus Involves Mutations in the MmpL5 Transcriptional Repressor MAB_4384.* Antimicrob Agents Chemother, 2017. **61**(4).

108. Domenech, P., M.B. Reed, and C.E. Barry, 3rd, *Contribution of the Mycobacterium tuberculosis MmpL protein family to virulence and drug resistance.* Infect Immun, 2005. **73**(6): p. 3492-501.

109. Pasca, M.R., et al., *mmpL7 gene of Mycobacterium tuberculosis is responsible for isoniazid efflux in Mycobacterium smegmatis.* Antimicrob Agents Chemother, 2005. **49**(11): p. 4775-7.

110. Hartkoorn, R.C., S. Uplekar, and S.T. Cole, *Cross-resistance between clofazimine and bedaquiline through upregulation of MmpL5 in Mycobacterium tuberculosis.* Antimicrob Agents Chemother, 2014. **58**(5): p. 2979-81.

111. Melly, G. and G.E. Purdy, *MmpL Proteins in Physiology and Pathogenesis of M. tuberculosis.* Microorganisms, 2019. **7**(3).

112. Dubee, V., et al., *beta-Lactamase inhibition by avibactam in Mycobacterium abscessus.* J Antimicrob Chemother, 2015. **70**(4): p. 1051-8.

113. Story-Roller, E., et al., *Mycobacterium abscessus and beta-Lactams: Emerging Insights and Potential Opportunities.* Front Microbiol, 2018. **9**: p. 2273.

114. Soroka, D., et al., *Characterization of broad-spectrum Mycobacterium abscessus class A beta-lactamase.* J Antimicrob Chemother, 2014. **69**(3): p. 691-6.

115. Hurst-Hess, K., P. Rudra, and P. Ghosh, *Mycobacterium abscessus WhiB7 Regulates a Species-Specific Repertoire of Genes To Confer Extreme Antibiotic Resistance.* Antimicrob Agents Chemother, 2017. **61**(11).

116. Mathias Richard, A.V.G., Laurent Kremer, *Dissecting erm(41)-Mediated Macrolide-Inducible Resistance in Mycobacterium abscessus.* Antimicrobial Agents and Chemotherapy, 2020. **64**(2): p. e01879-19.

117. Hurst-Hess, K., et al., *Hierarchy and interconnected networks in the WhiB7 mediated transcriptional response to antibiotic stress in Mycobacterium abscessus.* PLoS Genet, 2023. **19**(12): p. e1011060.

118. Pryjma, M., et al., *Antagonism between Front-Line Antibiotics Clarithromycin and Amikacin in the Treatment of Mycobacterium abscessus Infections Is Mediated by the whiB7 Gene.* Antimicrob Agents Chemother, 2017. **61**(11).

119. Bastian, S., et al., *Assessment of clarithromycin susceptibility in strains belonging to the Mycobacterium abscessus group by erm(41) and rrl sequencing.* Antimicrob Agents Chemother, 2011. **55**(2): p. 775-81.

120. Maurer, F.P., et al., *Acquisition of clarithromycin resistance mutations in the 23S rRNA gene of Mycobacterium abscessus in the presence of inducible erm(41).* J Antimicrob Chemother, 2012. **67**(11): p. 2606-11.

121. Brown-Elliott, B.A., et al., *Utility of sequencing the erm(41) gene in isolates of Mycobacterium abscessus subsp. abscessus with low and intermediate clarithromycin MICs.* J Clin Microbiol, 2015. **53**(4): p. 1211-5.

122. Mougari, F., et al., *Standardized interpretation of antibiotic susceptibility testing and resistance genotyping for Mycobacterium abscessus with regard to subspecies and erm41 sequevar.* J Antimicrob Chemother, 2016. **71**(8): p. 2208-12.

123. Ubeda, C. and E.G. Pamer, *Antibiotics, microbiota, and immune defense.* Trends Immunol, 2012. **33**(9): p. 459-66.

124. Patangia, D.V., et al., *Impact of antibiotics on the human microbiome and consequences for host health.* Microbiologyopen, 2022. **11**(1): p. e1260.

125. Day, N.J., P. Santucci, and M.G. Gutierrez, *Host cell environments and antibiotic efficacy in tuberculosis.* Trends Microbiol, 2023.

126. Park, H.E., et al., *Understanding the Reciprocal Interplay Between Antibiotics and Host Immune System: How Can We Improve the Anti-Mycobacterial Activity of Current Drugs to Better Control Tuberculosis?* Front Immunol, 2021. **12**: p. 703060.

127. Bergman, P., et al., *Host Directed Therapy Against Infection by Boosting Innate Immunity.* Front Immunol, 2020. **11**: p. 1209.

128. Giraud-Gatineau, A., et al., *The antibiotic bedaquiline activates host macrophage innate immune resistance to bacterial infection.* Elife, 2020. **9**.

129. Tousif, S., et al., *Isoniazid induces apoptosis of activated CD4+ T cells: implications for post-therapy tuberculosis reactivation and reinfection.* J Biol Chem, 2014. **289**(44): p. 30190-30195.

130. Manca, C., et al., *Host targeted activity of pyrazinamide in Mycobacterium tuberculosis infection.* PLoS One, 2013. **8**(8): p. e74082.

131. Singhal A, J.L., Kumar P, et al., *Metformin as adjunct antituberculosis therapy.* Sci Transl Med, 2014. **6**(263).

132. Padmapriydarsini, C., et al., *Randomized Trial of Metformin With Anti-Tuberculosis Drugs for Early Sputum Conversion in Adults With Pulmonary Tuberculosis.* Clin Infect Dis, 2022. **75**(3): p. 425-434.

133. Roca, F.J., et al., *Tumor necrosis factor induces pathogenic mitochondrial ROS in tuberculosis through reverse electron transport.* Science, 2022. **376**(6600): p. eabh2841.

134. Ordway, D., Henao-Tamayo, M., Smith, E., Shanley, C., Harton, M., Troudt, J., et al., *Animal model of Mycobacterium abscessus lung infection.* J. Leukoc. Biol., 2008. **83**: p. 1502-1511.

135. Obregon-Henao, A., et al., *Susceptibility of Mycobacterium abscessus to antimycobacterial drugs in preclinical models.* Antimicrob Agents Chemother, 2015. **59**(11): p. 6904-12.

136. Bernut, A., et al., *In vivo assessment of drug efficacy against Mycobacterium abscessus using the embryonic zebrafish test system.* Antimicrob Agents Chemother, 2014. **58**(7): p. 4054-63.

137. Keith M. Astrofsky, M.D.S., Robert A. Bullis, Roxanna M. Smolowitz and James G. Fox, *Diagnosis and Management of Atypical Mycobacterium spp. Infections in Established Laboratory Zebrafish (Brachydanio rerio) Facilities.* Comparative Medicine, 2000. **50**(6): p. 666-672.

138. Watral, V., and Kent, M. L., *Pathogenesis of Mycobacterium spp. in zebrafish (Danio rerio) from research facilities.* Comp Biochem Physiol C Toxicol Pharmacol, 2007. **145**(1): p. 55-60.

139. Dancourt, M., *Looking in amoebae as a source of mycobacterium.* Microb Pathog, 2014. **77**: p. 199-24.

140. Bakala N'Goma, J.C., et al., *Mycobacterium abscessus phospholipase C expression is induced during coculture within amoebae and enhances M. abscessus virulence in mice.* Infect Immun, 2015. **83**(2): p. 780-91.

141. Austin, P.E., McCulloch, E. A., Till, J. E., *Characterization of the factor in L-cell conditioned medium capable of stimulating colony formation by mouse marrow cells in culture.* Journal of Cellular Physiology, 1971. **77**(2): p. 121-133.

142. Johnson BK, T.S., Olive AJ, Abramovitch RB, *Macrophage Infection Models for Mycobacterium tuberculosis.* Methods in Molecular Biology, 2021. **2314**: p. 167-182.

143. Spera, I., et al., *The J2-Immortalized Murine Macrophage Cell Line Displays Phenotypical and Metabolic Features of Primary BMDMs in Their M1 and M2 Polarization State.* Cancers (Basel), 2021. **13**(21).

144. Blasi, E., Mathieson, B. J., Varesio, L, *Selective immortalization of murine macrophages from fresh bone marrow by raf/myc recombinant murine retrovirus.* J Neuroimmunol, 1990. **27**(2): p. 229-37.

145. Seager Danciger, J., Lutz, M., Hama, S., Cruz, D., Castrillo, A., Lazaro, J., Phillips, R., Premack, B., Berliner, J., *Method for large scale isolation, culture and cryopreservation of human monocytes suitable for chemotaxis, cellular adhesion assays, macrophage and dendritic cell differentiation.* J Immunol Methods, 2004. **388**(1): p. 123-34.

146. Marim, F.M., et al., *A method for generation of bone marrow-derived macrophages from cryopreserved mouse bone marrow cells.* PLoS One, 2010. **5**(12): p. e15263.

147. Kiritsy, M.C., et al., *A genetic screen in macrophages identifies new regulators of IFNgamma-inducible MHCII that contribute to T cell activation.* Elife, 2021. **10**.

148. Nayak, D.K., et al., *Isolation and In Vitro Culture of Murine and Human Alveolar Macrophages.* J Vis Exp, 2018(134).

149. Cohen, A.B., and Cline M. J., *The Human Alveolar Macrophage: Isolation, Cultivation in Vitro, and Studies of Morphologic and Functional Characteristics.* J Clin Invest, 1971. **50**: p. 1390-1398.

150. Maler, M.D., et al., *Key Role of the Scavenger Receptor MARCO in Mediating Adenovirus Infection and Subsequent Innate Responses of Macrophages.* mBio, 2017. **8**(4).

151. Thomas, S.T., et al., *Fetal Liver-Derived Alveolar-like Macrophages: A Self-Replicating Ex Vivo Model of Alveolar Macrophages for Functional Genetic Studies.* Immunohorizons, 2022. **6**(2): p. 156-169.

152. S Kusunoki, T.E., *Proposal of Mycobacterium peregrinum sp. nov., nom. rev., and elevation of Mycobacterium chelonae subsp. abscessus (Kubica et al.) to species status: Mycobacterium abscessus comb. nov.* Int J Syst Bacteriol, 1992. **42**(2): p. 240-5.

153. Lopeman, R.C., et al., *Mycobacterium abscessus: Environmental Bacterium Turned Clinical Nightmare.* Microorganisms, 2019. **7**(3).

CHAPTER 2: A Genome-Wide Screen in Macrophages Defines Host Genes Regulating the Uptake of *Mycobacterium abscessus.*

DECLARATIONS

Authors

Haleigh N. Gilliland[1], Olivia K. Beckman[1], and Andrew J. Olive[1]

1 Michigan State University

Contributions

HG and AO designed the studies. HG investigated the role of UGDH, B3GAT3 and B4GALT7 in iBMDM uptake of *M. abscessus* during early infection. OB quantified total sGAGs in sgNTC, sgUGDH, sgB3GAT3 and sgB4GALT7 iBMDMs. HG and AO wrote the chapter, and OB reviewed it.

Publication Notice

The following chapter is published at doi.org/10.1128/msphere.00663-22. Reprint permissions are reserved to the authors for use in this dissertation. This chapter was also published as a preprint at doi.org/10.1101/2022.12.20.521338. Reprint permissions are reserved to the authors for use in this dissertation.

ABSTRACT

The interactions between a host cell and a pathogen can dictate disease outcomes and are important targets for host-directed therapies. *Mycobacterium abscessus* (Mab) is a highly antibiotic resistant, rapidly growing non-tuberculous mycobacterium that infects patients with chronic lung diseases. Mab can infect host immune cells, such as macrophages, which contribute to its pathogenesis. However, our understanding of initial host-Mab interactions remains unclear. Here, we developed a functional genetic approach to define these host-Mab interactions by coupling a Mab fluorescent reporter with a genome-wide knockout library in murine macrophages. We used this approach to conduct a forward genetic screen to define host genes that contribute to the uptake of Mab by macrophages. We identified known regulators of phagocytosis, such as the integrin ITGB2, and uncovered a key requirement for glycosaminoglycan (sGAG) synthesis for macrophages to efficiently take up Mab. CRISPR-Cas9 targeting of three key sGAG biosynthesis regulators, Ugdh, B3gat3 and B4galt7 resulted in reduced uptake of both smooth and rough Mab variants by macrophages. Mechanistic studies suggest that sGAGs function upstream of pathogen engulfment and are required for the uptake of Mab, but not *Escherichia coli* or latex beads. Further investigation found that the loss of sGAGs reduced the surface expression, but not the mRNA expression, of key integrins suggesting an important role for sGAGs in modulating surface receptor availability. Together, these studies globally define and characterize important regulators of macrophage-Mab interactions and are a first step to understanding host genes that contribute to Mab pathogenesis and disease.

IMPORTANCE

Pathogen interactions with immune cells like macrophages contribute to pathogenesis, yet the mechanisms underlying these interactions remain largely undefined. For emerging respiratory pathogens, like *Mycobacterium abscessus*, understanding these host-pathogen interactions is important to fully understand disease progression. Given that *M. abscessus* is broadly recalcitrant to antibiotic treatments, new therapeutic approaches are needed. Here, we leveraged a genome-wide knockout library in murine macrophages to globally define host genes required for *M. abscessus* uptake. We identified new macrophage uptake regulators during *M. abscessus* infection, including a subset of integrins and the glycosaminoglycan synthesis (sGAG) pathway. While ionic characteristics of sGAGs are known to drive pathogen cell interactions, we discovered a previously unrecognized requirement for sGAGs to maintain robust surface expression of key uptake receptors. Thus, we developed a flexible forward genetic pipeline to define important interactions during *M. abscessus* infection and more broadly identified a new mechanism by which sGAGs control pathogen uptake.

INTRODUCTION

Mycobacterium abscessus (Mab) is a rapidly growing non-tuberculous mycobacterium (NTM) that causes opportunistic infections in patients with chronic lung diseases, like cystic fibrosis and chronic obstructive pulmonary disease (COPD) [1, 2]. Mab is the second most common NTM respiratory pathogen recovered in the United States, accounting for a significant number of rapidly growing mycobacterial respiratory disease isolates [3]. Due to its recalcitrance to many antibiotics, current treatment success rates remain below 50% [4-6]. Treatment is further complicated by the ability of Mab to transition from a smooth to rough morphology that drives biofilm formation and decreases antibiotic sensitivity [7]. Thus, Mab is an emerging pathogen of clinical importance and there is a critical need to develop new treatment options.

Developing more effective therapies requires a deeper understanding of Mab pathogenesis and host-pathogen interactions that drive infection. Recent work suggests that Mab interactions with macrophages are critical for disease progression [3, 8, 9]. Both smooth and rough Mab variants can survive in macrophages with rough variants initiating more rapid cell death cascades [3, 8, 9]. Transposon mutagenesis studies and other genetic approaches in Mab have identified many genes that are required for effective antibiotic killing and intracellular survival, including the ESX-IV system [10-12]. This virulence determinant contributes to the inhibition of lysosomal fusion enabling intracellular survival of Mab in macrophages [12]. In contrast to what is known about Mab, little is known about macrophage genes required for Mab uptake and survival. While studies have shown that Mab interacts with TLR2 and Dectin-1 to initiate uptake, a systematic characterization of Mab uptake by macrophages remains lacking [13, 14].

Uptake of pathogens requires effective interactions between the pathogen and macrophages. Macrophages use surface pattern recognition receptors (PRRs), including toll-like receptors, mannose receptors and scavenger receptors, for the initial recognition of many pathogens [15-19]. Other modifications to surface proteins, including sulfated glycosaminoglycan (sGAG) modifications such as heparin sulfate and chondroitin sulfate, affect the efficiency of pathogen attachment to the cell surface [20, 21]. On epithelial cells, sGAGs play an important role for the attachment of several pathogens including Coronavirus and *Chlamydia trachomatis* [22-24]. It is predicted that these surface modifications alter the charge interactions between pathogens and the host cell surface to modulated initial attachment [25, 26].

Following adherence, phagocytosis or receptor mediated engulfment of pathogens enables internalization. While each phagocytic cargo has unique components, the general pathway for phagocytosis is conserved. Phagocytosis begins with the generation of a phagosome following a ligand binding to macrophage surface receptors [27]. This binding event activates downstream signaling cascades that remodel the actin cytoskeleton to drive the progressive engagement of additional receptors around the particle [28, 29]. After engulfment, controlled membrane fusion events result in the formation of the nascent phagosome. The phagosome then interacts with various endosome components that acidify the compartment and ultimately lead to compartment fusion with the lysosome [30-35]. Several elegant studies have dissected unique pathways that contribute to phagocytosis of distinct cargos, defining receptors and signaling cascades that are essential [36-38]. However, no studies have globally examined host genes that control Mab interactions with macrophages.

Here, we defined the host genes that control the uptake of Mab into macrophages by coupling a brightly fluorescent Mab reporter with a genome-wide CRISPR-Cas9-mediated

macrophage knockout library in murine immortalized bone marrow-derived macrophages (iBMDMs). We performed a forward genetic screen to enrich for macrophages that could or could not take up Mab identifying several previously defined phagocytosis components. Follow up studies uncovered a strong requirement for sGAG production in macrophages for efficient Mab uptake. While loss of sGAGs did not affect general phagocytosis pathways or opsonized uptake of Mab, sGAGs were essential for initial interactions of both smooth and rough Mab variants with macrophages. Mechanistic studies uncovered a role for sGAGs in maintaining high surface expression of the key integrins ITGB2 and ITGAL, suggesting a new role for sGAGs in maintaining receptor availability on the cell surface. These results uncover important host pathways that modulate the interactions between Mab and macrophages during infection.

RESULTS

Fluorescent Mab reporter enables dissection of Macrophage-Mab interactions.

While Mab infects macrophages, our understanding of these interactions remains limited. To help address this gap in knowledge we developed a brightly fluorescent Mab reporter strain. A constitutive mEmerald GFP vector was transformed into the smooth variant of Mab strain ATCC-19977. Comparisons to non-fluorescent Mab showed that bacterial growth and antibiotic mediated killing with rifampicin in liquid media were unaffected by fluorescent protein expression (Figure 1.1A). We next examined the utility of the fluorescent Mab strain to dissect host-pathogen interactions with macrophages. We first examined the robustness of the fluorescent reporter by infecting immortalized bone marrow derived macrophages (iBMDMs) from C57BL/6J mice. One previous study using a GFP fluorescent Mab was unable to detect increased fluorescence in macrophages until 24 hours of infection, when attachment, uptake and bacterial growth all contribute to differential fluorescence [39]. We hypothesized that earlier

timepoints could be examined using the brighter mEmerald GFP, allowing us to distinguish uptake from intracellular growth. To test this hypothesis, we quantified the number of mEmerald positive macrophages by flow cytometry six hours after infecting iBMDMs with fluorescent Mab at increasing multiplicities of infection (MOIs). We noted that increasing the MOI resulted in an increase in the percent of mEmerald+ cells and the mean fluorescence intensity of these infected cells (Figure 1.1B-1.1D). We next quantified the mEmerald+ cells over the first six hours of infection of iBMDMs at an MOI of 5. We observed the number of infected cells 2-hours post-infection showed a minimal increase compared to uninfected controls, while there was a significant increase in infected cells at four- and six-hours post-infection (Figure 1.1E and 1.1F). Thus, the mEmerald GFP reporter does not affect Mab growth while enabling the dissection of early interactions between Mab and macrophages.

CRISPR-Cas9 loss-of-function (LOF) screen identifies host genes required for Mab uptake by macrophages.

Host pathways required for macrophage uptake of Mab remain almost entirely unknown. To test if the flow cytometry-based uptake assay could identify host pathways required for Mab uptake, we used a known phagocytosis inhibitor, Cytochalasin D, to inhibit actin polymerization [40]. iBMDMs were pretreated with Cytochalasin D then infected with mEmerald Mab. The percent of cells that were infected were then quantified four hours later by flow cytometry. We observed a nearly 50% decrease in mEmerald+ macrophages treated with Cytochalasin D compared to vehicle controls (Figure 1.2A and 1.2B). These data highlight the sensitivity of the uptake assay to dissect early interactions between Mab and macrophages. Next, we leveraged the uptake assay to globally identify host regulators required for Mab uptake by macrophages (Figure 1.2C). We previously generated a robust and reproducible pooled genome-wide loss-of-

function library in Cas9+ iBMDMs [41]. Knockouts in this pool were generated with sgRNAs from the Brie library which targets four independent single guide RNA molecules (sgRNAs) per coding gene and over 1,000 non-targeting controls (NTC) [42]. To identify regulators of Mab uptake, we infected the loss-of-function library of macrophages with mEmerald Mab for four hours. Fluorescence activated cells sorting (FACS) was then used to isolate over 200x sgRNA coverage of the library from mEmerald+ cells and mEmerald- cells. Following genomic DNA extraction, sgRNA abundances for each sorted bin were quantified by deep sequencing. To test for statistical enrichment of sgRNAs and genes, we used the modified robust rank algorithm (α-RRA) employed by Model-based Analysis of Genome-wide CRISPR/Cas9 Knockout (MAGeCK). This algorithm ranks sgRNAs by effect before filtering low ranking sgRNAs to improve significance testing. To identify macrophage genes required for Mab uptake during early infection, we compared the enrichment of sgRNAs in the mEmerald - (Mab uninfected) directly to the mEmerald+ (Mab infected) population. The α-RRA analysis identified 100 genes with a p value <0.01 and a fold change of 2 with at least 2 independent sgRNAs. Among the top 100 candidates, we identified known regulators of macrophage phagocytosis including Manea, M6PR, Itgb2 (CD18), Itgam (CD11b), CD46 and Rac1 with each gene showing enrichment in the mEmerald- population (Figure 1.2D) [43]. Guide-level analysis showed agreement with all four sgRNAs targeting these genes suggesting they are bona fide hits and that our screen was robust.

To confirm the screen results, we validated the role of Manea, M6PR, Itgb2 and Itgam in controlling Mab uptake by macrophages. We generated two independent iBMDM lines targeting two distinct sgRNAs per gene, in addition to a non-targeting control. These cells were then infected with mEmerald Mab and uptake was quantified four hours later. In agreement with our

screen results, we found that targeting each candidate gene resulted in a significant decrease in mEmerald+ iBMDMs compared to NTC cells (Figure 1.2E). Taken together these results show that the genome-wide screen identified host genes that contribute to early interactions between Mab and macrophages.

Sulfated glycosaminoglycans (sGAGs) are required for macrophage uptake of Mab.

To discover new pathways that are required for Mab uptake by macrophages, we next used DAVID analysis and gene set enrichment analysis (GSEA) to identify functional enrichments from our uptake screen dataset. These analyses identified the sulfated glycosaminoglycan (sGAG) synthesis pathway as required for efficient uptake of Mab (Figure 1.3A). While a variety of pathogens use sGAGs to facilitate attachment and invasion of epithelial cells, little is known about their role in macrophages. Within the top candidates in the screen were multiple genes within the sGAG biosynthesis pathway (Figure 1.3B – Blue Dots). Three of these genes, UGDH, B3GAT3, and B4GALT7 encode UDP-glucose 6-dehydrogenase, galactosyltransferase I and glucuronosyltransferase I, respectively and were among the top 30 candidates while showing strong agreement among the four independent sgRNAs. These data suggest that sGAGs contribute to Mab uptake by macrophages.

To validate the importance of macrophage sGAGs for Mab uptake, we targeted Ugdh, B3gat3 and B4galt7 directly in iBMDMs. Using an approach targeting two independent sgRNAs simultaneously we generated a panel of iBMDMs with editing efficiency ranging from 60-95% in each gene, and one cell line per gene was selected for follow up studies [42]. We first examined functional differences following gene editing by quantifying the total sGAGs in sGAG- targeted and NTC iBMDMs. We found that iBMDMs targeted for Ugdh, B3gat3 and B4galt7 each resulted in a significant reduction in sGAGs compared to NTC macrophages

(Figure 1.3C). We next used these sGAG-targeted cells to examine differences in Mab uptake. NTC and sGAG-targeted iBMDMs were infected with mEmerald Mab for four hours with increasing MOIs and bacterial uptake was quantified. At each MOI we observed a significant decrease in Mab uptake in sGAG targeted iBMDMs compared to the NTC cells (Figure 1.3D and 1.3E). These results confirm that sGAGs contribute to the effective uptake of Mab by macrophages, validating our genome-wide screen and bioinformatic analysis.

sGAGs are required for macrophage uptake of rough Mab variants.

While our data suggest sGAGs are needed for uptake of smooth Mab variants by macrophages, it remained unclear if this host pathway was also required for rough variant uptake. To directly test this question, a rough Mab variant derived from ATCC 19977 was transformed with the mEmerald reporter. Similar to the smooth variant, we noted no defects in growth or antibiotic killing in broth culture (Figure 1.4A) and robust uptake by iBMDMs in an MOI dependent manner (Figure 1.4B-1.4D). To test if sGAGs are also required for uptake of rough Mab we next infected NTC and sGAG-targeted iBMDMs with the rough mEmerald Mab reporter for four hours at increasing MOI and quantified the percentage of infected cells. We observed over a 50% decrease of rough Mab uptake in sGAG-targeted macrophages compared to control macrophages at all MOIs (Figure 1.4E and 1.4F). Thus, sGAGs are required for macrophage uptake of both smooth and rough Mab variants.

sGAGs function upstream of Mab internalization.

We next examined the mechanisms underlying sGAG-mediated control of Mab uptake. To understand if sGAGs control specific or general uptake pathways, we tested whether sGAGs were necessary for uptake of other phagocytic cargo by macrophages. First, we quantified the uptake of latex beads by incubating yellow-green-labeled beads at increasing concentrations with

control or sGAG-targeted iBMDMs. In contrast to our results with Mab, we found no differences in the uptake of latex beads between control or sGAG-targeted iBMDMs (Figure 1.5A and 1.5B). We next examined whether sGAGs contribute to the uptake of *Escherichia coli*, a gram negative bacterium. mEmerald expressing *E. coli* was incubated with NTC or sGAG-targeted iBMDMs for four hours then uptake was quantified. Similar to latex beads, we observed no significant differences in *E. coli* uptake between control or sGAG-targeted macrophages (Figure 1.5C and 1.5D). Taken together, these results suggest that sGAG-mediated uptake in macrophages occurs independently of general phagocytosis mechanisms and has pathogen specificity.

Given that the uptake of pathogens can be influenced by opsonization, we next examined whether the sGAG pathway overlaps with complement-mediated uptake mechanisms. Both smooth and rough mEmerald Mab reporters were incubated in active or heat killed serum for thirty minutes. Following serum incubation, control or sGAG-targeted iBMDMs were infected and the percent uptake of Mab was quantified four hours later. Opsonization of the smooth Mab variant with active serum resulted in no significant change in uptake compared to heat-inactivated serum (Figure 1.5E). For the rough Mab variant, while uptake was significantly increased following incubation with active serum in all cells, the uptake differences between NTC and sGAG-targeted iBMDMs remained significant (Figure 1.5F). These data show that while smooth and rough Mab variants are differentially susceptible to complement-mediated phagocytosis, this uptake pathway is independent of sGAGs.

To distinguish if sGAGs are required for internalization or attachment of Mab we next treated control or sGAG-targeted macrophages with Cytochalasin D. We hypothesized that if sGAGs control initial attachment that blocking actin polymerization with Cytochalasin D would further inhibit Mab uptake in sGAG-targeted macrophages. To test this hypothesis, we pre-

treated NTC and sGAG-targeted macrophages with DMSO or Cytochalasin D for two hours. Cells were then infected with smooth or rough variants of mEmerald Mab and uptake was quantified four hours later. We found that Cytochalasin D treatment significantly reduced uptake of both smooth and rough Mab variants compared to vehicle controls in all cell lines tested (Figure 1.5G and 1.5H). These data suggest that sGAGs are needed upstream of bacterial internalization as they function additively with actin polymerization inhibitors.

Loss of sGAGs reduces the surface integrin expression on macrophages.

While sGAGs directly modulate ionic interactions at the cellular surface, it remained possible that sGAG-modifications also regulate the surface levels of the receptors that are required for pathogen uptake (26). Given the importance of integrins for Mab uptake from our screen, we examined the expression of a subset of integrins including ITGB2, ITGAM, and ITGAL. When we quantified the mRNA levels of these integrins we found no changes in the mRNA expression of integrins between NTC and sGAG-targeted macrophages (Figure 6A). In contrast, while we observed no difference in the surface expression of ITGAM, we observed a significant decrease in ITGB2 and ITGAL expression on the surface of sGAG-targeted iBMDMs (Figure 1.6B and 1.6C). We next directly examined surface levels of the ITGB2/ITGAL heterodimer (LFA-1) and found significantly reduced expression on the surface of sGAG-targeted iBMDMs (Figure 1.6D and 1.6E). Taken together these data suggest that sGAGs modulate the surface expression of key integrins that contribute to Mab uptake by macrophages.

FIGURES

Figure 1.1. Early interactions with fluorescent *Mycobacterium abscessus* and macrophages can be detected by flow cytometry. (**A**) The optical density of control or mEmerald transformed *M. abscessus* ATCC-19977 was monitored over 48 hours in 7H9 broth in the presence or absence of Rifampicin (128 µg/ml). (**B-D**) iBMDMs from C57BL6J mice were infected with increasing MOI (5-20) of mEmerald M. abscessus for six hours. Flow cytometry was used to measure (**B**) the percent of cells that were infected (mEmerald+) and (**C**) the mean fluorescence intensity of infected cells. (**D**) Representative flow cytometry plots gated on live and single cells are shown for each MOI. Data are from one of three independent experiments. (**E-F**) iBMDMs from C57BL6/J mice were infected with mEmerald *M. abscessus* at an MOI of 5 for two, four or six hours. (**E**) Flow cytometry was used to measure the percent of cells that were infected (mEmerald+). **(F)** Shown are representative flow cytometry plots gated on live and single cells for each time point. All results shown are representative results from one of three independent experiments. ****p<.0001 ***p<.001 by one-way ANOVA with Dunnett's multiple comparison test.

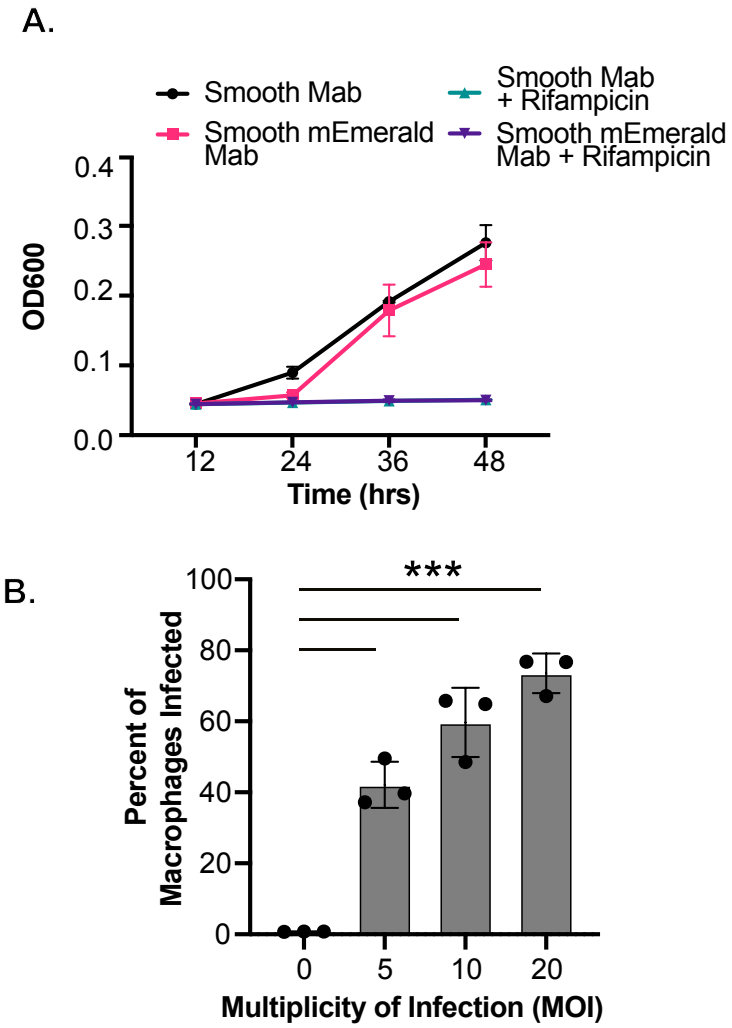

Figure 1.1 (cont'd)

C.

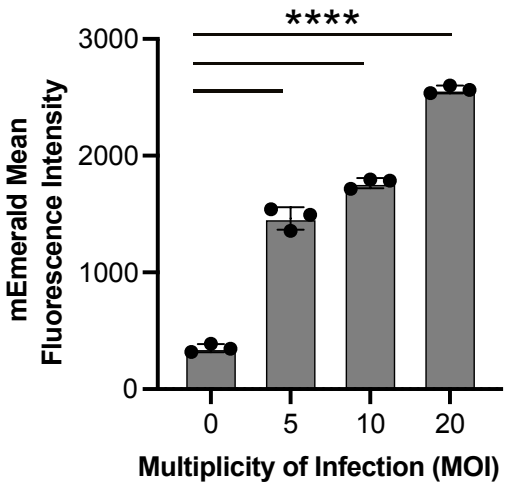

D.

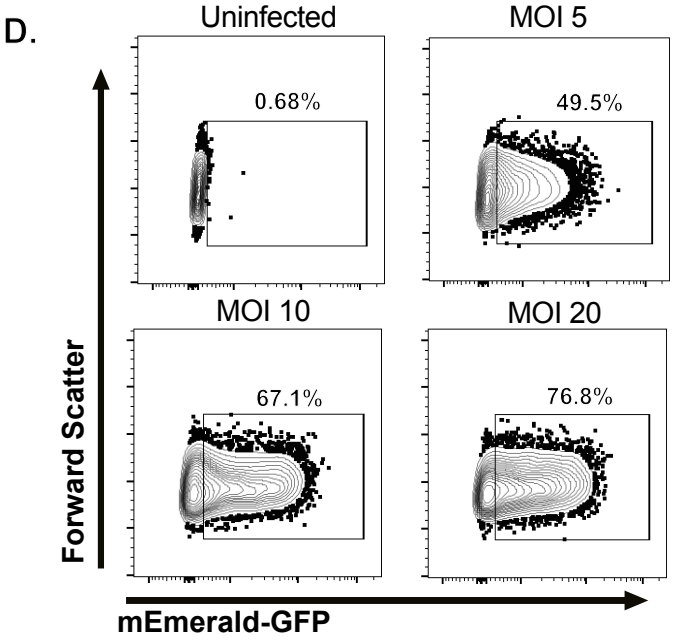

Figure 1.1 (cont'd)

E.

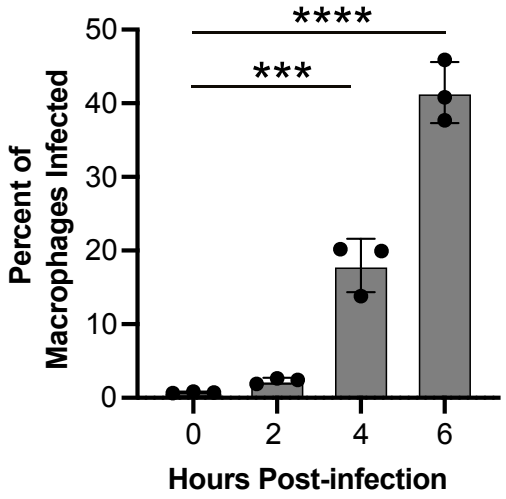

F.

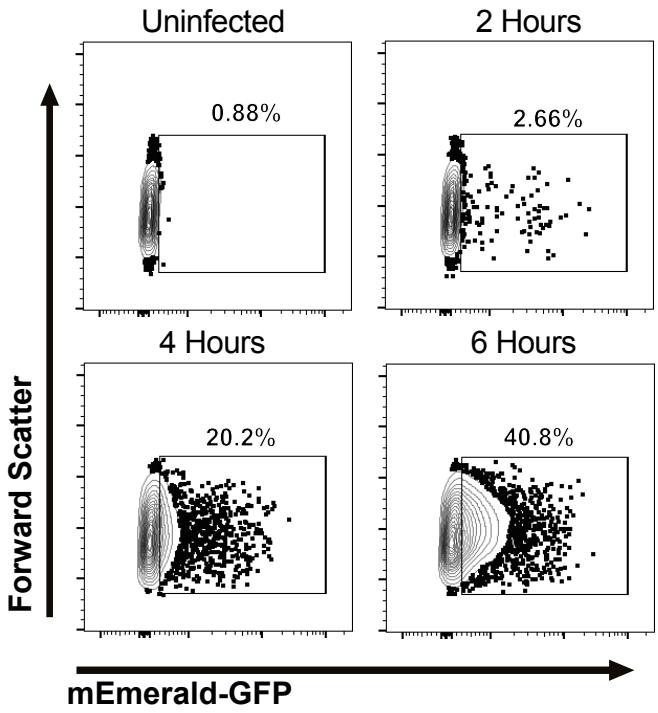

Figure 1.2. Genome-wide loss-of-function screen in iBMDMs identifies host genes required for uptake of *M. abscessus.* (**A**). iBMDMs were treated with DMSO or Cytochalasin D (10µg/ml or 20µg/ml) for two hours then infected with mEmerald *M. abscessus* at an MOI of 5 for four hours. The percent uptake was quantified by flow cytometry. Results are normalized to the mean percent uptake of the NTC + DMSO condition (**B**) Shown are representative flow cytometry plots gated on live single cells for each treatment. (**C**) A schematic of the genome-wide screen to identify host genes that are required for *M. abscessus* uptake by macrophages. A genome wide CRISPR-Cas9 library generated in Cas9+ iBMDMs with sgRNAs from the Brie library (4 sgRNAs per gene) was infected with mEmerald *M. abscessus* for four hours and mEmerald+ and mEmerald- populations were isolated by FACS. The representation of sgRNAs in each population were determined by sequencing. Figure made in Biorender. (**D**) Shown is the score determined by the alpha-robust rank algorithm (α-RRA) in MAGeCK for each gene in the CRISPR-Cas9 library that passed filtering metrics from three independent screen replicates. Highlighted genes represent known host factors that contribute to uptake of pathogens. (**E**) Cas9+ iBMDMs targeted with the indicated sgRNAs for candidates (2 per candidate gene) were infected with mEmerald *M. abscessus* for 4 hours at an MOI of 5. The uptake of M. abscessus was quantified by flow cytometry. These data are normalized to the mean percent of uptake of *M. abscessus* by non-targeting control cells. The results are representative of at least three independent experiments. ***p<.001 ** p<.01 by one-way ANOVA with Dunnett's multiple comparison test. For the data in panel 1.2E each candidate sgRNA is p<.001 compared to the NTC.

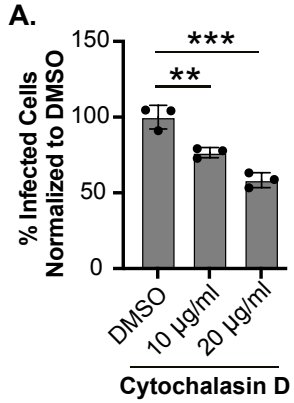

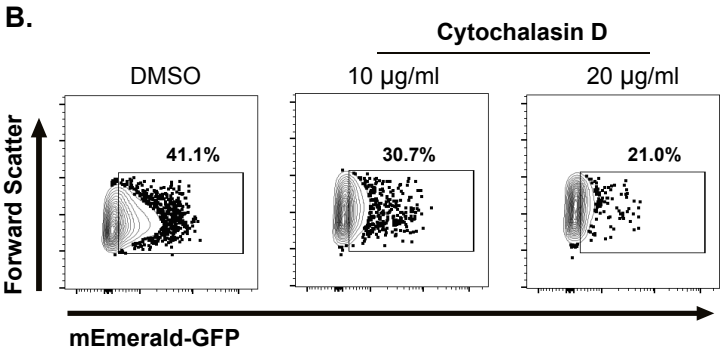

Figure 1.2 (cont'd)

C.

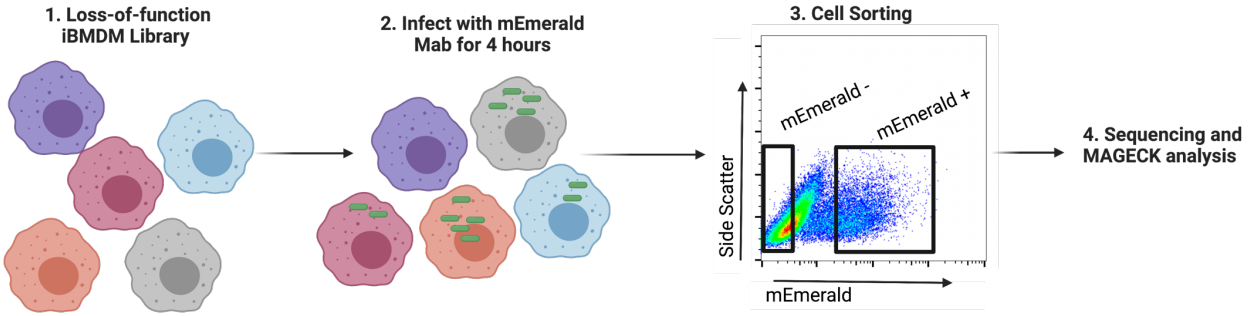

D.

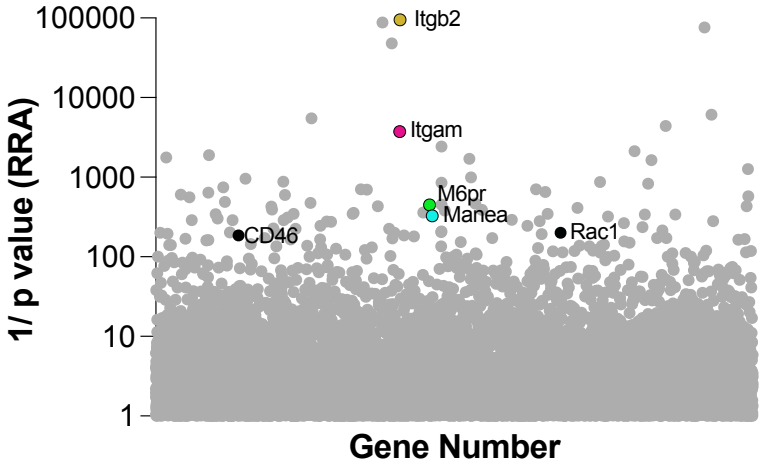

E.

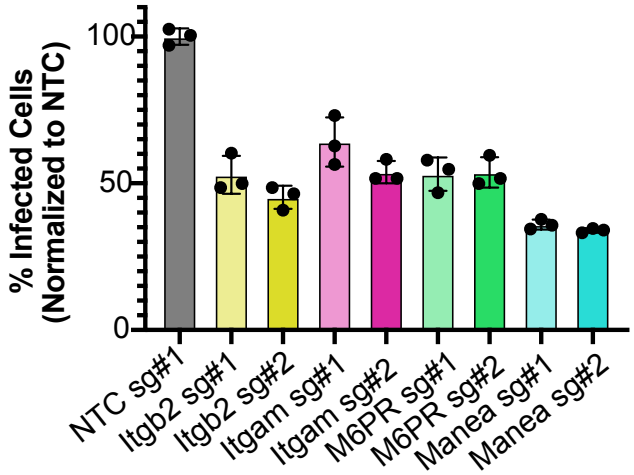

Figure 1.3. Sulfated glycosaminoglycans are required for effective uptake of *M. abscessus* by macrophages. (**A**) Gene set enrichment analysis was used to identify enriched pathways from the ranked forward genetic screen. Shown is a leading-edge analysis plot representing a top enriched KEGG pathway related to glycosaminoglycan biosynthesis. (**B**) The α-RRA ranking of sGAG biosynthesis related genes identified in the genome-wide screen highlighted as blue dots. (**C**) Total sGAGs were quantified in sgNTC, sgUGDH, sgB3GAT3 and sgB4GALT7 iBMDMs and normalized to total protein content. Shown is a representative result from four independent experiments. (**D**) sgNTC, sgUGDH, sgB3GAT3 and sgB4GALT7 iBMDMs were infected with mEmerald *M. abscessus* at increasing MOI for four hours then the percent infected cells were quantified by flow cytometry. Shown is the percent of infected cells normalized to the mean of the uptake of NTC at each MOI. These results are representative of four independent experiments. (**E**) Shown is a representative flow cytometry plot gated on live and single cells for the indicated genotypes at an MOI of 5. ***p<.001 **p<.01 by one-way ANOVA with Dunnett's multiple comparison test.

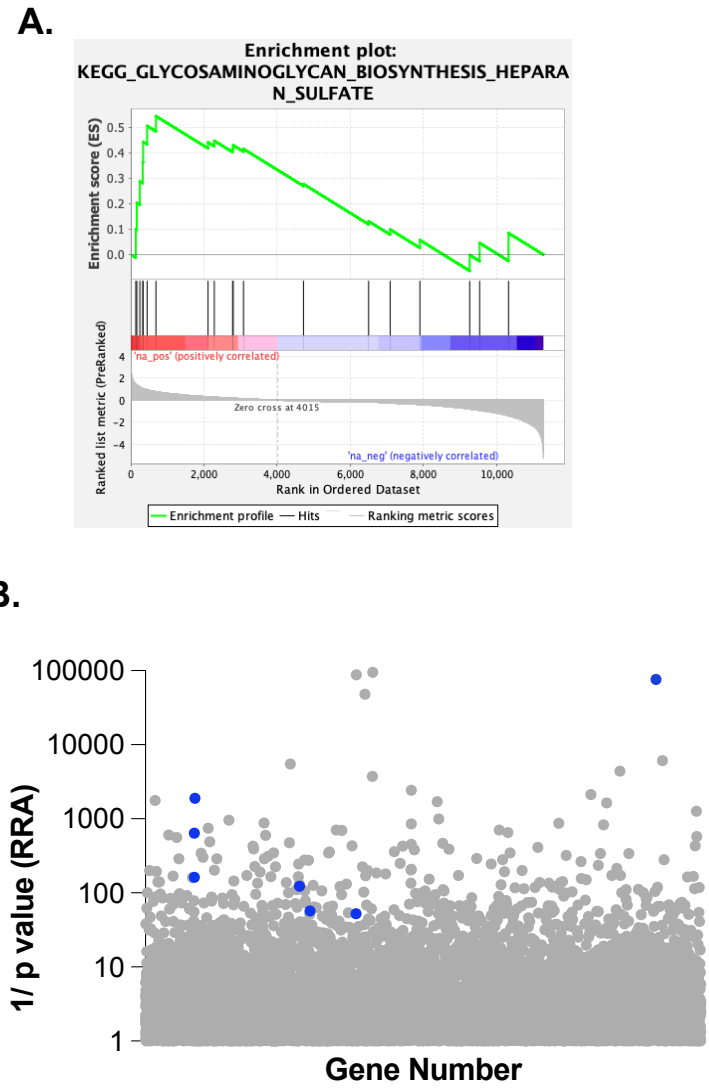

Figure 1.3 (cont'd)

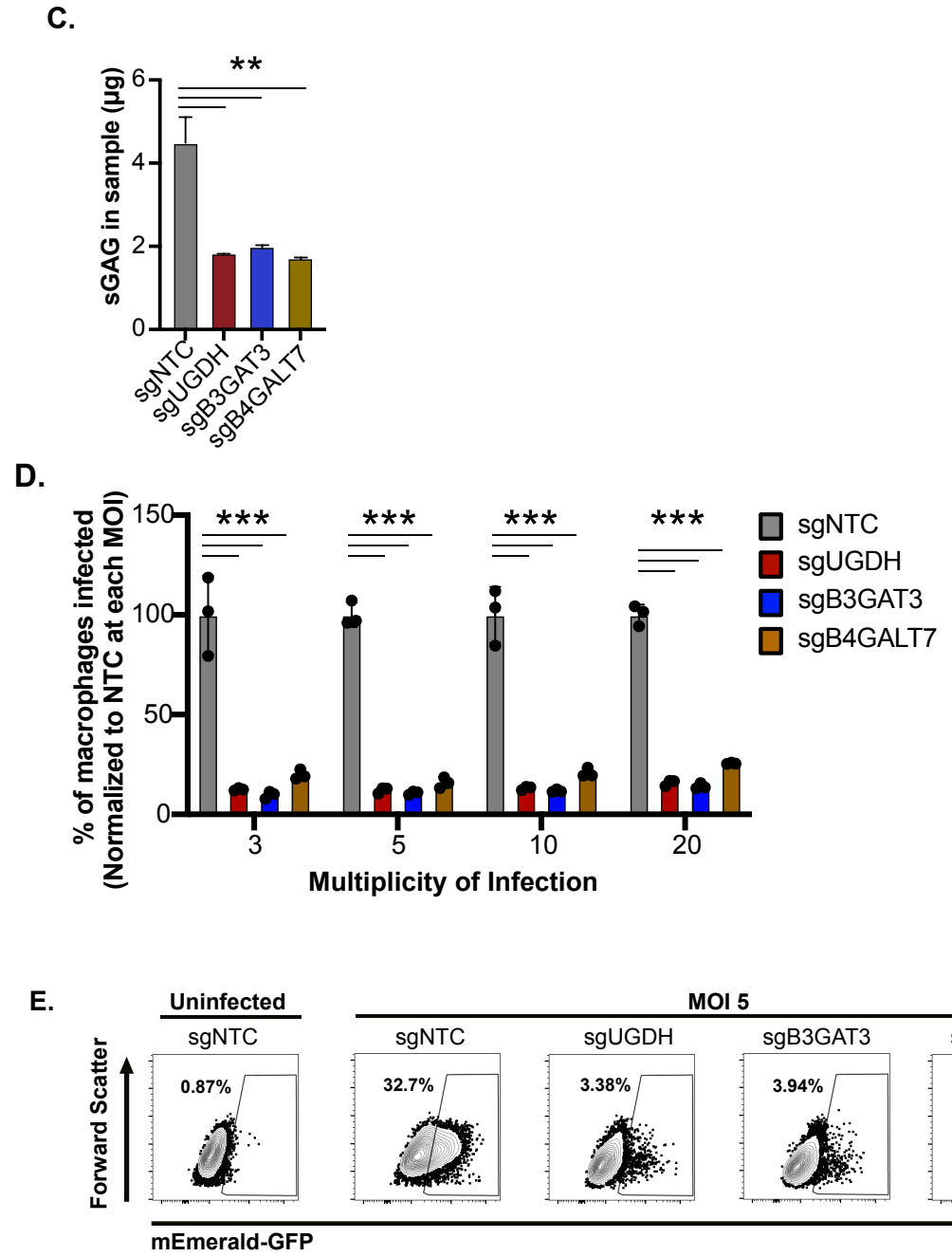

Figure 1.4. Rough variants of *M. abscessus* require sGAGs for efficient uptake by macrophages. (**A**) The optical density of control or mEmerald transformed rough variant of *M. abscessus* ATCC-19977 was monitored over 48 hours in 7H9 broth in the presence or absence of Rifampicin (128 µg/ml). (**B**) iBMDMs from C57BL6/J mice were infected with increasing MOI (5- 20) of mEmerald rough variant of *M. abscessus* for four hours and flow cytometry was used to measure the percent of cells that were infected (mEmerald+). Shown are representative flow cytometry plots gated on live and single cell for an MOI of five. (**C**) The percent of macrophages infected with rough Mab and (**D**) the mean fluorescence intensity of infected cells at the indicated MOIs. (**E**) sgNTC, sgUGDH, sgB3GAT3 and sgB4GALT7 iBMDMs were infected with mEmerald rough variant of *M. abscessus* at increasing MOIs for four hours then the percent uptake of cells was quantified by flow cytometry. Shown is a representative flow cytometry plot gated on live and single cells for the indicated genotypes infected at an MOI of 5. (**F**) Shown is the percent of infected cells normalized to the mean of the percent uptake for the NTC at each MOI. Results in (**A-F**) are all representative of at least three independent experiments. ***p<.001 **p<.01 by one-way ANOVA with Dunnett's multiple comparison test.

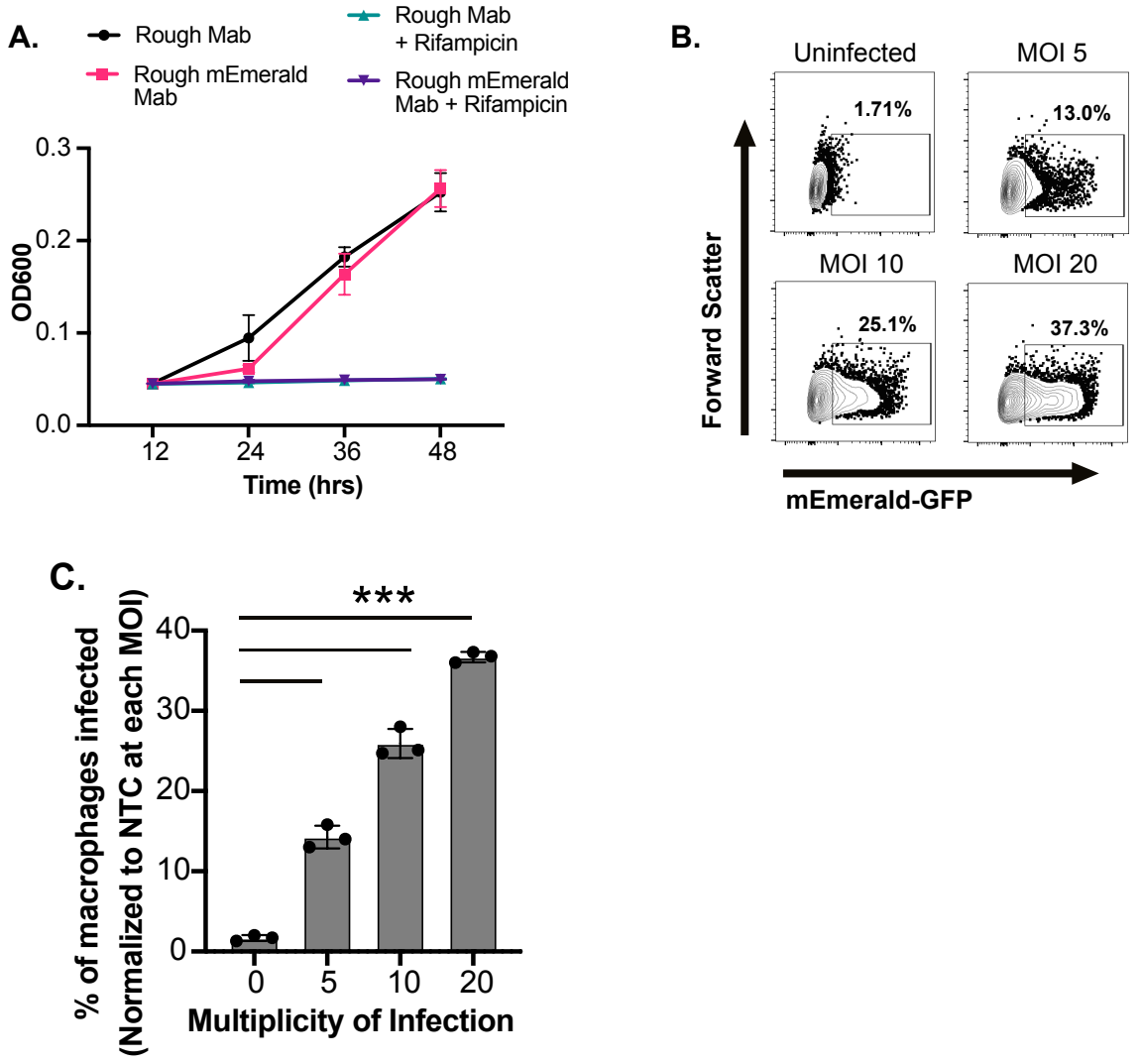

Figure 1.4 (cont'd)

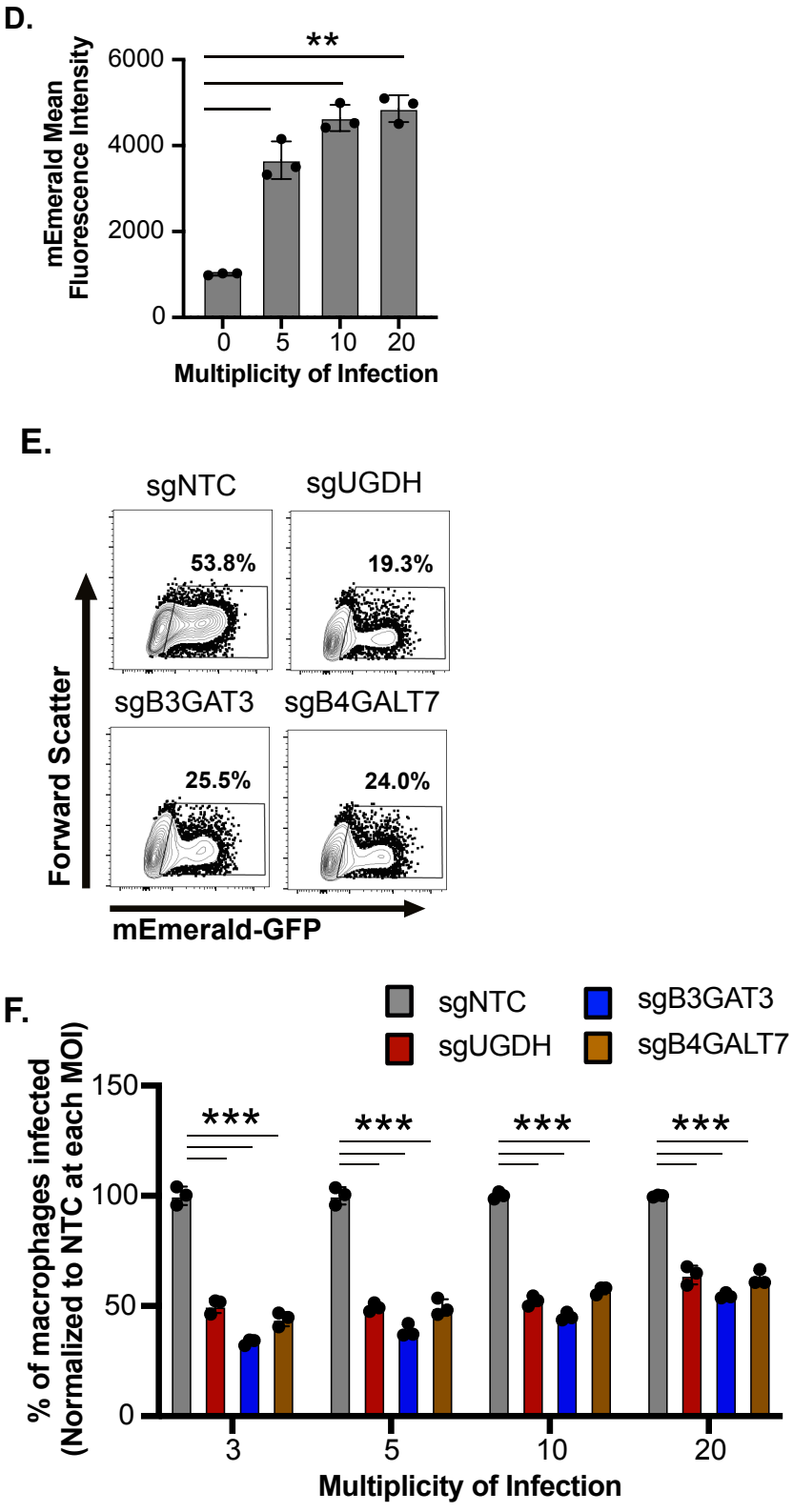

Figure 1.5. sGAGs do not alter general macrophage phagocytosis mechanisms and require viable bacteria to contribute to uptake. (**A**) Yellow-green-labeled latex beads were added at increasing concentrations (Bead:Cell ratio 3-50) to sgNTC, sgUGDH, sgB3GAT3 and sgB4GALT7 iBMDMs for four hours then the percent of cells with beads was quantified by flow cytometry. Shown is the percent of cells with beads normalized to the mean of the percent uptake of NTC at each concentration. (**B**) Shown are representative flow cytometry plots gated on live and single cells for the indicated genotypes treated with a bead:cell ratio of 5. (**C**) The indicated genotypes of iBMDMs were infected with mEmerald E. coli for four hours at an MOI of five. The percent infected cells were quantified by flow cytometry and were normalized to the mean of the percent uptake of NTC. (**D**) Shown are representative flow cytometry plots gated on live and single cells for the indicated genotyped infected with *E. coli* at an MOI of 5 (**E**) Smooth or (**F**) rough variants of mEmerald *M. abscessus* were incubated with heat-killed or active fetal bovine serum for thirty minutes then used to infect iBMDMs of the indicated genotypes for four hours at an MOI of five. The percent infected cells were quantified by flow cytometry and were normalized to the mean of sgNTC uptake in heat-killed serum for either smooth or rough variants. (**G**) iBMDMs of the indicated genotypes were treated with DMSO or Cytochalasin D (10µg/ml or 20µg/ml) for two hours then infected with mEmerald *M. abscessus* smooth or (**H**) rough variants at an MOI of 5 for four hours. The percent uptake was quantified by flow cytometry and all samples were normalized to the mean of sgNTC uptake in DMSO for either smooth or rough variants. All results are representative of at least 3 independent experiments with similar results. ***p<.001 **p<.01 by two-way ANOVA with Dunnett's multiple comparison test.

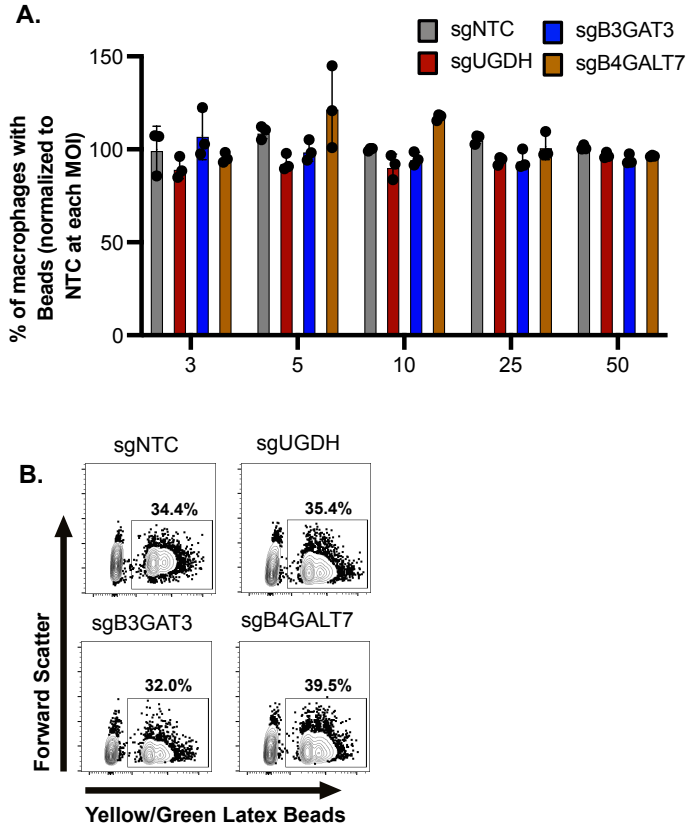

Figure 1.5 (cont'd)

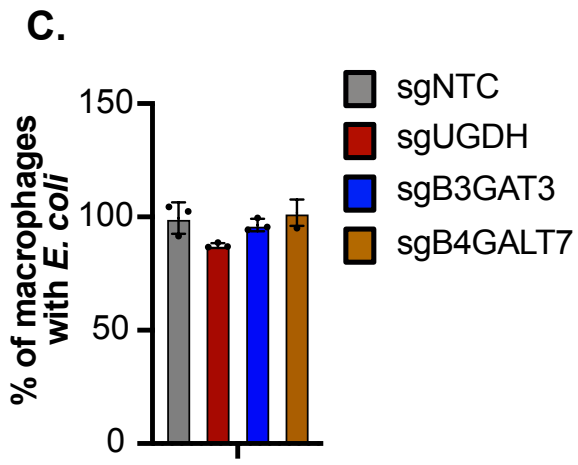

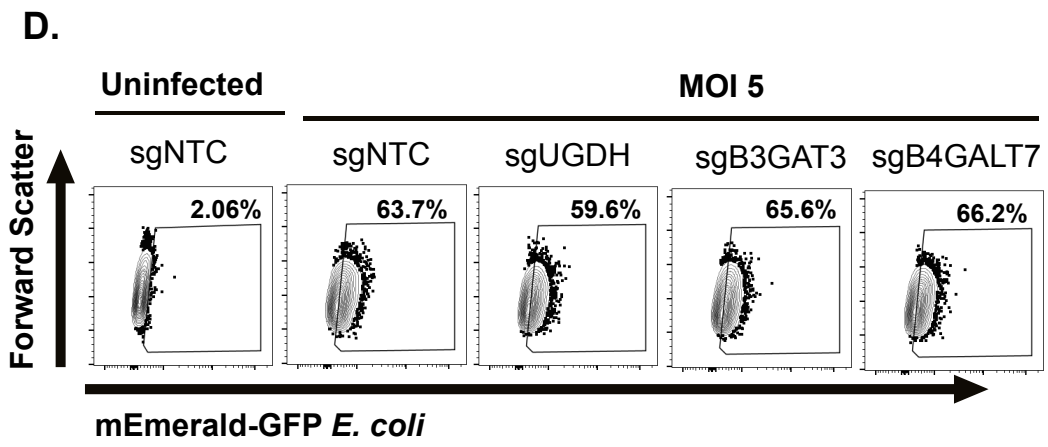

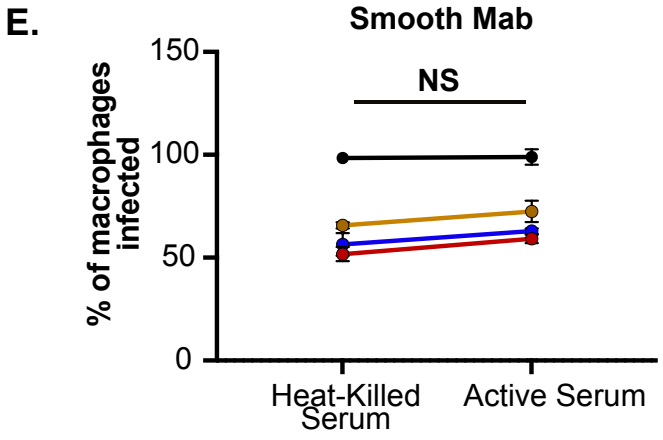

Figure 1.5 (cont'd)

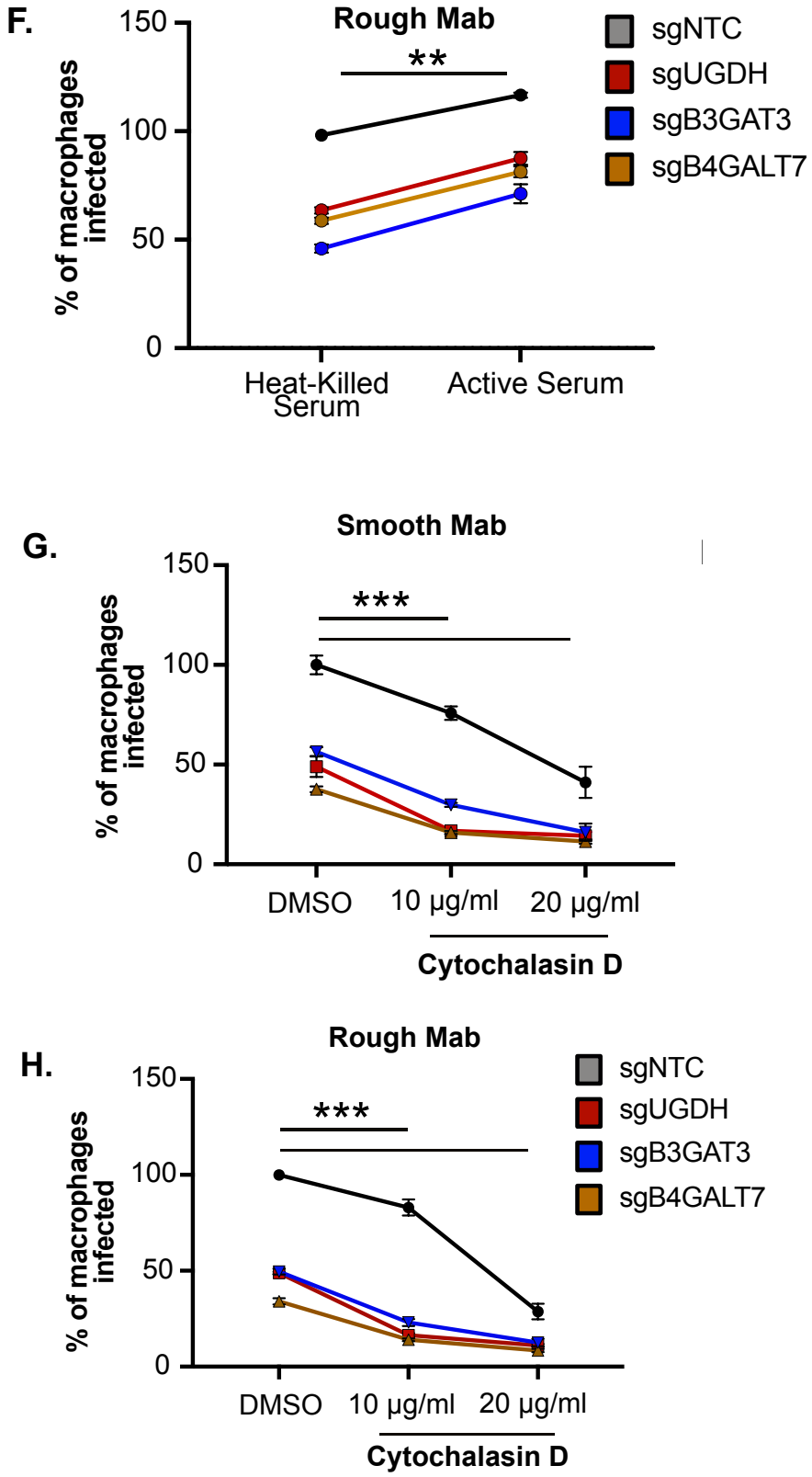

Figure 1.6. Reduced sGAGs results in lower surface expression of integrins on macrophages. (**A**) RNA was isolated from sgNTC, sgUGDH, sgB3GAT3 and sgB4GALT7 iBMDMs and the expression of Itgb2, Itgal and Itgam relative to Gapdh was quantified by qRT-PCR. (**B**) The surface expression of ITGB2, ITGAL and ITGAM was quantified in NTC and sGAG-targeted iBMDMs by flow cytometry. Shown is the mean fluorescence intensity of each integrin and (**C**) a representative histogram for each sGAG-targeted gene for each integrin overlaid with NTC is shown. (**D**) The surface expression of ITGB2-ITGAL heterodimers (LFA-1) were quantified on NTC and sGAG-targeted iBMDMs. Shown is the quantification of the mean fluorescence intensity and (**F**) a representative histogram for each iBMDM genotype overlaid with NTC. All results are representative of at least 2-3 independent experiments with similar results. ***p<.001 **p<.01 by one-way ANOVA with Dunnett's multiple comparison test.

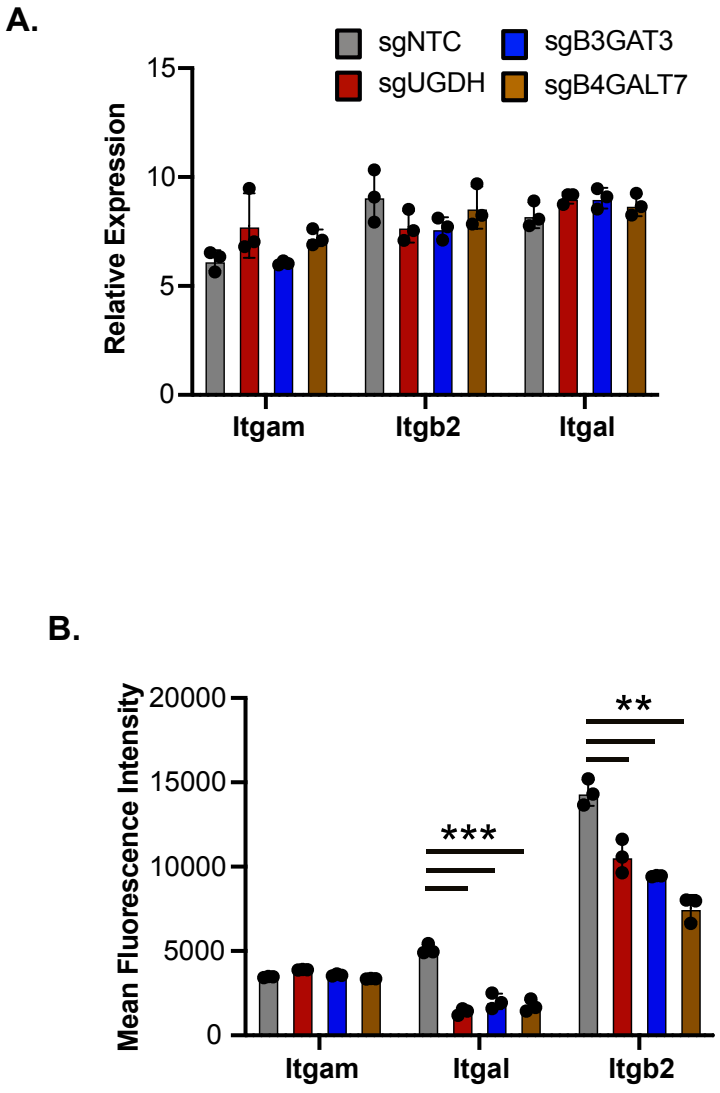

Figure 1.6 (cont'd)

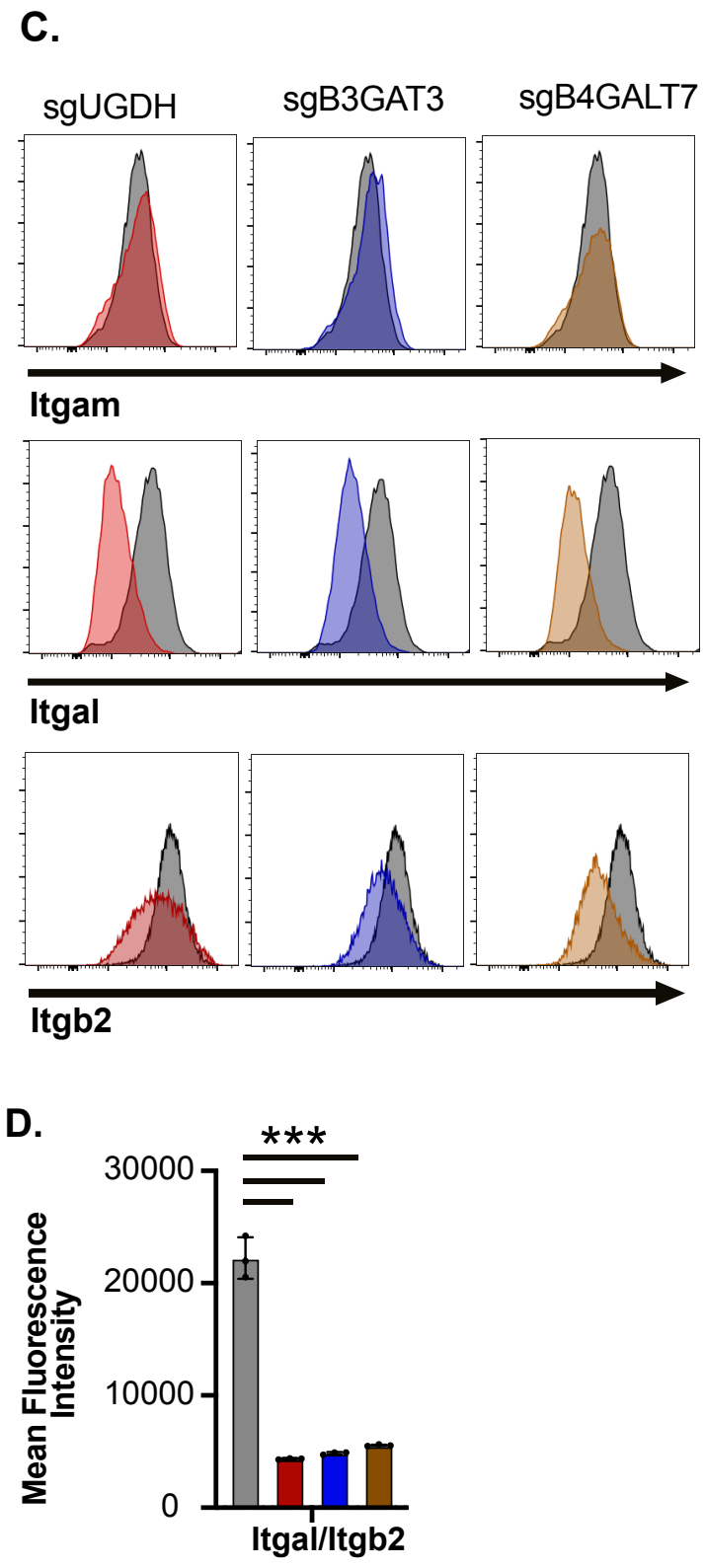

Figure 1.6 (cont'd)

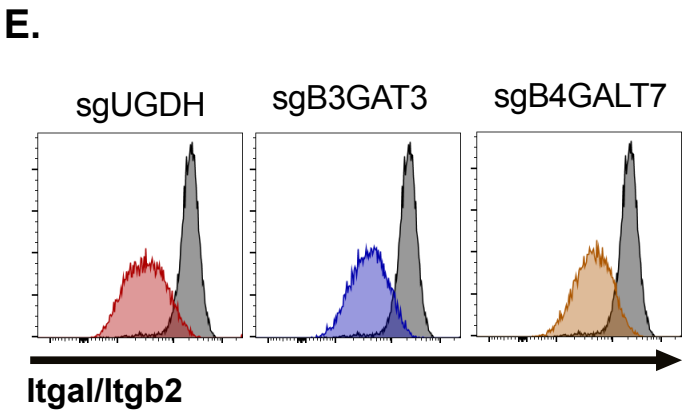

DISCUSSION

Infections with *M. abscessus* are on the rise globally and their recalcitrance to antibiotic therapy is driving treatment failure [44-46]. Designing effective treatments against Mab, including host-directed therapies, will require a fundamental understanding of critical host-Mab interactions that occur during infection. Here, we developed a Mab fluorescent reporter-based approach to investigate interactions of Mab with macrophages and conducted a forward genetic screen to globally identify host genes that are required for Mab uptake. Our screen identified many candidates including previously described players in pathogen uptake such as Itgb2, Itgam, Manea and M6pr [47, 48] which together with our validation highlight the robustness of this dataset and the strengths of the functional genetic approach.

As part of our bioinformatic analysis to uncover new pathways required for efficient Mab uptake, we identified a strong signature for the sGAG biosynthesis pathway. sGAGs are modified glycosaminoglycans, which consist of repeating polysaccharides attached to the cell surface and surface proteins [26]. We targeted three independent genes in the sGAG synthesis pathway that all resulted in decreased uptake of both smooth and rough Mab variants by macrophages. While sGAGs have previously been shown to modulate host-pathogen interactions in epithelial cells, very little is known about their role in macrophages [22-24]. We found that sGAGs did not affect latex bead or *E. coli* uptake, showing that general macrophage uptake mechanisms are intact in sGAG-targeted cells. In addition, Cytochalasin D treatment of sGAG-targeted macrophages further reduced Mab uptake, suggesting sGAGs contribute upstream of the actin polymerization required for Mab internalization. Together these data point towards a role for sGAGs in the adherence of Mab to macrophages. While many models suggest sGAGs modulate ionic interactions between pathogens and the cellular surface, our results suggest a

parallel mechanism by which sGAGs contribute to pathogen uptake [26]. In all sGAG-targeted iBMDMs we discovered a significant decrease in the surface expression of the integrins ITGB2 and ITGAL but no change in the mRNA expression. We propose that one previously overlooked function of sGAGs in pathogen uptake is maintaining the surface expression of critical receptors, including key integrins. How broadly sGAGs control the surface proteome of cells and if this function of sGAGs contributes to other host-pathogen interactions will be of great interest.

Multiple lines of evidence from our study point towards a central role for ITGB2 in the uptake of Mab. Not only was Itgb2 the number one hit in the genome-wide screen, but we found the top enriched pathway, sGAG-biosynthesis, directly modulates ITGB2 surface expression. ITGB2 is known to complex with different integrin alpha receptors to serve as a key trafficking molecule and complement receptor [49]. ITGB2, in complex with ITGAM, was previously shown to modulate LC3-associated phagocytosis (LAP) during *Listeria monocytogenes* infections and control the uptake of *Pseudomonas aeruginosa*, suggesting multiple uptake pathways intersect with ITGB2 [47, 50]. The identification of both Itgam and Itgb2 among the top candidates in the screen suggests a key role for this heterodimer in Mab uptake. ITGB2 also complexes with other integrins like ITGAL, yet the contribution of each of these distinct receptors in Mab uptake remains unknown and will be examined in the future [49]. While human and murine ITGB2 proteins are highly similar, it will be important to directly test the role of this integrin in Mab uptake in human macrophages [51]. In addition, investigating how Mab uptake by distinct receptors alters intracellular trafficking and/or bacterial control will better define key host-pathogen interactions during Mab infections.

How Mab mediates interactions with distinct macrophage uptake pathways remains unknown. Surface glycopeptidolipids (GPLs) are thought to contribute to macrophage infections

[52, 53]. However, given that both smooth and rough variants of Mab required sGAG dependent pathways for effective uptake, there must be GPL-independent mechanisms that contribute during infection. One interesting observation from our study was that rough variants are more susceptible to complement-mediated uptake than smooth variants. This suggests a model where GPL evade complement-mediated uptake which may modulate Mab survival. Several other Mab factors have been associated with macrophage infection, including the ATPase EccB4 and glycosyl-diacylated-nondecyl-diols (GDND), but the direct role of these genes in macrophage uptake remain unknown [12, 54-56]. More broadly dissecting Mab determinants of macrophage infection will require unbiased bacterial genetic approaches, such as transposon-based approaches that were recently developed in Mab [10, 12]. This approach will link macrophage uptake pathways directly with specific Mab-encoded factors.

In addition to understanding how Mab adheres to macrophages, the role of sGAGs during lung infection is important to consider. While Mab is mostly associated with monocytes and macrophages *in vivo*, current mouse models to test Mab pathogenesis remain challenging [55, 57]. Sustained Mab infection in mice requires multiple immune deficiencies that disrupt normal host-pathogen interactions [57]. In addition, since sGAGs are essential to development, understanding how sGAGs contribute to *in vivo* disease will require the generation of conditional knockout animals in immune knockout backgrounds [58]. While improved Mab *in vivo* models are being developed, the approach described here highlights a framework for leveraging unbiased genetic approaches to glean important mechanistic understanding of host Mab interactions.

Altogether, we optimized a host genetic platform to define important macrophage pathways during Mab infection. By coupling a brightly fluorescent Mab reporter with a genome-

wide knockout macrophage library, we are positioned to rapidly screen for diverse phenotypes related to macrophage-Mab interactions. Here, we leveraged this approach to dissect Mab uptake during early infection. Yet, this same approach can be used to understand host pathways that control Mab growth or contribute to macrophage cell death. Thus, our host focused functional genetic approach will broadly identify potential host-directed therapeutic targets, with the goal of improving treatment success during Mab infection.

MATERIALS AND METHODS

Mab culture conditions, generation of fluorescent reporter, and growth assays.

Isogenic pairs of smooth and rough Mab (ATCC 19977) were used throughout this study. The Mab or *E. coli* mEmerald strains were built by transforming pmV261 hsp60::mEmerald into either the smooth or rough Mab variant by electroporation or DH5α *E. coli* by heat shock followed by selection on zeocin. All Mab cultures were grown aerobically in Middlebrook 7H9 medium supplemented with 10% Middlebrook OADC (oleic acid, dextrose, catalase, and bovine albumin) at 37°C. mEmerald GFP-expressing strains were propagated in medium containing 5μg/ml zeocin (Invivogen).

To quantify bacterial growth, non-fluorescent and mEmerald GFP-Mab single cell suspensions were inoculated in 7H9 at starting concentration of $5x10^5$ bacteria/ml. To examine antibiotic killing, rifampicin was included at a final concentration of 128 μg/ml. Optical density was quantified by measuring the absorbance at 600nm on a Tecan Spark 20M plate reader at the indicated timepoints.

Cell culture.

J2-virus immortalized murine bone marrow derived macrophages (iBMDMs) and Cas9+ iBMDMs were maintained in Dulbecco's Modified Eagle Medium (DMEM; Hyclone) supplemented with 10% heat inactivated fetal bovine serum (FBS; Seradigm) as previously described (42). All macrophage cell lines were incubated in 5% CO2 at 37°C.

Macrophage infections and uptake assays.

Single cell Mab or *E. coli* suspensions were prepared by resuspending logarithmic phase bacteria in DMEM with 10% heat inactivated FBS (Seradigm) followed by a soft spin (800g) to pellet large bacterial clumps. The supernatant was then used to infect macrophages, seeded at

$5x10^5$ /well in a 12-well plate, at the indicated MOIs for the indicated time points (2-6 hours). Following infection, macrophages were washed with PBS, lifted from plates by scrapping, then fixed in 4% paraformaldehyde. Macrophage uptake was quantified using the BD LSRII flow cytometer (BD Biosciences) at the Michigan State University Flow Cytometry Core. Live and single macrophages were identified using forward and side scatter and the number of infected cells was determined by the fluorescence in the GFP channel. All experiments include an uninfected control to set gates for uptake quantification during analysis that was performed using FlowJo v10. For complement-mediated uptake experiments mEmerald Mab was first incubated in heat-inactivated or active FBS for thirty minutes prior to macrophage infections. For actin polymerization inhibitor experiments, cells were treated with DMSO or Cytochalasin D (Cayman Chemicals) for 2 hours prior to infection.

For the bead uptake assay, 1µm carboxylate-modified polystyrene latex beads expressing yellow-green fluorescence (Sigma-Aldrich) were diluted in PBS to $5x10^8$ beads per ml. Beads were incubated with iBMDMs at the indicated number of latex beads per macrophage for four hours. Following bead exposure, macrophages were washed with PBS and fixed in 4% paraformaldehyde solution. The percent uptake of yellow-green fluorescence latex beads was quantified by flow cytometry as described above.

CRISPR screen and analysis.

Mouse Brie CRISPR knockout pooled library was a gift from David Root and John Doench (Addgene #73633) (42) and infected with our smooth mEmerald-GFP Mab reporter strain at an MOI of five for four hours. Following the infection, macrophages were washed with PBS then fixed with 4% paraformaldehyde. Infected library was then sorted using a BioRad S3e cell sorter to isolate mEmerald+ and mEmerald- macrophages. $1.5\text{-}2.5x10^7$ cells were sorted into

each bin from triplicate experiments. Genomic DNA was isolated from each sorted population using Qiagen DNeasy kits after reversing DNA crosslinks following a 55°C incubation overnight. Amplification of sgRNAs by PCR was performed as previously described using Illumina compatible primers from IDT (42) and amplicons were sequenced on an Illumina NextSeq 500 at the Genomics Core at Michigan State University.

Sequenced reads were first trimmed to remove any adapter sequence and to adjust for the p5 primer stagger. We used model-based analysis of genome-wide CRISPR-Cas9 knockout (MAGeCK) to map reads to the sgRNA library index without allowing for any mismatch. Subsequent sgRNA counts were median normalized to control sgRNAs in MAGeCK to account for variable sequencing depth. To test for sgRNA and gene enrichment, we used the "test" command in MAGeCK to compare the distribution of sgRNAs in the GFP+ and GFP- bins. The MAGeCK output Gene Summary provided a ranked list of genes significantly underrepresented in the mEmerald+ bin based on 4 independent sgRNAs that was used to curate the candidate gene list.

CRISPR-targeted knockouts.

Individual sgRNAs were cloned as previously described using sgOPTI that was a gift from Eric Lander (Addgene plasmid no. 85681) (42). In short, annealed oligos containing the sgRNA targeting sequence were phosphorylated, then cloned into a dephosphorylated and BsmBI (New England Biolabs) digested sgOPTI. To facilitate rapid and efficient generation of sgRNA plasmids with different selectable markers, we used sgOPTI-Blasticidin-Zeocin (BZ) and sgOPTI Puromycin-Ampicillin (PA) as previously described (42). The simultaneous use of sgOPTI-BZ and sgOPTI-PA plasmids allowed for pooled cloning in which a given sgRNA was ligated into a mixture of BsmBI-digested plasmids. Successful transformants for each plasmid

were by plating on ampicillin or zeocin in parallel. Next, two sgRNA-plasmid constructs per gene were packaged into lentivirus as previously described (42), then used to transduce Cas9+ iBMDMs. Transductants were selected with blasticidin and/or puromycin then genomic DNA was isolated and PCR was used to amplify edited regions and sent for Sanger Sequencing (Genewiz). The resultant ABI files were used for Tracking of Idels by Decomposition (TIDE) analysis to assess the frequency and size of indels in each population compared to control macrophages (59). Three sgRNAs were targeted per gene and one targeted line was selected for follow-up studies with editing efficiency 60%-95% for each gene. sgRNA sequences and primers for Tide analysis are included in Table 1.3.

Quantification of sulfated glycosaminoglycans.

Sulfated Glycosaminoglycans (sGAGs) were isolated following the Blyscan Sulfated Glycosaminoglycan Assay (BioVision). In short, macrophages were washed with PBS, then 1ml of Papain Extraction Reagent containing 1mg/ml of Papain (Sigma-Aldrich) was added. Plates were incubated in 5% CO2 at 37°C for 1 minute. Cell Suspensions were transferred to 1.5ml microcentrifuge tubes and immediately placed in an ice-water bath. To extract sGAGs, 200µl of cell suspension was transferred to a 1.5ml microcentrifuge tube and incubated at 65°C for three hours.

sGAG were then quantified using the Blyscan Sulfated Glycosaminoglycan Assay Protocol (BioVision). Briefly, 25µl of test sample was transferred into a 1.5ml microcentrifuge tube. Reagent blanks, sGAG standards and test samples were prepared according to the Blyscan Sulfated Glycosaminoglycan Assay General Protocol and adjusted to a 100µl final volume. To stain sGAGs, 1ml of Blyscan Dye Reagent (BioVision) was added to each tube, then tubes were placed in a gentle mechanical shaker for 30 minutes at room temperature. To pellet stained

sGAGs, tubes were centrifuged at 13,000xg for 10 minutes, then supernatant was discarded. To release the recovered sGAGs, 500µl of Dissociation Reagent (BioVision) was added to each tube and vortexed until pellets were dissolved. 200µl of reagent blanks, sGAG standards and test samples were transferred to a 96-well plate and absorbance readings at 656nm were obtained from an Agilent BioTek Synergy H1 Hybrid multi-Mode Plate Reader.

RNA isolation and quantitative real-time PCR.

Macrophages were resuspended in 500µL of TRIzol reagent (Life Technologies) and incubated for 5 minutes at room temperature. 100µL of chloroform was added to the homogenate, vortexed and centrifuged at 10,000xg for 18 minutes at 4°C to separate nucleic acids. The clear, RNA containing layer was removed and combined with equal parts ethanol. This mixture was placed into a collection tube and protocols provided by the Zymo Research Direct-zol RNA extraction kit were followed. Quantity and purity of the RNA were checked using a NanoDrop and diluted to 5ng/µL in nuclease-free water.

PCR amplification of the RNA was completed using the One-step Syber Green RT-PCR kit (Qiagen). 25ng of total RNA was added to a master mix reaction of the provided RT mix, Syber green, gene specific primers (5uM of forward and reverse primer), and nuclease-free water. For each biological replicate (triplicate), reactions were conducted in technical triplicates in 96-well plates. PCR product was monitored using the QuantStudio3 (ThermoFisher). The number of cycles needed to reach the threshold of detection (Ct) was determined for all reactions. The mean CT of each experimental sample in triplicate was determined. The average mean of glyceraldehyde 3-phosphate dehydrogenase (GAPDH) was subtracted from the experimental sample mean CT for each gene of interest (dCT).

Bioinformatics analysis.

Gene set enrichment analysis (GSEA) was used to identify enriched pathways in the MAGeCK analyzed dataset based on the full ranked list as done previously. For GSEA analysis, the "GSEA Preranked" function was used to complete functional enrichment using default settings for Kyoto Encyclopedia of Genes and Genomes (KEGG) and Gene Ontology terms. DAVID analysis was used to identify enriched pathways within the positive regulators of Mab uptake. Using the robust rank aggregation (RRA) the top enriched positive regulators (2-fold change with at least 3 sgRNAs) were used as a "candidate list". Functional analysis and functional annotation analysis were completed, and top enriched pathways and protein families were identified.

Data availability.

Raw sequencing data in FASTQ and processed formats are available for download from NCBI Gene Expression Omnibus (GEO) accession number GSE221413.

Statistical analysis.

Statistical analysis and data visualization were performed using Prism version 9 (GraphPad Software) or Biorender, as indicated in figure legends. Data are presented, unless otherwise indicated, as the mean ± SD and individual data points are shown for each experiment. For parametric data, one-way or two-way ANOVA followed by Tukey's or Dunnett's multiple comparisons test were used to identify significant differences between multiple groups.

REFERENCES

1. Daley CL, Iaccarino JM, Lange C, Cambau E, Wallace RJ, Andrejak C, Böttger EC, Brozek J, Griffith DE, Guglielmetti L, Huitt GA, Knight SL, Leitman P, Marras TK, Olivier KN, Santin M, Stout JE, Tortoli E, van Ingen J, Wagner D, Winthrop KL. 2020. Treatment of nontuberculous mycobacterial pulmonary disease: an official ATS/ERS/ESCMID/IDSA clinical practice guideline. Clin Infect Dis 71:e1–e36. https://doi.org/10.1093/cid/ciaa241.

2. Victoria L, Gupta A, Gomez JL, Robledo J. 2021. Mycobacterium abscessus complex: a review of recent developments in an emerging pathogen. Front Cell Infect Microbiol 11:659997. https://doi.org/10.3389/fcimb.2021 .659997.

3. Roux A-L, Viljoen A, Bah A, Simeone R, Bernut A, Laencina L, Deramaudt T, Rottman M, Gaillard J-L, Majlessi L, Brosch R, Girard-Misguich F, Vergne I, de Chastellier C, Kremer L, Herrmann J-L. 2016. The distinct fate of smooth and rough Mycobacterium abscessus variants inside macrophages. Open Biol 6:160185. https://doi.org/10.1098/rsob.160185.

4. Rominski A, Roditscheff A, Selchow P, Bottger EC, Sander P. 2017. Intrinsic rifamycin resistance of Mycobacterium abscessus is mediated by ADP-ribosyltransferase MAB_0591. J Antimicrob Chemother 72:376–384. https://doi.org/ 10.1093/jac/dkw466.

5. Hurst-Hess K, Rudra P, Ghosh P. 2017. Mycobacterium abscessus WhiB7 regulates a species-specific repertoire of genes to confer extreme antibiotic resistance. Antimicrob Agents Chemother 61. https://doi.org/10.1128/AAC .01347-17.

6. Nash KA, Brown-Elliott BA, Wallace RJ, Jr. 2009. A novel gene, erm(41), confers inducible macrolide resistance to clinical isolates of Mycobacterium abscessus but is absent from Mycobacterium chelonae. Antimicrob Agents Chemother 53:1367–1376. https://doi.org/10.1128/AAC.01275-08.

7. Howard ST, Rhoades E, Recht J, Pang X, Alsup A, Kolter R, Lyons CR, Byrd TF. 2006. Spontaneous reversion of Mycobacterium abscessus from a smooth to a rough morphotype is associated with reduced expression of glycopeptidolipid and reacquisition of an invasive phenotype. Microbiology (Reading) 152:1581–1590. https://doi.org/10.1099/mic.0.28625-0.

8. Pawlik A, Garnier G, Orgeur M, Tong P, Lohan A, Le Chevalier F, Sapriel G, Roux A-L, Conlon K, Honoré N, Dillies M-A, Ma L, Bouchier C, Coppée J-Y, Gaillard J-L, Gordon SV, Loftus B, Brosch R, Herrmann JL. 2013. Identification and characterization of the genetic changes responsible for the characteristic smooth-to-rough morphotype alterations of clinically persistent Mycobacterium abscessus. Mol Microbiol 90:612–629. https://doi.org/10 .1111/mmi.12387.

9. Medjahed H, Reyrat JM. 2009. Construction of Mycobacterium abscessus defined glycopeptidolipid mutants: comparison of genetic tools. Appl Environ Microbiol 75:1331–1338. https://doi.org/10.1128/AEM.01914-08.

10. Aguilo JI, Alonso H, Uranga S, Marinova D, Arbués A, de Martino A, Anel A, Monzon M, Badiola J, Pardo J, Brosch R, Martin C. 2013. ESX-1-induced apoptosis is involved in cell-to-cell spread of Mycobacterium tuberculosis. Cell Microbiol 15:1994–2005. https://doi.org/10.1111/cmi.12169.

11. Kim BR, Kim BJ, Kook YH, Kim BJ. 2019. Phagosome escape of rough Mycobacterium abscessus strains in murine macrophage via phagosomal rupture can lead to Type I interferon production and their cell-to-cell spread. Front Immunol 10:125. https://doi.org/10.3389/fimmu.2019.00125.

12. Gutierrez AV, Viljoen A, Ghigo E, Herrmann JL, Kremer L. 2018. Glycopeptidolipids, a double-edged sword of the Mycobacterium abscessus complex. Front Microbiol 9:1145. https://doi.org/10.3389/fmicb.2018.01145.

13. Akusobi C, Benghomari BS, Zhu J, Wolf ID, Singhvi S, Dulberger CL, Ioerger TR, Rubin EJ. 2022. Transposon mutagenesis in Mycobacterium abscessus identifies an essential penicillin-binding protein involved in septal peptidoglycan synthesis and antibiotic sensitivity. Elife 11:e71947. https://doi.org/ 10.7554/eLife.71947.

14. Viljoen A, Blaise M, de Chastellier C, Kremer L. 2016. MAB_3551c encodes the primary triacylglycerol synthase involved in lipid accumulation in Mycobacterium abscessus. Mol Microbiol 102:611–627. https://doi.org/10 .1111/mmi.13482.

15. Laencina L, Dubois V, Le Moigne V, Viljoen A, Majlessi L, Pritchard J, Bernut A, Piel L, Roux A-L, Gaillard J-L, Lombard B, Loew D, Rubin EJ, Brosch R, Kremer L, Herrmann J-L, Girard-Misguich F. 2018. Identification of genes required for Mycobacterium abscessus growth in vivo with a prominent role of the ESX-4 locus. Proc Natl Acad Sci U S A 115:E1002–E1011.

16. Shin D-M, Yang C-S, Yuk J-M, Lee J-Y, Kim KH, Shin SJ, Takahara K, Lee SJ, Jo E-K. 2008. Mycobacterium abscessus activates the macrophage innate immune response via a physical and functional interaction between TLR2 and dectin-1. Cell Microbiol 10:1608–1621. https://doi.org/10.1111/j.1462 -5822.2008.01151.x.

17. Rhoades ER, Archambault AS, Greendyke R, Hsu FF, Streeter C, Byrd TF. 2009. Mycobacterium abscessus Glycopeptidolipids mask underlying cell wall phosphatidyl-myo-inositol mannosides blocking induction of human macrophage TNF-alpha by preventing interaction with TLR2. J Immunol 183:1997–2007. https://doi.org/10.4049/jimmunol.0802181.

18. Kang PB, Azad AK, Torrelles JB, Kaufman TM, Beharka A, Tibesar E, DesJardin LE, Schlesinger LS. 2005. The human macrophage mannose receptor directs Mycobacterium

tuberculosis lipoarabinomannan-mediated Macrophage Genes Required for M. abscessus Uptake mSphere March/April 2023 Volume 8 Issue 2 10.1128/msphere.00663-22 15 phagosome biogenesis. J Exp Med 202:987–999. https://doi.org/10.1084/ jem.20051239.

19. Sever-Chroneos Z, Tvinnereim A, Hunter RL, Chroneos ZC. 2011. Prolonged survival of scavenger receptor class A-deficient mice from pulmonary Mycobacterium tuberculosis infection. Tuberculosis (Edinb) 91 Suppl 1:S69–74. https://doi.org/10.1016/j.tube.2011.10.014.

20. Means TK, Jones BW, Schromm AB, Shurtleff BA, Smith JA, Keane J, Golenbock DT, Vogel SN, Fenton MJ. 2001. Differential effects of a Toll-like receptor antagonist on Mycobacterium tuberculosis-induced macrophage responses. J Immunol 166:4074–4082. https://doi.org/10.4049/jimmunol.166 .6.4074.

21. Taban Q, Mumtaz PT, Masoodi KZ, Haq E, Ahmad SM. 2022. Scavenger receptors in host defense: from functional aspects to mode of action. Cell Commun Signal 20:2. https://doi.org/10.1186/s12964-021-00812-0.

22. Hirayama D, Iida T, Nakase H. 2017. The phagocytic function of macrophage-enforcing innate immunity and tissue homeostasis. Int J Mol Sci 19:92. https://doi.org/10.3390/ijms19010092.

23. Capila I, Linhardt RJ. 2002. Heparin-protein interactions. Angew Chem Int Ed Engl 41:391–412.

24. Rostand KS, Esko JD. 1997. Microbial adherence to and invasion through proteoglycans. Infect Immun 65:1–8. https://doi.org/10.1128/iai.65.1.1-8 .1997.

25. Thammawat S, Sadlon TA, Hallsworth PG, Gordon DL. 2008. Role of cellular glycosaminoglycans and charged regions of viral G protein in human metapneumovirus infection. J Virol 82:11767–11774. https://doi.org/10 .1128/JVI.01208-08.

26. Milewska A, Zarebski M, Nowak P, Stozek K, Potempa J, Pyrc K. 2014. Human coronavirus NL63 utilizes heparan sulfate proteoglycans for attachment to target cells. J Virol 88:13221–13230. https://doi.org/10.1128/JVI.02078-14.

27. Bucior I, Mostov K, Engel JN. 2010. Pseudomonas aeruginosa-mediated damage requires distinct receptors at the apical and basolateral surfaces of the polarized epithelium. Infect Immun 78:939–953. https://doi.org/10 .1128/IAI.01215-09.

28. Shi D, Sheng A, Chi L. 2021. Glycosaminoglycan-protein interactions and their roles in human disease. Front Mol Biosci 8:639666. https://doi.org/ 10.3389/fmolb.2021.639666.

29. Smock RG, Meijers R. 2018. Roles of glycosaminoglycans as regulators of ligand/receptor complexes. Open Biol 8:180026. https://doi.org/10.1098/rsob .180026.

30. Griffin FM, Griffin JA, Leider JE, Silverstein SC. 1975. Studies on the mechanism of phagocytosis: I. requirements for circumferential attachment of particlebound ligands to specific receptors on the macrophage plasma membrane. J Exp Med 142:1263–1282. https://doi.org/10.1084/jem.142.5.1263.

31. Kheir WA, Gevrey JC, Yamaguchi H, Isaac B, Cox D. 2005. A WAVE2-Abi1 complex mediates CSF-1-induced F-actin-rich membrane protrusions and migration in macrophages. J Cell Sci 118:5369–5379. https://doi.org/10 .1242/jcs.02638.

32. Scott CC, Dobson W, Botelho RJ, Coady-Osberg N, Chavrier P, Knecht DA, Heath C, Stahl P, Grinstein S. 2005. Phosphatidylinositol-4,5-bisphosphate hydrolysis directs actin remodeling during phagocytosis. J Cell Biol 169: 139–149. https://doi.org/10.1083/jcb.200412162.

33. Marie-Anais F, Mazzolini J, Herit F, Niedergang F. 2016. Dynamin-actin cross talk contributes to phagosome formation and closure. Traffic 17: 487–499. https://doi.org/10.1111/tra.12386.

34. Fratti RA, Backer JM, Gruenberg J, Corvera S, Deretic V. 2001. Role of phosphatidylinositol 3-kinase and Rab5 effectors in phagosomal biogenesis and mycobacterial phagosome maturation arrest. J Cell Biol 154:631–644. https://doi.org/10.1083/jcb.200106049.

35. Hackam DJ, Rotstein OD, Zhang WJ, Demaurex N, Woodside M, Tsai O, Grinstein S. 1997. Regulation of phagosomal acidification. Differential targeting of Na1/H1 exchangers, Na1/K1-ATPases, and vacuolar-type H1- atpases. J Biol Chem 272:29810–29820. https://doi.org/10.1074/jbc.272.47 .29810.

36. Lee HJ, Woo Y, Hahn TW, Jung YM, Jung YJ. 2020. Formation and maturation of the phagosome: a key mechanism in innate immunity against intracellular bacterial infection. Microorganisms 8:1298. https://doi.org/10 .3390/microorganisms8091298.

37. Poteryaev D, Datta S, Ackema K, Zerial M, Spang A. 2010. Identification of the switch in early-to-late endosome transition. Cell 141:497–508. https://doi.org/10.1016/j.cell.2010.03.011.

38. Roberts EA, Chua J, Kyei GB, Deretic V. 2006. Higher order Rab programming in phagolysosome biogenesis. J Cell Biol 174:923–929. https://doi.org/10.1083/jcb.200603026.

39. Park JS, Helble JD, Lazarus JE, Yang G, Blondel CJ, Doench JG, Starnbach MN, Waldor MK. 2019. A FACS-based genome-wide CRISPR screen reveals a requirement for COPI in Chlamydia trachomatis invasion. iScience 11: 71–84. https://doi.org/10.1016/j.isci.2018.12.011.

40. Haney MS, Bohlen CJ, Morgens DW, Ousey JA, Barkal AA, Tsui CK, Ego BK, Levin R, Kamber RA, Collins H, Tucker A, Li A, Vorselen D, Labitigan L, Crane E, Boyle E, Jiang L, Chan J, Rincón E, Greenleaf WJ, Li B, Snyder MP, Weissman IL, Theriot JA, Collins SR, Barres BA, Bassik MC. 2018. Identification of phagocytosis regulators using magnetic genome-wide CRISPR screens. Nat Genet 50:1716–1727. https://doi.org/10.1038/s41588-018-0254-1.

41. Yeung ATY, Choi YH, Lee AHY, Hale C, Ponstingl H, Pickard D, Goulding D, Thomas M, Gill E, Kim JK, Bradley A, Hancock REW, Dougan G. 2019. A genome-wide knockout screen in human macrophages identified host factors modulating Salmonella infection. mBio 10:e02169-19. https://doi.org/ 10.1128/mBio.02169-19.

42. Brzostek J, Fatin A, Chua WH, Tan HY, Dick T, Gascoigne NRJ. 2020. Single cell analysis of drug susceptibility of Mycobacterium abscessus during macrophage infection. Antibiotics 9:711. https://doi.org/10.3390/antibiotics9100711.

43. Schliwa M. 1982. Action of cytochalasin d on cytoskeletal networks. J Cell Biol 92:79–91. https://doi.org/10.1083/jcb.92.1.79.

44. Kiritsy MC, Ankley LM, Trombley J, Huizinga GP, Lord AE, Orning P, Elling R, Fitzgerald KA, Olive AJ. 2021. A genetic screen in macrophages identifies new regulators of IFNgamma-inducible MHCII that contribute to T cell activation. Elife 10:e65110. https://doi.org/10.7554/eLife.65110.

45. Kiritsy MC, Ankley LM, Trombley JD, Huizinga GP, Lord AE, Orning P. 2021. A genome-wide screen in macrophages identifies new regulators of IFNg-inducible MHCII that contribute to T cell activation. eLIFE.

46. Li W, Xu H, Xiao T, Cong L, Love MI, Zhang F, Irizarry RA, Liu JS, Brown M, Liu XS. 2014. MAGeCK enables robust identification of essential genes from genome-scale CRISPR/Cas9 knockout screens. Genome Biol 15:554. https://doi.org/10.1186/s13059-014-0554-4.

47. Johansen MD, Herrmann JL, Kremer L. 2020. Non-tuberculous mycobacteria and the rise of Mycobacterium abscessus. Nat Rev Microbiol 18:392–407. https://doi.org/10.1038/s41579-020-0331-1.

48. Luthra S, Rominski A, Sander P. 2018. The role of antibiotic-target-modifying and antibiotic-modifying enzymes in Mycobacterium abscessus drug resistance. Front Microbiol 9:2179. https://doi.org/10.3389/fmicb.2018.02179.

49. Renna M, Schaffner C, Brown K, Shang S, Tamayo MH, Hegyi K, Grimsey NJ, Cusens D, Coulter S, Cooper J, Bowden AR, Newton SM, Kampmann B, Helm J, Jones A, Haworth CS, Basaraba RJ, DeGroote MA, Ordway DJ, Rubinsztein DC, Floto RA. 2011. Azithromycin blocks autophagy and may predispose cystic fibrosis patients to mycobacterial infection. J Clin Invest 121:3554–3563. https://doi.org/10.1172/JCI46095.

50. Herb M, Gluschko A, Schramm M. 2018. LC3-associated phagocytosis initiated by integrin ITGAM-ITGB2/Mac-1 enhances immunity to Listeria monocytogenes. Autophagy 14:1462–1464. https://doi.org/10.1080/15548627 .2018.1475816.

51. Saraiva EM, Andrade AF, de Souza W. 1987. Involvement of the macrophage mannose-6-phosphate receptor in the recognition of Leishmania mexicana amazonensis. Parasitol Res 73:411–416. https://doi.org/10.1007/ BF00538197.

52. Dustin ML. 2016. Complement receptors in myeloid cell adhesion and phagocytosis. Microbiol Spectr 4:10.1128. https://doi.org/10.1128/ microbiolspec.MCHD-0034-2016.

53. Demirdjian S, Hopkins D, Cumbal N, Lefort CT, Berwin B. 2020. Distinct contributions of CD18 integrins for binding and phagocytic internalization of Pseudomonas aeruginosa. Infect Immun 88:e00011-20. https://doi .org/10.1128/IAI.00011-20.

54. Wen L, Marki A, Wang Z, Orecchioni M, Makings J, Billitti M, Wang E, Suthahar SSA, Kim K, Kiosses WB, Mikulski Z, Ley K. 2022. A humanized beta(2) integrin knockin mouse reveals localized intra- and extravascular neutrophil integrin activation in vivo. Cell Rep 39:110876. https://doi.org/ 10.1016/j.celrep.2022.110876.

55. Ryan K, Byrd TF. 2018. Mycobacterium abscessus: shapeshifter of the Mycobacterial World. Front Microbiol 9:2642. https://doi.org/10.3389/ fmicb.2018.02642.

56. Daher W, Leclercq L-D, Viljoen A, Karam J, Dufrêne YF, Guérardel Y, Kremer L. 2020. O-methylation of the glycopeptidolipid acyl chain defines surface hydrophobicity of Mycobacterium abscessus and macrophage invasion. ACS Infect Dis 6:2756–2770. https://doi.org/10.1021/acsinfecdis .0c00490.

57. Ferrell KC, Johansen MD, Triccas JA, Counoupas C. 2022. Virulence mechanisms of Mycobacterium abscessus: current knowledge and implications Macrophage Genes Required for M. abscessus Uptake mSphere March/April 2023 Volume 8 Issue 2 10.1128/msphere.00663-22 16 for vaccine design. Front Microbiol 13:842017. https://doi.org/10.3389/ fmicb.2022.842017.

58. Halloum I, Carrère-Kremer S, Blaise M, Viljoen A, Bernut A, Le Moigne V, Vilchèze C, Guérardel Y, Lutfalla G, Herrmann J-L, Jacobs WR, Kremer L. 2016. Deletion of a dehydratase important for intracellular growth and cording renders rough Mycobacterium abscessus avirulent. Proc Natl Acad Sci U S A 113:E4228–37.

59. Obregón-Henao A, Arnett KA, Henao-Tamayo M, Massoudi L, Creissen E, Andries K, Lenaerts AJ, Ordway DJ. 2015. Susceptibility of Mycobacterium abscessus to antimycobacterial drugs in preclinical models. Antimicrob Agents Chemother 59:6904–6912. https://doi.org/ 10.1128/AAC.00459-15.

60. Maggioncalda EC, Story-Roller E, Mylius J, Illei P, Basaraba RJ, Lamichhane G. 2020. A mouse model of pulmonary Mycobacteroides abscessus infection. Sci Rep 10:3690. https://doi.org/10.1038/s41598-020-60452-1.

61. Brinkman EK, Chen T, Amendola M, van Steensel B. 2014. Easy quantitative assessment of genome editing by sequence trace decomposition. Nucleic Acids Res 42:e168. https://doi.org/10.1093/nar/gku936.

CHAPTER 3: *Mycobacterium abscessus* Infection in Fetal Liver-derived Alveolar-like Macrophages Activates Distinct Inflammatory Responses Compared to Myeloid-derived Macrophages.

DECLARATIONS

Authors

Haleigh N. Gilliland[1*], Soledad Soverina[1*], Kayla Conner[1], Taryn Vielma[1] and Andrew J. Olive[1]

1 Michigan State University

* Authors contributed equally

Contributions

The following chapter investigates the global transcriptional and cytokine profile differences between two macrophage subsets during *Mycobacterium abscessus* infection. HG, SS and AO conceptualized the idea to test how alveolar macrophages and myeloid derived macrophages differentially respond to Mab infection. HG completed all flow cytometry, Griess assay and qPCR experiments. SS conducted all colony forming unit (CFU) and ELISA assays. KC did all the bioinformatics analysis on RNAseq and multiplex Luminex datasets. TV completed all CellTiter Glo experiments. AO and HG wrote the chapter together and all other authors reviewed it.

ABSTRACT

Pulmonary infections caused by *Mycobacterium abscessus* (Mab), a rapidly growing nontuberculous mycobacterium (NTM), are on the rise in patients with chronic or acquired lung disease. In contrast to immunocompetent individuals, these patient cohorts exhibit abnormal pulmonary function that result from chronic inflammation and mucus build-up. Treatment regimens rely on multi-drug cocktails yet Mab's natural recalcitrance to common antibiotics extends treatment timelines and increases the frequency of treatment failures. Thus, it is important to understand the mechanisms by which immunocompetent individuals clear Mab with relative ease while susceptible individuals do not, to identify new treatment options that may protect at-risk patients. In the lungs, macrophages are the first immune cell Mab encounters following infection, with both resident alveolar macrophages and recruited myeloid derived macrophages playing important roles during infection control. However, the specific role of these distinct macrophage populations in regulating control and inflammatory responses during Mab remains limited due to a lack of *ex vivo* models that recapitulate the functions of different macrophage subsets. Here, we leverage a fetal-liver derived alveolar macrophage (FLAM) model to define the mechanistic interactions occurring at the Mab-macrophage interface compared to bone-marrow derived macrophages (BMDMs). Even though both FLAMs and BMDMs similarly control intracellular Mab, the inflammatory response between these macrophage populations is significantly different. While BMDMs robustly activated NF-κB transcriptional targets that include important chemokines and inflammatory cytokines like TNF, FLAMs transiently induced these genes following Mab infection. While activation of FLAMs or BMDMs with IFNγ prior to Mab infection did not alter Mab intracellular dynamics, it did drive FLAMs to be more inflammatory. However, while we found IFNγ activated FLAMs more robustly activate NF-κB

during Mab infection, there remain important differences compared to BMDMs. This includes lower expression of the inducible nitric oxide synthase, which we found was reversed with chemical activation of HIF1α. We conclude that FLAMs and BMDMs differentially respond to Mab infection due to differences in signaling networks activated following innate immune sensing, with FLAMs being more hypo-inflammatory than BMDMs. More broadly our results highlight a key need to better understand the initial interactions with Mab and distinct macrophage populations to define pathways that contribute to pulmonary protection or disease during respiratory infections.

INTRODUCTION

Pulmonary infections caused by rapidly growing nontuberculous mycobacterium (NTM) are on the rise, with a 400% increase in prevalence from 1987 to 2015 [1-3]. Of these infections, those caused by *Mycobacterium abscessus* (Mab) are the second most common [4]. While the majority of immunocompetent hosts control Mab infections, patients with pre-existing pulmonary conditions including cystic fibrosis (CF), chronic obstructive pulmonary disease (COPD), or bronchiectasis are at a particularly high-risk for chronic Mab pulmonary infection [5-8]. Complicating matters, Mab remains intrinsically resistant to many antibiotics, requiring multi-drug treatment regimens and high rates of treatment failure [9-11]. The lungs of susceptible patient cohorts are characterized by structural damage, inflammation, and/or changes in mucus regulation, changing the pulmonary environment in dramatic ways [7, 12, 13]. How these structural and inflammatory changes directly alter Mab-host interactions remains unclear. With no protective vaccine and limited drug options, understanding how immunocompetent hosts control Mab is of critical importance to develop more clinically relevant host-directed therapies.

Central to host-pathogen interactions in the lungs are macrophages, key innate immune cells tasked with sensing the environment, initiating inflammation, and controlling infections [14, 15]. In the lungs, several macrophage sub-populations including fetal-derived resident macrophages and myeloid-derived interstitial/recruited macrophages play important roles in maintaining pulmonary homeostasis and protecting the lungs against respiratory pathogens [15-17]. The difference in ontogeny and the local environment drives important phenotypic differences in these distinct macrophage subtypes [14, 16]. Resident lung macrophages, such as alveolar macrophages (AMs), are maintained in the airspace to recycle surfactants produced by lung epithelial cells [15-17]. AMs are the first immune cells to detect inhaled pathogens and

control initial immune responses during pulmonary infection. Work examining other respiratory infections, including *Mycobacterium tuberculosis*, suggest AMs are hypo-inflammatory and restrain their interactions with T cells to prevent robust adaptive immune activation [18, 19]. In contrast, myeloid-derived macrophages are highly inflammatory cells that drive increased pathogen control and T cell activation [18, 20, 21]. Combined, these inflammatory responses result in tissue inflammation that modulates macrophage function.

During lung infections, inflammatory signals can further modify the local environment to drive protection or pathology [22-24]. One key inflammatory cue is the production of the cytokine interferon-gamma (IFNγ) [25]. This protective cytokine is primarily produced by NK and Th1-activated T cells and is required for humans to control mycobacterial infections, as the loss of IFNγ signaling results in mendelian susceptibility to mycobacterial disease (MSMD) [26, 27]. IFNγ contributes to immune control by upregulating antimicrobial and T cell mediated restriction pathways [19, 28]. These pathways include the production of reactive oxygen species (ROS) and nitric oxide (NO) that directly control pathogens and inflammatory signaling [27, 28]. Recent work suggests IFNγ responses are distinct in different macrophage subtypes, with these differences driving alternative immune functions [18, 29]. Given that Mab susceptible patient cohorts are characterized by chronic inflammatory lung environments, it is important to understand how distinct macrophage subsets respond to Mab in both resting and inflammatory states.

To date, the majority of studies examining Mab-Macrophage interactions have used murine bone marrow-derived macrophages (BMDMs) and/or immortalized macrophage cell lines including RAW, J774, and Thp1 cells [30-33]. These studies identified important host genes required for the uptake of Mab as well as roles for TLR2 and Nod2 in activating pathways that

drive TNF, type I IFN, and NO production to control Mab [30, 34, 35]. Mab infected Zebrafish embryo studies have found TNF signaling and IL8-mediated neutrophil recruitment are required for granuloma formation [36, 37]. However, we continue to lack an understanding of the early interactions between Mab and AMs. One reason for this gap in knowledge is the limited approaches available to understand AMs. AMs are particularly challenging to isolate and to maintain in the AM-like states observed in the lungs. Recent advances in *ex vivo* culturing now enable a mechanistic understanding of interactions with AM-like cells [38-40]. One model we recently developed are fetal liver-derived alveolar-like macrophages (FLAMs) [38]. These cells are isolated from the fetal liver, which is the source of AMs *in vivo*, and cultured with two key lung cytokines GM-CSF and TGFβ [38, 41, 42]. FLAMs are transcriptionally similar to AMs yet distinct from myeloid-derived BMDMs in both resting and IFNγ-activated states [18], thus, serving as a useful model to understand mechanistic AM responses during infection.

Here, we defined macrophage subset specific responses to Mab infection. We first compared the uptake and bacterial growth kinetics in BMDMs and FLAMs to model distinct populations in the lungs in both resting and IFNγ-activated cells. In parallel, we used transcriptional profiling and cytokine analysis to define macrophage-subset specific responses during Mab infection. Our results suggest few differences in Mab intracellular bacterial control or cell death between FLAMs and BMDMs. However, we observed significant differences in the innate response in resting and IFNγ-activated FLAMs and BMDMs that was dependent on Mab infection. Mechanistic studies found that Nrf2, a transcription factor previously associated with AM innate responses to Mtb, does not play a role in the hypo-inflammatory response in FLAMs directly to Mab infection [43, 44]. We also found that NF-κB is a key driver of cytokine production in BMDMs but is not as robustly activated in FLAMs. Finally, we observed that

while IFNγ-activated FLAMs are more inflammatory, they do not induce high levels of the inducible nitric oxide synthase (*Nos2*) compared BMDMs. This deficiency was overcome by chemical activation of HIF1α. These data uncover key differences in the transcriptional response of distinct macrophage subtypes, identifying cell-type specific inflammation that may play an important role regulating disease control or progression during respiratory infections.

RESULTS

Mab persists in BMDMs and FLAMs over 48 hours of infection.

As a first step to understand differences in host-Mab interactions between macrophage subsets we compared whether BMDMs or FLAMs phagocytose Mab with different efficiency. To test this, we infected resting BMDMs or FLAMs with the smooth ATCC Mab strain 19977 expressing constitutively active mEmerald GFP at increasing multiplicities of infection (MOIs) [31]. Four hours later, flow cytometry was used to quantify the percent of cells that were GFP positive. While we noted an increase in the percent of infected cells as the MOI increased, we did not observe any significant differences in uptake between BMDMs and FLAMs (Figure 2.1A). In addition to percent of infected cells, we wondered whether the mean fluorescence intensity (MFI) of infected cells could be used a surrogate for intracellular bacterial level. To test this prediction, we first infected immortalized BMDMs with mEmerald-Mab and used cell sorting to isolate infected cells with high or low GFP MFI and plated for CFU (Figure 2.1B). We found that cells sorted from the high GFP MFI contained more Mab on a per cell basis than the same number of cells from the low GFP group (Figure 2.1C). These data show that MFI is a useful correlate of intracellular bacterial levels. When we examined the MFI of cells infected with increasing MOI of Mab at 4 hours, we observed no significant differences between BMDMs and

FLAMs (Figure 2.1D). These data show that the uptake of Mab by BMDMs and FLAMs is similar.

We next characterized the intracellular dynamics of Mab in distinct macrophage subsets over time. BMDMs or FLAMs were infected with mEmerald-Mab at an MOI of 5 and 12, 24 and 48 hours later cells were lysed for quantification of colony forming units (CFU) (Figure 2.1E). We found no significant increase or decrease of viable Mab in either cell type over time and very small differences in total CFU between cell types. In parallel, flow cytometry was used to monitor intracellular Mab. In agreement with our CFU quantification, we observed no significant increases in the percent of infected cells or the MFI of infected cells over time (Figure 2.1F). These data suggest that Mab persists in resting BMDMs and FLAMs over several days.

Mab infection of FLAMs results in distinct cytokine production independent of cell death.

Given the similar intracellular Mab dynamics between BMDMs and FLAMs, we next tested whether there are differences in cell death and inflammation during infection. FLAMs and BMDMs were infected with Mab at an MOI of 5 and 12, 24 and 48 hours later cell death was quantified by flow cytometry using a viability dye (Figure 2.2A) or by quantifying ATP via a CellTiter Glo assay (Figure 2.2B). Our results found limited induction of cell death following infection in either cell type. While BMDMs trended towards more cell death, the overall percentage remained very low. These data suggests that over the first two days of infection, when the intracellular levels of Mab are similar between BMDMs and FLAMs, there is very little change in macrophage viability.

We next examined whether the inflammatory response was different between Mab infected BMDMs and FLAMs. Cells were infected with Mab at an MOI of 5 and 12, 24 and 48 hours later pro-inflammatory cytokines was quantified in the cell culture supernatants by a

multiplex Luminex assay. We observed significant differences between BMDMs and FLAMs, with BMDMs producing high levels of the cytokines CCL3, CCL4, CXCL2, CXCL5, CXCL10, TNF and G-CSF while FLAMs induced very limited amounts of these cytokines (Figure 2.2C). We noted no major induction of the cytokines IL1α or IL1β in either macrophage subset. Taken together, these results show that Mab infected BMDMs have significantly higher and broader inflammatory responses that are independent of changes in bacterial viability or cell death.

Transcriptional analysis finds Mab infection of BMDMs is more inflammatory than FLAMs.

We next characterized changes to the global transcriptome of both FLAMs and BMDMs over time during Mab infection. Cells were infected with Mab at an MOI of 5, then 6 and 24 hours later RNA was isolated and global mRNA sequencing analysis was performed. PCA analysis showed a strong separation between BMDMs and FLAMs in all conditions along PC1, in line with our previous studies (Figure 2.3A) [18]. While there was a major shift in BMDMs at 24 hours following infection along PC2, this was not observed in FLAMs. This suggests that Mab infection induces a less dramatic effect on the transcriptome of FLAMs compared to BMDMs. We next compared genes that were differentially expressed in either FLAMs or BMDMs over time (Figure 2.3B). We noted 3x more genes were significantly induced and 4.8x more genes were significantly repressed uniquely in BMDMs at 6 hours and 24 hours post-infection compared to FLAMs. There was a significant number of genes that were uniquely induced or repressed in either BMDMs or FLAMs. Pathway analysis of these gene lists found that BMDMs repress oxidative phosphorylation and nucleotide metabolism, while FLAMs induce cell cycle and proliferative genes. To identify other key differences in transcriptional activation during Mab infection of BMDMs and FLAMs, we used clustering analysis to group

genes whose expression changes similarly across all conditions. We identified seven unique clusters and conducted pathway and transcription factor analysis to identify transcriptional networks that were associated with each cluster (Figure 2.3C). Of note, we found that Cluster 3 contained genes that were uniquely induced during Mab infection in FLAMs. KEGG pathway analysis found significant enrichment of genes associated with metabolism, including glycine, serine, and threonine metabolism as well as peroxisomes, a key hub of lipid metabolism. Cluster 5 contained genes that were induced in both FLAMs and BMDMs and was enriched for pathways related to lysosome and phagosomes, as well as antigen presentation. In contrast, Cluster 6 contained genes that were uniquely induced in BMDMs and was enriched for inflammatory pathways including NF-κB and TNF. Transcription factor analysis of Cluster 6 agreed with the KEGG pathway analysis and identified a strong NF-κB signature. When we more closely examined a subset of NF-κB related genes, we found that in BMDMs many of these genes were more highly induced and the expression level of these pro-inflammatory transcripts was higher (Figure 2.3D). When we examined a subset of chemokines that were elevated in our multiplex analysis above, we noted high, persistent expression of each in BMDMs relative to FLAMs (Figure 2.3E). The exception to this pattern was IL1α and IL1β. These cytokines were robustly induced at high levels in FLAMs compared to BMDMs, suggesting unique regulation of IL1 in FLAMs. Taken together our transcriptional analysis found that while both FLAMs and BMDMs sense and respond to Mab infection, BMDMs drive a more inflammatory response than FLAMs.

Differential Nrf2 and NF-κB activation partially contributes to differences in inflammation of FLAMs and BMDMs during Mab infection.

We next examined possible mechanisms contributing to the hypo-inflammation we observed in FLAMs following Mab infection. Previous work with *Mycobacterium tuberculosis* infection found that activation of the transcription factor Nrf2 inhibited inflammatory pathways in AMs [43]. To directly test if Nrf2 was responsible for FLAMs hypo-inflammatory response we infected wild type and Nrf2 deficient FLAMs with Mab and examined pro-inflammatory cytokine production over time (Figure 2.4A). We found that in uninfected resting $Nrf2^{-/-}$ FLAMs there was an increase in the baseline production of the cytokines TNF and CXCL10 compared to wild type cells. Interestingly, we observed no change in these cytokines following Mab infection over time. These data suggest that while Nrf2 modulates the baseline expression of inflammatory cytokines, it does not suppress inflammatory signaling in response to Mab infection.

Our transcriptional analysis suggested that BMDMs induce NF-κB pathways more robustly than FLAMs. To examine the role of NF-κB in the hyper-inflammatory response of BMDMs, we inhibited NF-κB using the chemical inhibitor BAY 11-7082 in both FLAMs and BMDMs and quantified TNF, an NF-κB dependent transcript, by ELISA 6 and 24 hours following Mab infection (Figure 2.4B) [45]. We observed that blocking NF-κB in Mab-infected BMDMs resulted in minimal TNF production similar to infected FLAMs and uninfected BMDMs. These data suggest that NF-κB activation in BMDMs drives higher levels of inflammatory cytokines than FLAMs during Mab infection.

Activating BMDMs or FLAMs with IFNγ does not alter Mab control.

Patients who develop chronic Mab respiratory infections are characterized by previous lung damage and ongoing respiratory disfunctions [9, 46]. In these patients, the baseline

inflammatory state of macrophages is different from resting macrophages. IFNγ is produced during inflammatory responses and is a key cytokine that activates macrophages and can drive restriction of intracellular pathogens [27, 28]. To test if IFNγ differentially alters Mab-host interaction in FLAMs and BMDMs, cells were activated overnight with IFNγ, then infected with mEmerald-Mab before multiple parameters were examined. First, we examined whether IFNγ altered Mab uptake by BMDMs and FLAMs. We found that four hours following infection, IFNγ did not alter uptake efficiency between BMDMs and FLAMs at increasing MOIs (Figure 2.5A and B). We next examined intracellular dynamics overtime. Using flow cytometry, we noted a slight increase in the percent infected cells in both BMDMs and FLAMs, but this remained stable through 48 hours of infection (Figure 2.5C). We also noted a similar MFI of infected cells between resting and IFNγ-activated BMDMs and FLAMs (Figure 2.5D). In line with our flow cytometry approaches, when we quantified viable CFU, we found no significant differences in Mab viability in resting or IFNγ-activated FLAMs or BMDMs (Figure 2.5E). These data suggest that IFNγ-activation does not significantly alter the intracellular dynamics of Mab, which continues to persist in both activated BMDMs and FLAMs.

IFNγ drives more cell death and inflammatory cytokines following Mab infection in both BMDMs and FLAMs.

We next examined how IFNγ alters the host response to Mab infection. IFNγ activated BMDMs and FLAMs were infected with mEmerald Mab and changes in cell viability were quantified over time using two orthologous approaches. First, cell viability was quantified using flow cytometry (Figure 2.6A). In addition, total ATP was quantified using a CellTiter Glo assay (Figure 2.6B). Our results found that while IFNγ induced significant levels of cell death, this remained unchanged following Mab infection. These data suggest that while IFNγ activation

increases cell death pathways in both BMDMs and FLAMs compared to resting cells, it does so independently of Mab infection.

We next dissected if the inflammatory response of BMDMs and FLAMs was altered by IFNγ activation. IFNγ-stimulated FLAMs or BMDMs were infected with Mab at an MOI of 5 and 48 hours later pro-inflammatory cytokines in the supernatants were quantified by a multiplex Luminex assay (Figure 2.6C). We observed that IFNγ activation alone drove high levels of CCL3, CCL4 and CXCL10 in BMDMs but only CCL3 further increased following Mab infection. IFNγ-activated FLAMs did not robustly induce these cytokines in any condition. Similar to resting cells, IFNγ-activated BMDMs induced high levels of CXCL2 and CXCL5 following Mab infection, but this was not observed in FLAMs. Notably, G-CSF was similarly induced in both IFNγ-activated BMDMs and FLAMs. We observed that TNF was more robustly induced in IFNγ-activated FLAMs than resting FLAMs, yet the overall TNF levels remained significantly lower than BMDMs. Finally, we found that while both IL1α and IL1β were significantly induced in FLAMs but not BMDMs, the levels of induction were generally low. Together these results show that while IFNγ alters the inflammatory response of both BMDMs and FLAMs, these cell types continue to drive distinct cytokine profiles following Mab infection.

IFNγ-activation drives distinct transcriptional changes in Mab infected FLAMs and BMDMs.

We next compared the global transcriptomic changes of IFNγ-activated FLAMs and BMDMs during Mab infection. BMDMs and FLAMs were activated with IFNγ overnight then infected with Mab at an MOI of 5. 6 and 24 hours later RNA was isolated from cells and RNA sequencing analysis was performed. To identify general differences in the transcriptomes, we visualized the data using principal component analysis (Figure 2.7A). When we examined only

IFNγ-activated conditions with BMDMs and FLAMs, we noted separation between cell types along the PC1 axis. We noted separation on PC2 axis for BMDMs infected with Mab for 24 hours. In contrast, we did not observe any significant movement along PC2 with FLAMs. This analysis was remarkably similar to our PCA from resting BMDMs and FLAMs (see Figure 2.3A). To directly compare resting and IFNγ-activated cells, we generated a new PCA from all conditions (Figure 2.7A). While FLAMs clustered together for all conditions, both resting and IFNγ-activated BMDMs infected with Mab for 24 hours showed a strong shift from the other BMDMs. These data suggest that Mab infection drives a more robust transcriptional change in BMDMs compared to FLAMs.

We next compared genes that were differentially expressed in either IFNγ-activated FLAMs or BMDMs over time following Mab infection (Figure 2.7B). Similar to resting cells we noted more genes were significantly induced or repressed in BMDMs at 6 hours and 24 hours post-infection compared to FLAMs. When we compared the lists of differentially expressed genes from IFNγ-activated and resting cells from the same condition, we found that IFNγ drives more changes to gene expression than Mab infection alone in both FLAMs and BMDMs. To identify key patterns of transcriptional changes during Mab infection of BMDMs and FLAMs, we used clustering analysis to identify groups of genes whose expression changes similarly across each IFNγ-activated condition. We found four clusters of genes and using pathway and transcription factor analysis we identified transcriptional networks that were associated with each cluster (Figure 2.7C). Interestingly, cluster 1 contains genes that are induced in IFNγ-activated Mab infected FLAMs but are repressed in BMDMs. Among the top enriched KEGG pathways in this cluster was oxidative phosphorylation, suggesting key differences in the metabolic response of IFNγ-activated BMDMs and FLAMs to Mab infection. We also observed that Cluster 3

contained genes that were induced in IFNγ-activated Mab infected BMDMs but not FLAMs. In contrast to resting cells, we did not observe a significant enrichment of the NF-κB pathway from this cluster. This suggests that IFNγ-activation of FLAMs drives a more robust NF-κB response following Mab infection. To examine this directly we compared the normalized reads from FLAMs for NF-κB dependent genes examined in Figure 2.3 above. We found that IFNγ-activation of FLAMs drove significantly higher expression of NF-κB dependent genes following Mab infection (Figure 2.7D). Thus, NF-κB can be more robustly activated in Mab infected FLAMs following IFNγ-stimulation. When we examined a subset of genes examined by our multiplex analysis, we saw strong agreement for the majority of cytokines including CXCL1, CXCL2, TNF and G-CSF (Figure 2.7E). Interestingly, while we also observed that only FLAMs induce IL1α and IL1β in response to Mab, the magnitude of these changes at the transcriptional level was significantly higher compared to the released cytokines.

The lack of Nos2 expression following Mab Infection of IFNγ-activated FLAMs is overcome by the induction of HIF1a.

An important role of IFNγ-activation is to induce antimicrobial compounds, such as Nitric Oxide (NO). NO is known to play an important role during Mycobacterial infections, yet if it is differentially regulated during Mab infection remains unclear [21, 47-49]. When we compared gene sets between FLAMs and BMDMs during IFNγ activation, we noted significant differences in the expression of Nos2 and Ptgs2 (Figure 2.8A). Previous studies found these genes are induced in both a HIF1α-dependent manner that is also associated with a metabolic shift to aerobic glycolysis [50-52]. Given that we observed a specific increase in oxidative phosphorylation pathways in IFNγ-activated FLAMs, we hypothesized that HIF1α may not be as robustly induced in FLAMs compared to BMDMs. When we examined the expression of HIF1α

in our RNAseq dataset, we observed that while HIF1α expression was significantly induced during Mab infection of IFNγ-activated BMDMs, the expression remained unchanged in FLAMs (Figure 2.8B). We next wanted to test whether the activation of HIF1α was sufficient to increase Nos2 expression in FLAMs. FLAMs were left resting or were activated with IFNγ in the presence or absence of the HIF1α activator, DMOG. Cells were infected with Mab and 24 hours later RNA was isolated and the expression of Nos2 was quantified by RT-PCR. We found very low expression of Nos2 in all conditions except IFNγ-activated Mab infected FLAMs treated with DMOG (Figure 2.8C). When we repeated this experiment and examined nitrite production using a Griess assay, we observed a similar result (Figure 2.8D). FLAMs only produced high levels of nitrite in the presence of DMOG following IFNγ-activation and Mab infection. These data suggest that unlike BMDMs, HIF1α is not robustly induced in IFNγ-activated FLAMs during Mab infection, and this results in changes to the inflammatory response including low induction of Nos2 and nitric oxide production. Thus, IFNγ-activated FLAMs activate distinct pathways following Mab infection compared to BMDMs.

FIGURES

Figure 2.1. FLAMs and BMDMs similarly take up and control intracellular Mab. (A) BMDMs or FLAMs were infected for 4 hours with the indicated MOI of mEmerald-Mab and flow cytometry was used to quantify the percent of cells infected. **(B)** iBMDMs were infected with mEmerald-Mab for three days and 50,000 infected cells with either high mEmerald mean fluorescence intensity (MFI) or low MFI were sorted, plated and total CFU from each population was quantified. **(C)** BMDMs or FLAMs were infected for 4 hours with the indicated MOI of mEmerald-Mab and flow cytometry was used to quantify the MFI of infected cells. **(D)** BMDMs or FLAMs were infected for 4 hours with mEmerald-Mab (MOI 5) and flow cytometry was conducted at the indicated times post-infection to quantify the percent of cells infected and **(E)** the MFI of infected cells from each condition. **(F)** In parallel cells were lysed and intracellular Mab was quantified by CFU plating. Each experiment is representative of at least 3 independent experiments with at least three biological replicates per experiment. * p<.05 **p<.01 by two-way ANOVA with a Tukey correction for multiple comparisons (A and F) and unpaired t-test for B. All significant comparisons are indicated and remaining comparisons are not significant.

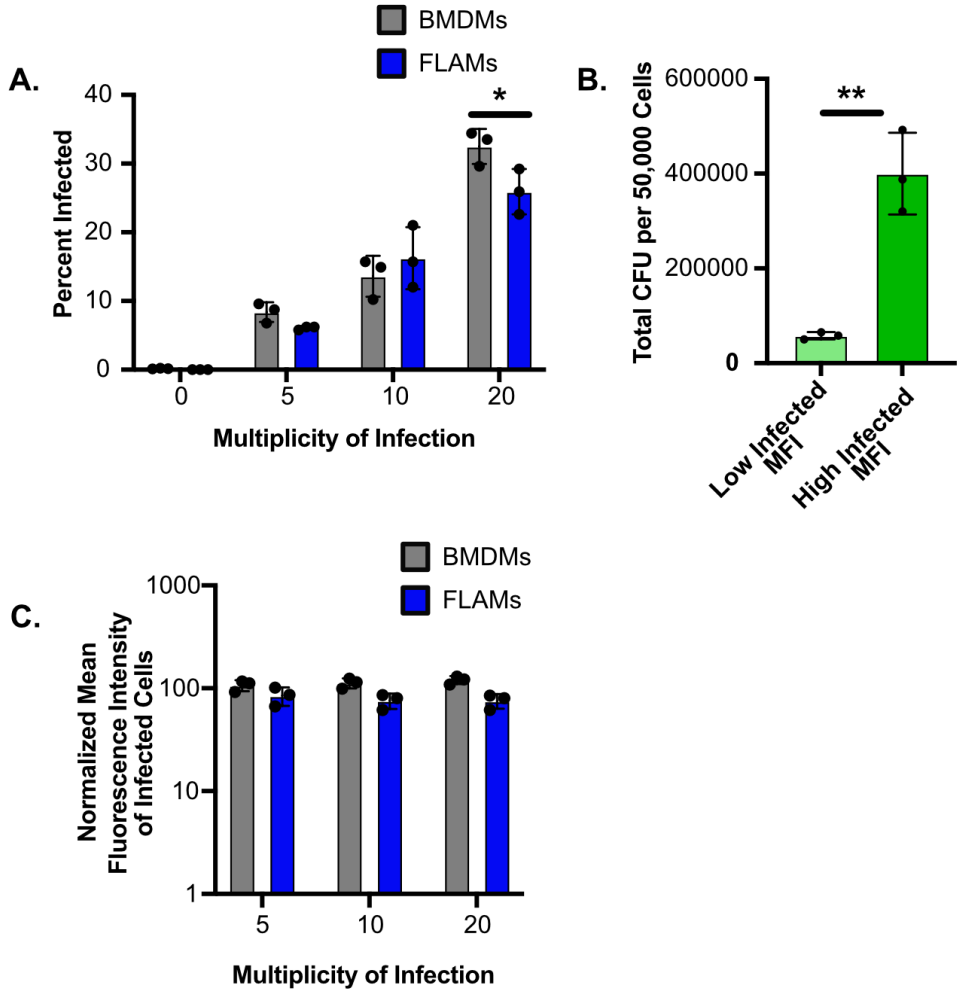

Figure 2.1 (cont'd)

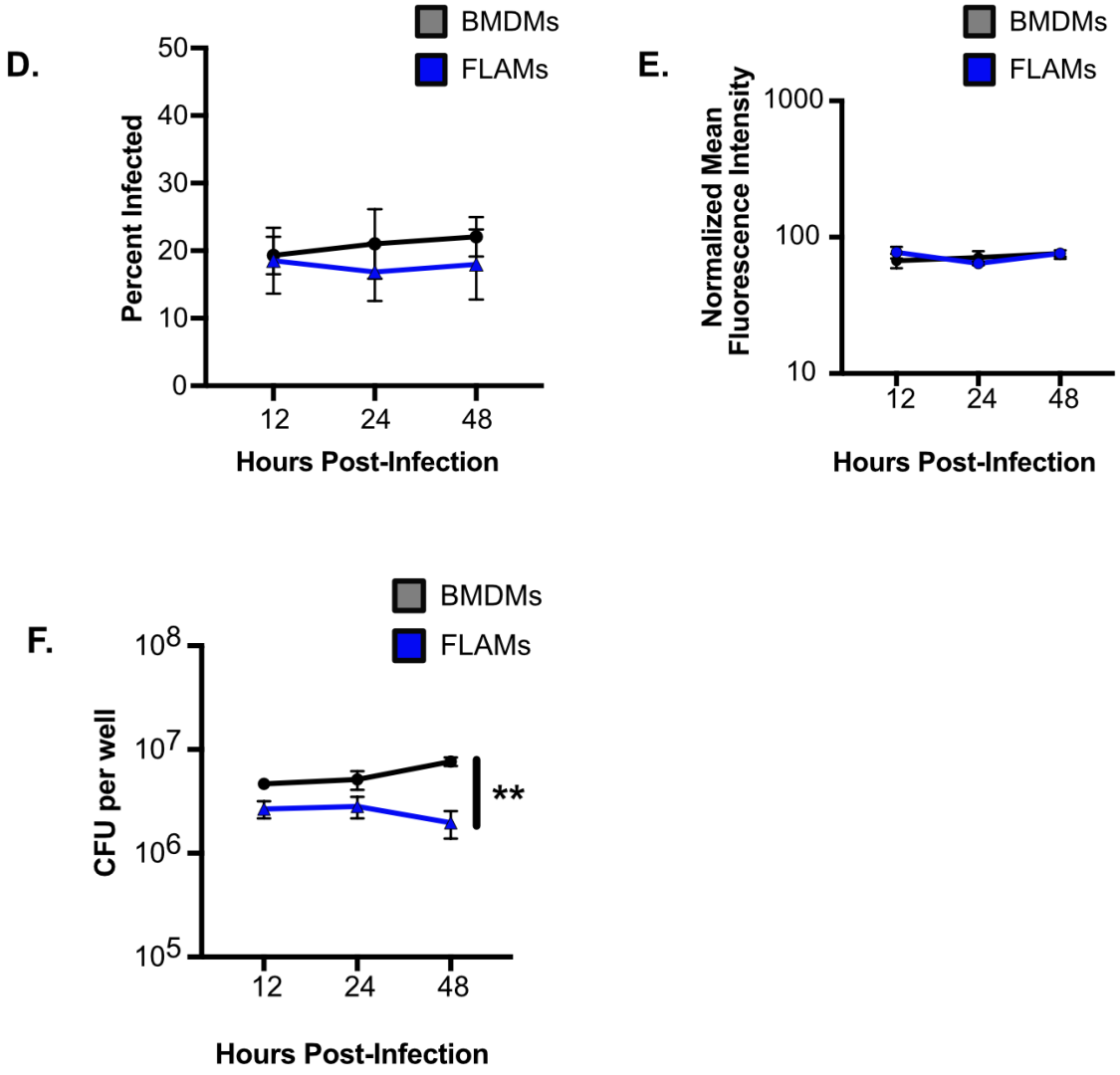

Figure 2.2. BMDMs are more inflammatory than FLAMs in response to Mab infection without driving more cell death. (A) Shown is the percent of viable cells (Live/Dead stain negative) quantified by flow cytometry for BMDMs or FLAMs infected with mEmerald-Mab (MOI 5) for 48 hours. **(B)** The percent of viable cells 24 and 48 hours following mEmerald-Mab infection of BMDMs or FLAMs (MOI 5) using CellTiter Glo. The percent cells that were alive was determined by normalizing each sample to the mean of the uninfected cell type control. **(C)** Shown is the concentration of cytokines from the supernatants of BMDMs or FLAMs infected with mEmerald-Mab (MOI 5) at the indicated timepoints. A & B are representative of three independent experiments with three biological replicates per group. Panel C is from a single multiplex experiment with three biological replicates per group. * p<.05 **p<.01 ***p<.001 ****p<.0001 by two-way ANOVA with a Tukey correction for multiple comparisons.

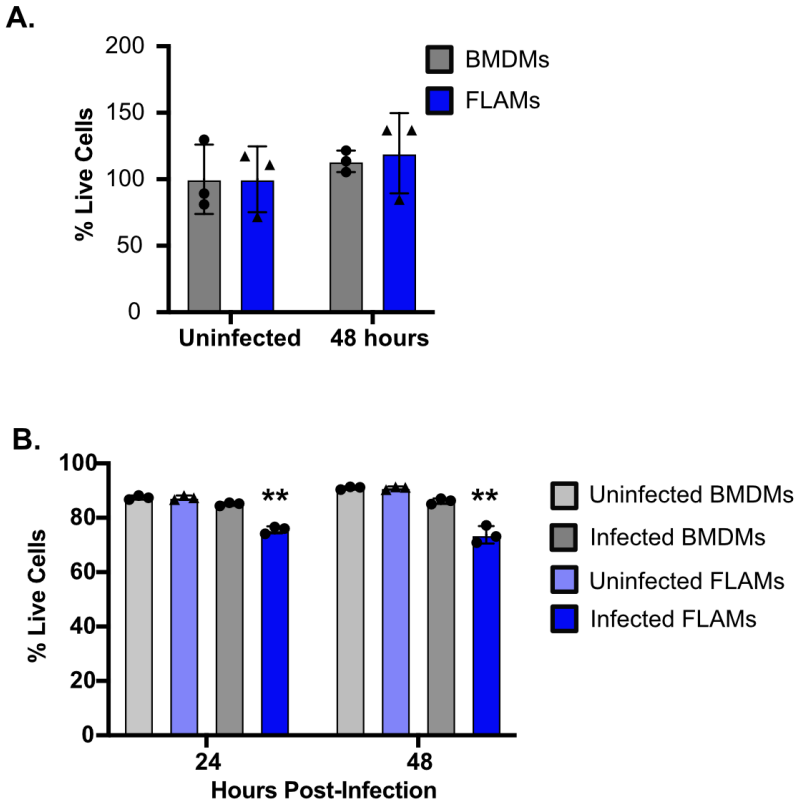

Figure 2.2 (cont'd)

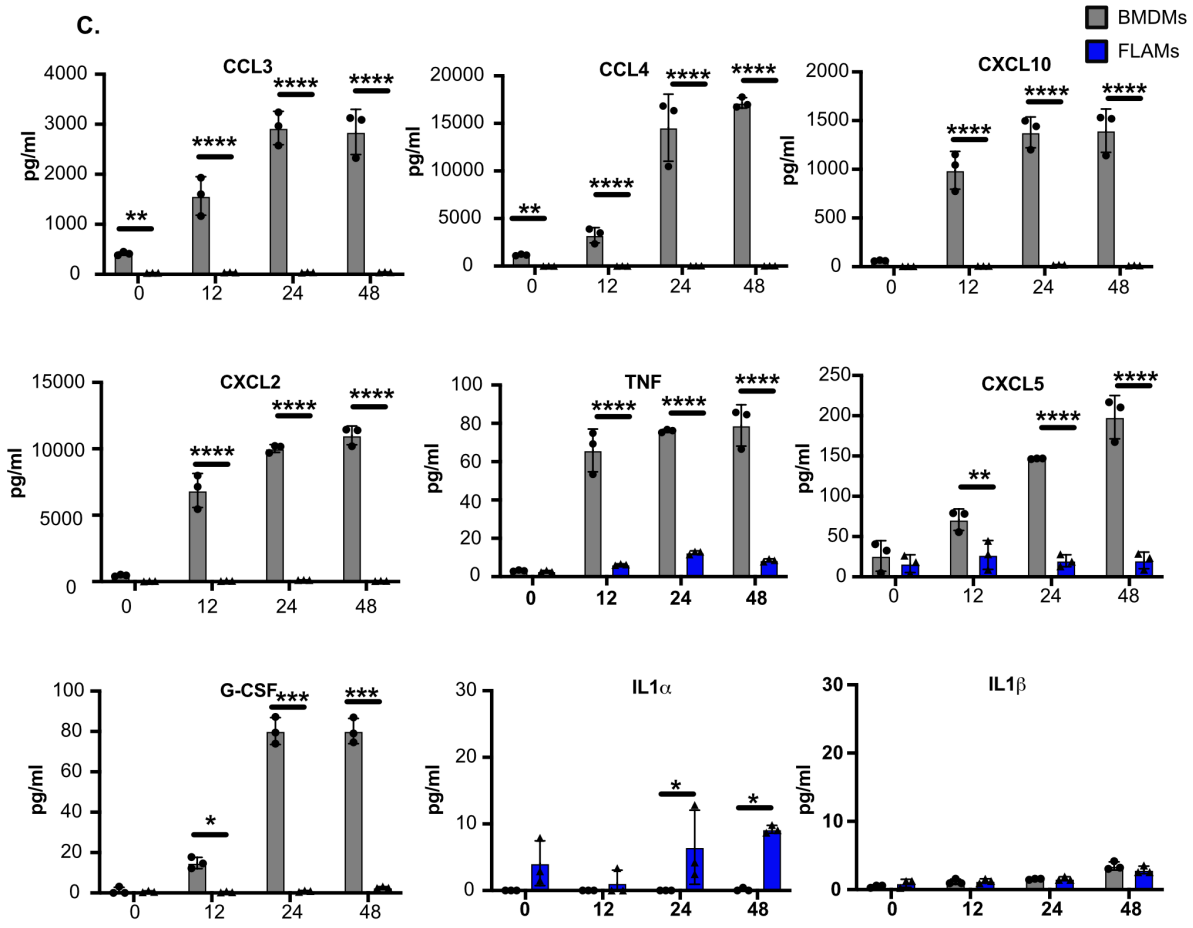

Figure 2.3. BMDMs induce a stronger NF-κB transcriptional signature during Mab infection compared to FLAMs. (A) A principal component analysis (PCA) plot comparing the similarity of the transcriptional responses of BMDMs and FLAMs during Mab infection. **(B)** Venn Diagrams showing shared and unique genes that were significantly induced or repressed in BMDMs and FLAMs during Mab infection using DeSeq2. **(C)** Representative clusters of genes that respond similarly to Mab infection in BMDMs and FLAMs over time. **(D)** Normalized counts of NF-κB genes from the KEGG pathway set were compared across samples of BMDMs and FLAMs infected with Mab over time and is expressed as a heat map. The color scale represents the z-score calculated from normalized read counts across samples for each gene. **(E)** Normalized counts of a subset of NF-κB genes that were differentially regulated in BMDMs (gray) and FLAMs (blue) during Mab infection. ***p<.001 based on adjusted *p*-values using DeSeq2 comparisons.

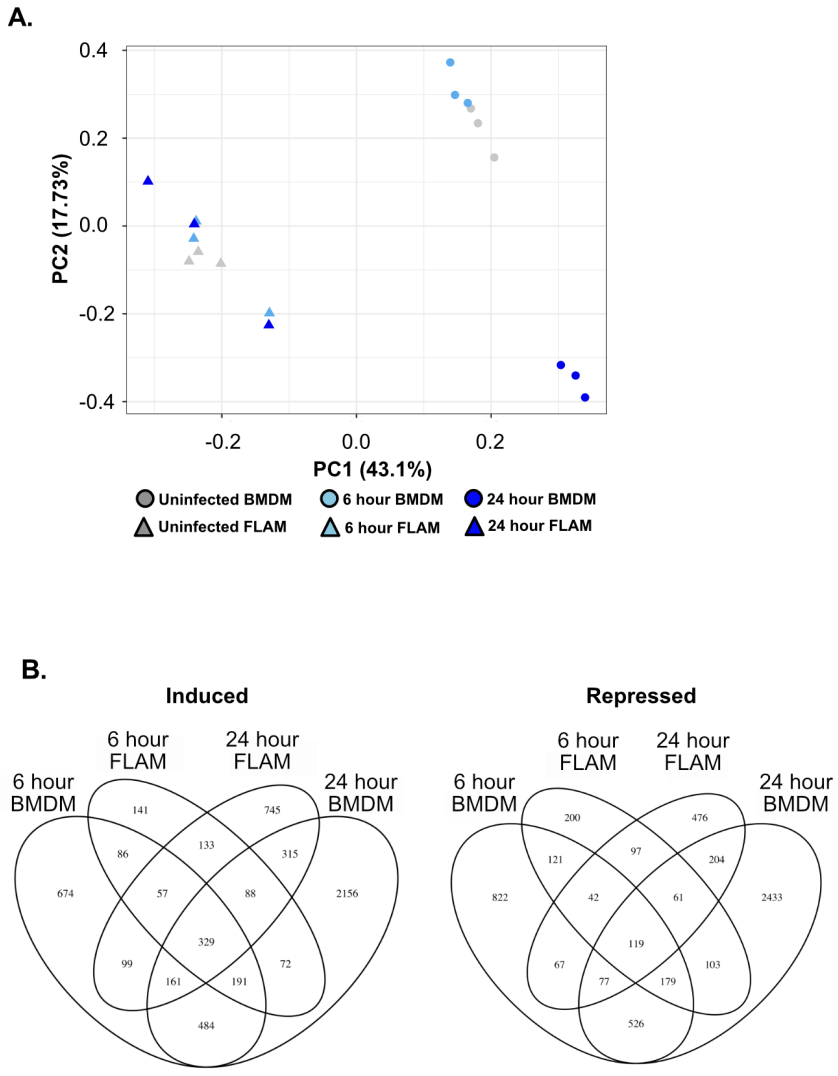

Figure 2.3 (cont'd)

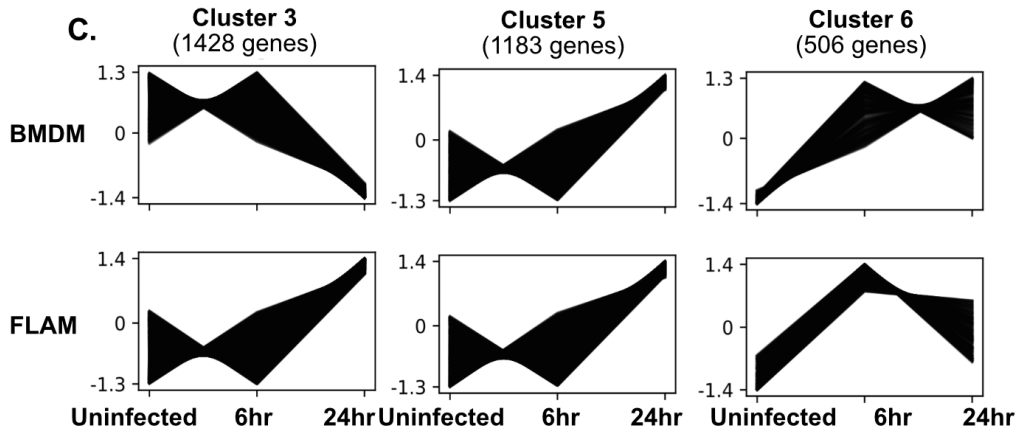

Figure 2.3 (cont'd)

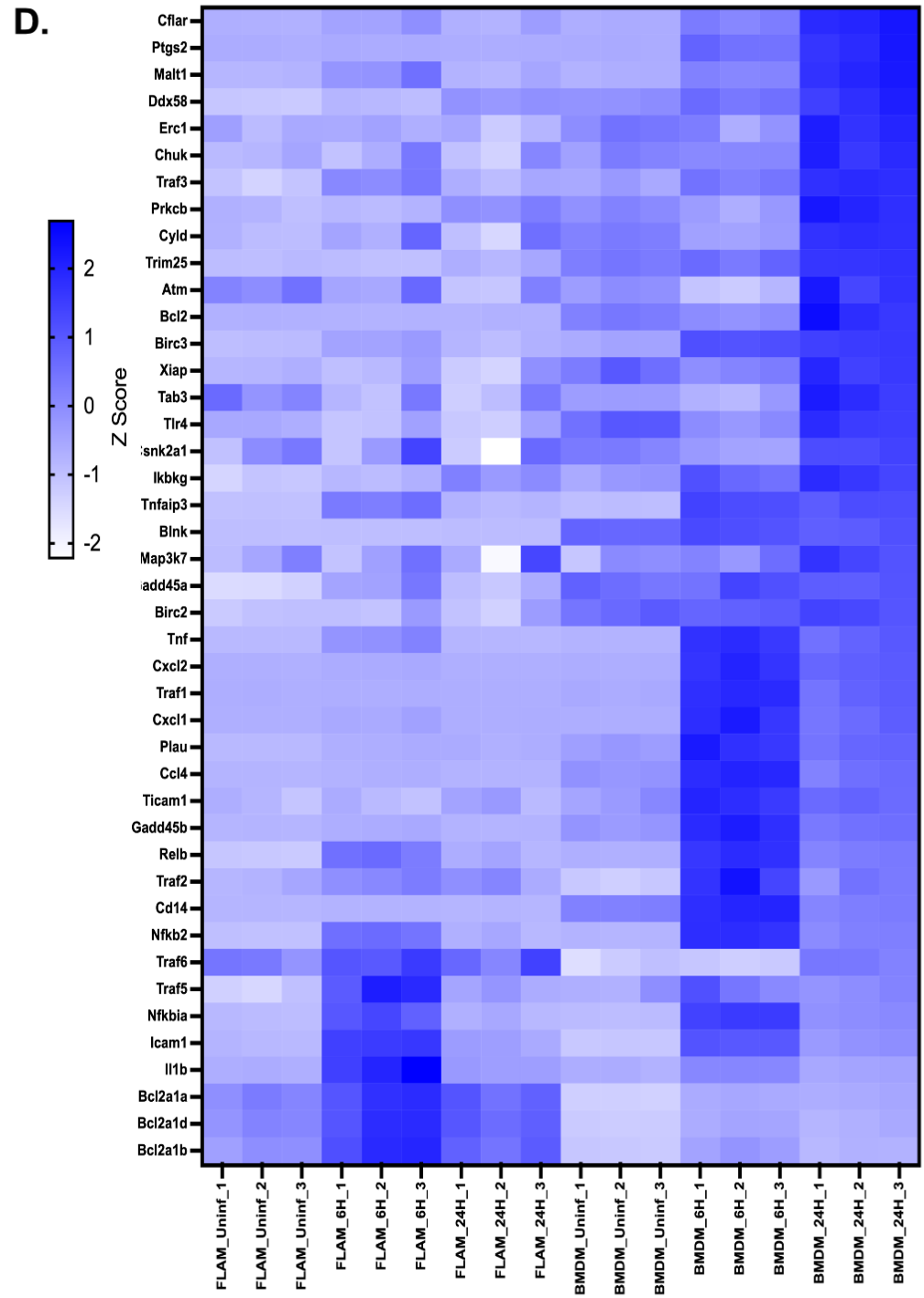

Figure 2.3 (cont'd)

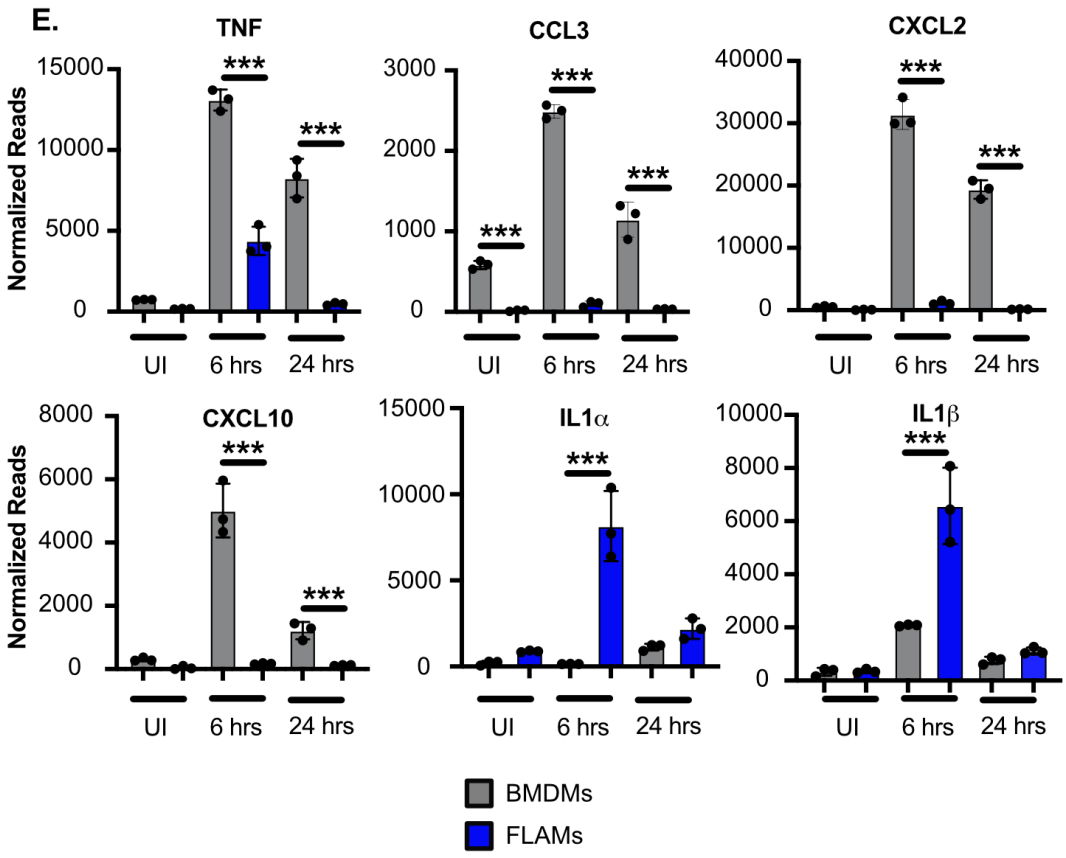

Figure 2.4. Inhibition of NF-κB equalizes the inflammatory response of BMDMs and FLAMs to Mab infection. (A) Shown is the concentration of TNF and CXCL10 from the supernatants of wild type or Nrf2$^{-/-}$ FLAMs infected with mEmerald-Mab (MOI 5) for 48 hours by ELISA. **(B)** Shown is the concentration of TNF and CXCL10 from the supernatants of BMDMs or FLAMs infected with mEmerald-Mab (MOI 5) for 48 hours in the presence and absence of the NF-κB inhibitor (5μM). Data are representative of two independent experiments with at least 3 biological replicates. * p<.05 ***p<.001 by two-way ANOVA with a Tukey correction for multiple comparisons. All significant comparisons are indicated and remaining comparisons are not significant.

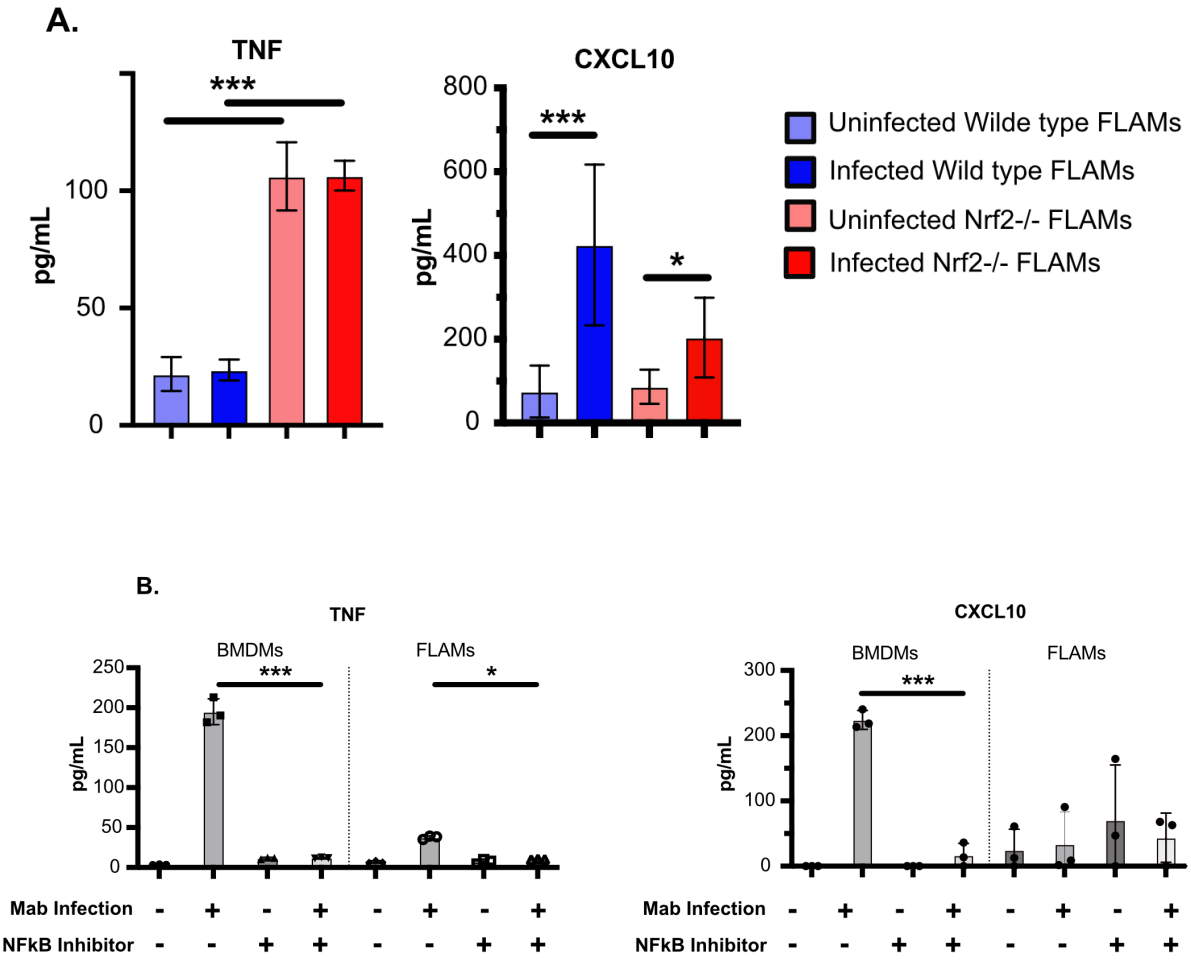

Figure 2.5. IFNγ activation of BMDMs or FLAMs does not alter Mab uptake or intracellular control. (A) The percent of infected cells and the **(B)** MFI of infected cells were quantified by flow cytometry from IFNγ-activated (25ng/ml) BMDMs or FLAMs that were infected with mEmerald-Mab at the indicated MOIs for 4 hours. **(C)** The percent of infected cells and the **(D)** MFI of infected cells were quantified by flow cytometry from untreated or IFNγ-activated (25ng/ml) BMDMs or FLAMs that were infected with mEmerald-Mab (MOI 5) for the indicated times post-infection. **(E)** Viable intracellular Mab was quantified by CFU assay from untreated or IFNγ-activated (25ng/ml) BMDMs or FLAMs that were infected with mEmerald-Mab (MOI 5) for the indicated times post-infection. Shown data are representative of three independent experiments with three replicates per group. Untreated data are from the same experiment shown in Figure 2.1D-2.1E and appropriate multiple hypothesis testing corrections have been made. No significance was observed in panels A and B. For C and D no significance was observed between IFNg-activated BMDM and FLAMs or between resting and activated BMDMs or FLAMs. For E **p<.01 by two-way ANOVA with Tukey correction between IFNg-activated FLAMs and IFNg-activated BMDMs.

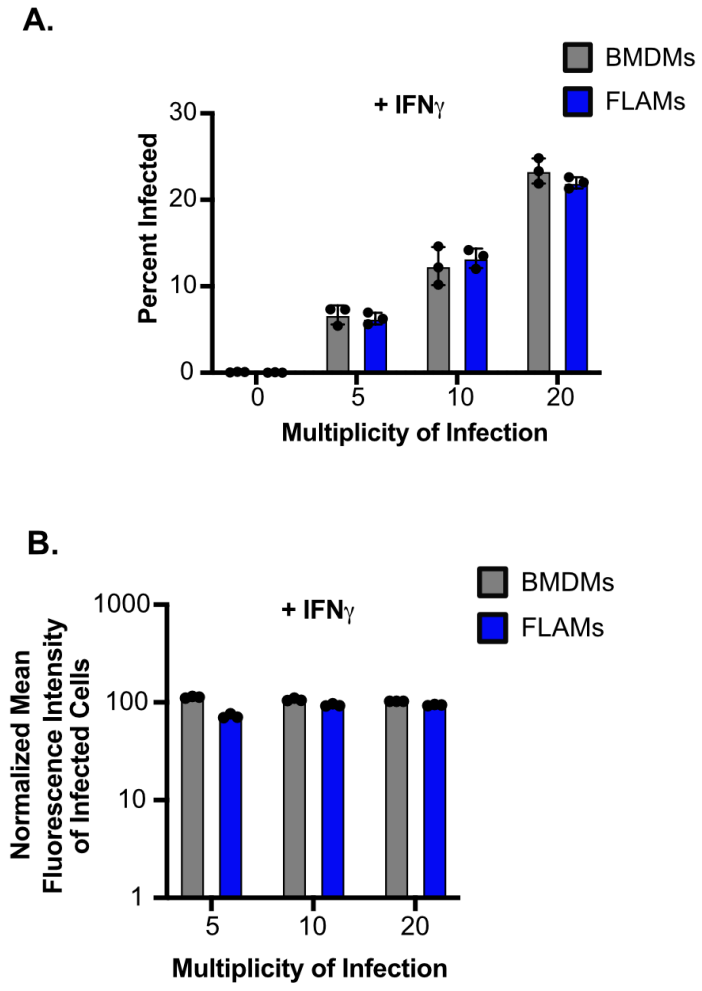

Figure 2.5 (cont'd)

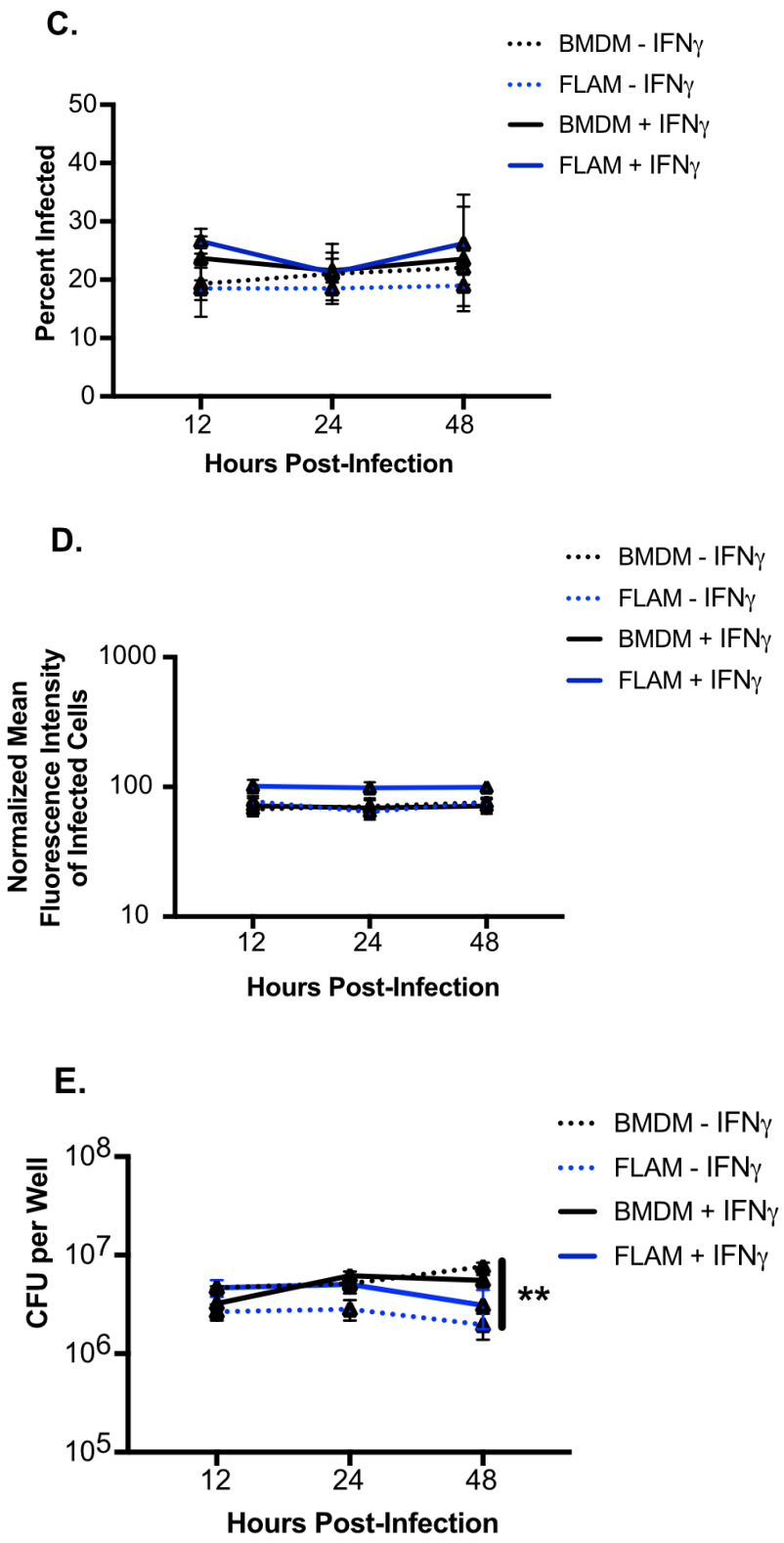

Figure 2.6. The inflammatory response of IFNγ-activated BMDMs and FLAMs remain distinct. (A) Shown is the percent of viable cells (Live/Dead stain negative) quantified by flow cytometry for IFNγ-activated (25ng/ml) BMDMs or FLAMs infected with mEmerald-Mab (MOI 5) for the indicated time. **(B)** The percent of viable cells 48 hours following mEmerald-Mab infection of untreated or IFNγ-activated (25ng/ml) BMDMs or FLAMs (MOI 5) using CellTiter Glo. The percent cells that were alive was determined by normalizing each sample to the mean of the uninfected cell type control. **(C)** Shown is the concentration of cytokines from the supernatants of IFNγ-activated (25ng/ml) BMDMs or FLAMs infected with mEmerald-Mab (MOI 5) and at the indicated timepoints. A & B are representative of three independent experiments with three biological replicates per group. Panel C is from a single multiplex experiment with three biological replicates per group. **p<.01 ***p<.001 by two-way ANOVA with a Tukey correction for multiple comparisons.

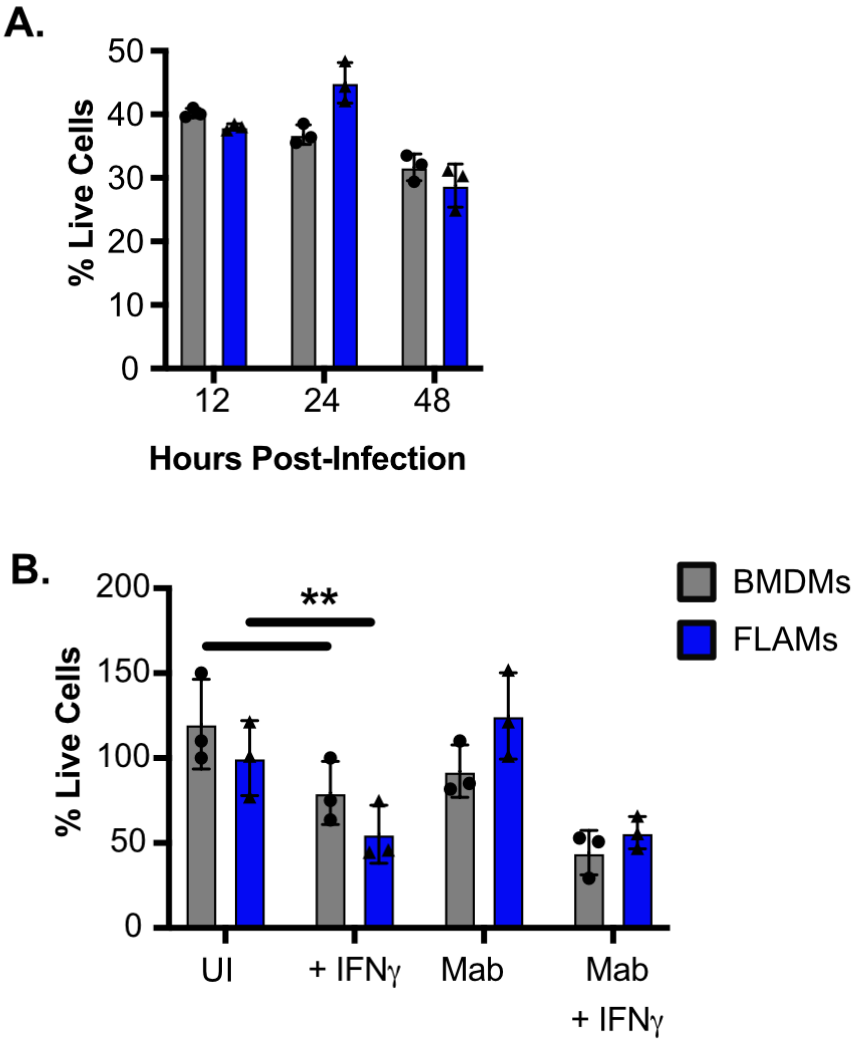

Figure 2.6 (cont'd)

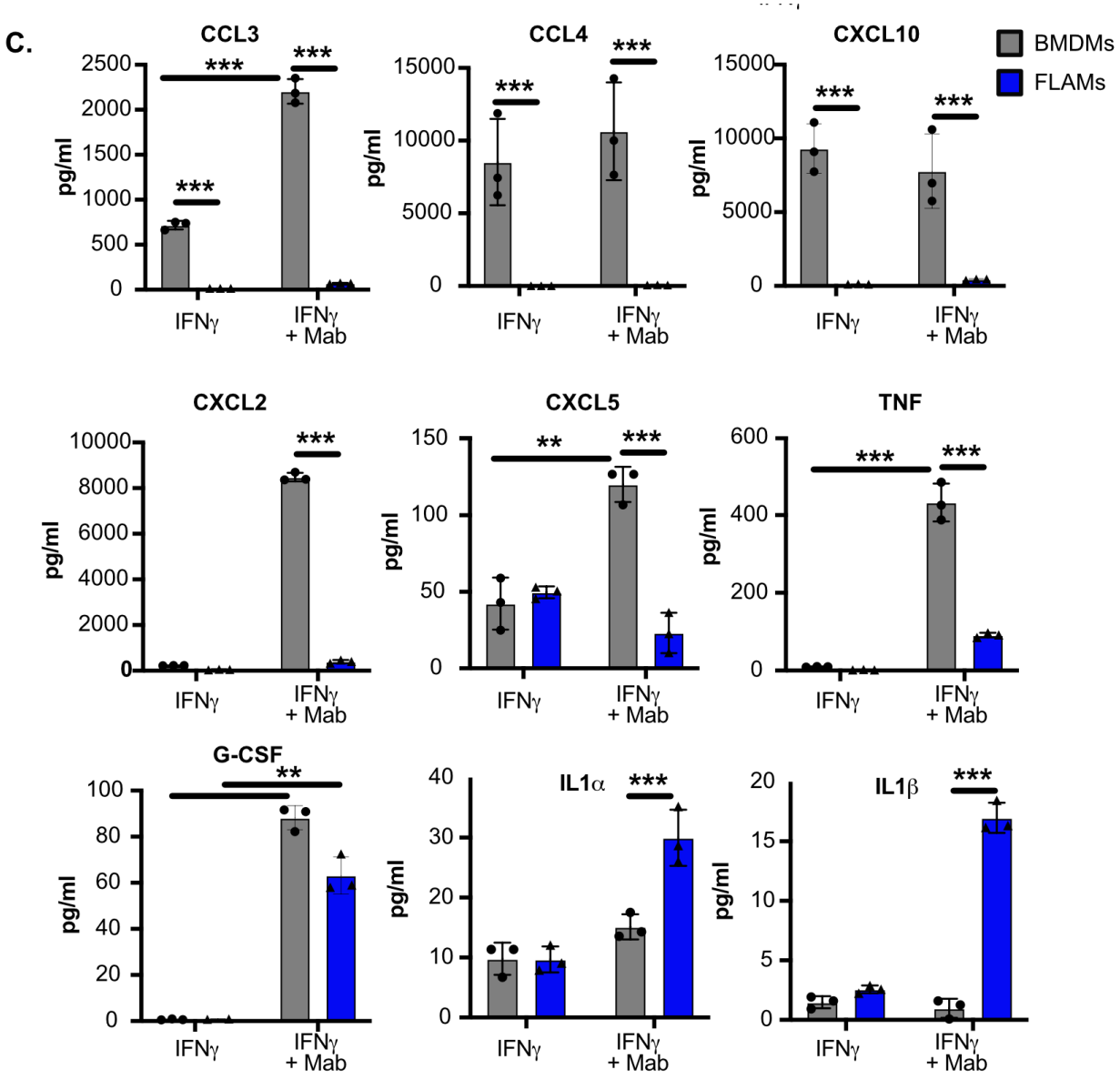

Figure 2.7. IFNγ drives more robust NF-κB activation in Mab infected FLAMs. (A) A principal component analysis (PCA) plot comparing the similarity of the transcriptional responses of (Top) IFNγ-activated BMDMs and FLAMs during Mab infection and (Bottom) all conditions examined in BMDMs and FLAMs during Mab infection. **(B)** Venn Diagrams showing shared and unique genes that were significantly induced or repressed in IFNγ-activated BMDMs and FLAMs during Mab infection using DeSeq2. **(C)** Representative clusters of genes that respond similarly to Mab infection in IFNγ-activated BMDMs and FLAMs over time. **(D)** Normalized counts of NF-κB genes from the KEGG pathway set were compared across the indicated conditions in FLAMs and is expressed as a heat map. The color scale represents the z-score calculated from normalized read counts across samples for each gene. **(E)** Normalized counts of a subset of NF-κB genes that were differentially regulated in BMDMs (gray) and FLAMs (blue) during Mab infection. Statistical significance was determined based on adjusted *p*-values using DeSeq2.

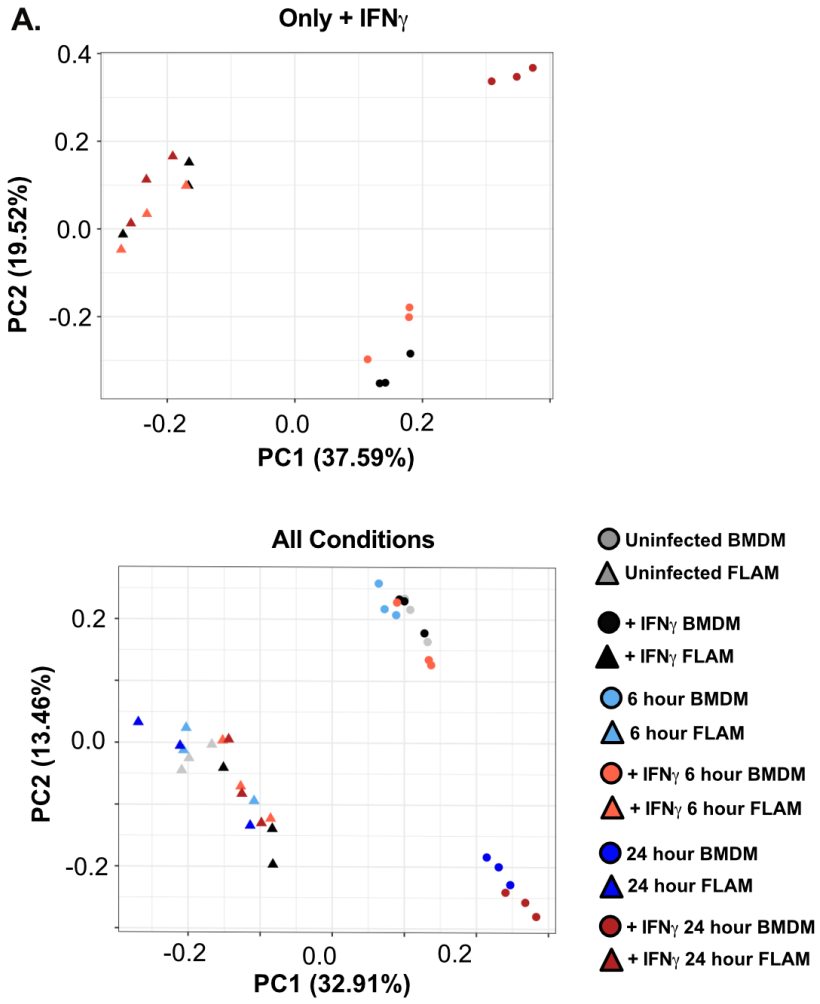

Figure 2.7 (cont'd)

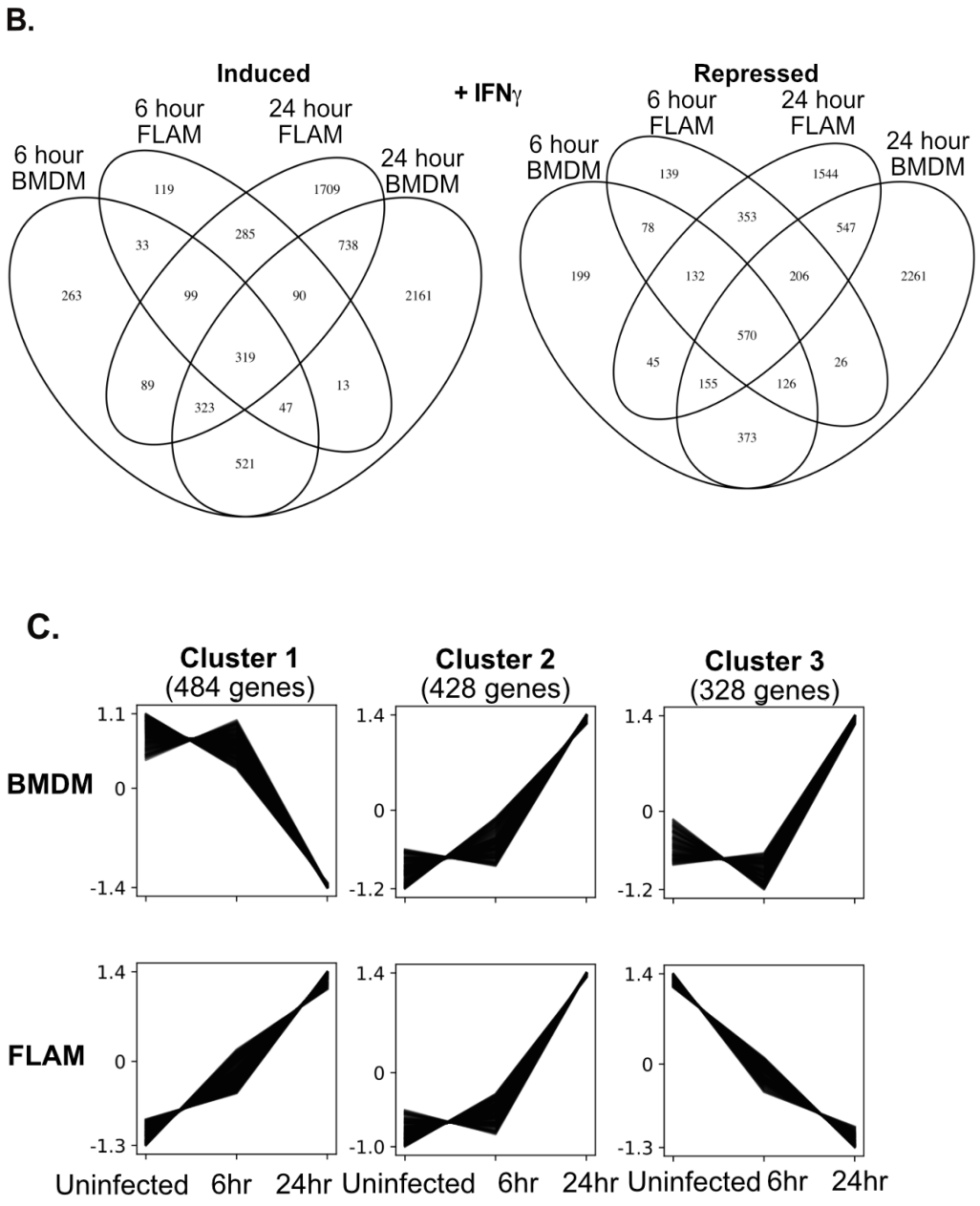

Figure 2.7 (cont'd)

Figure 2.7 (cont'd)

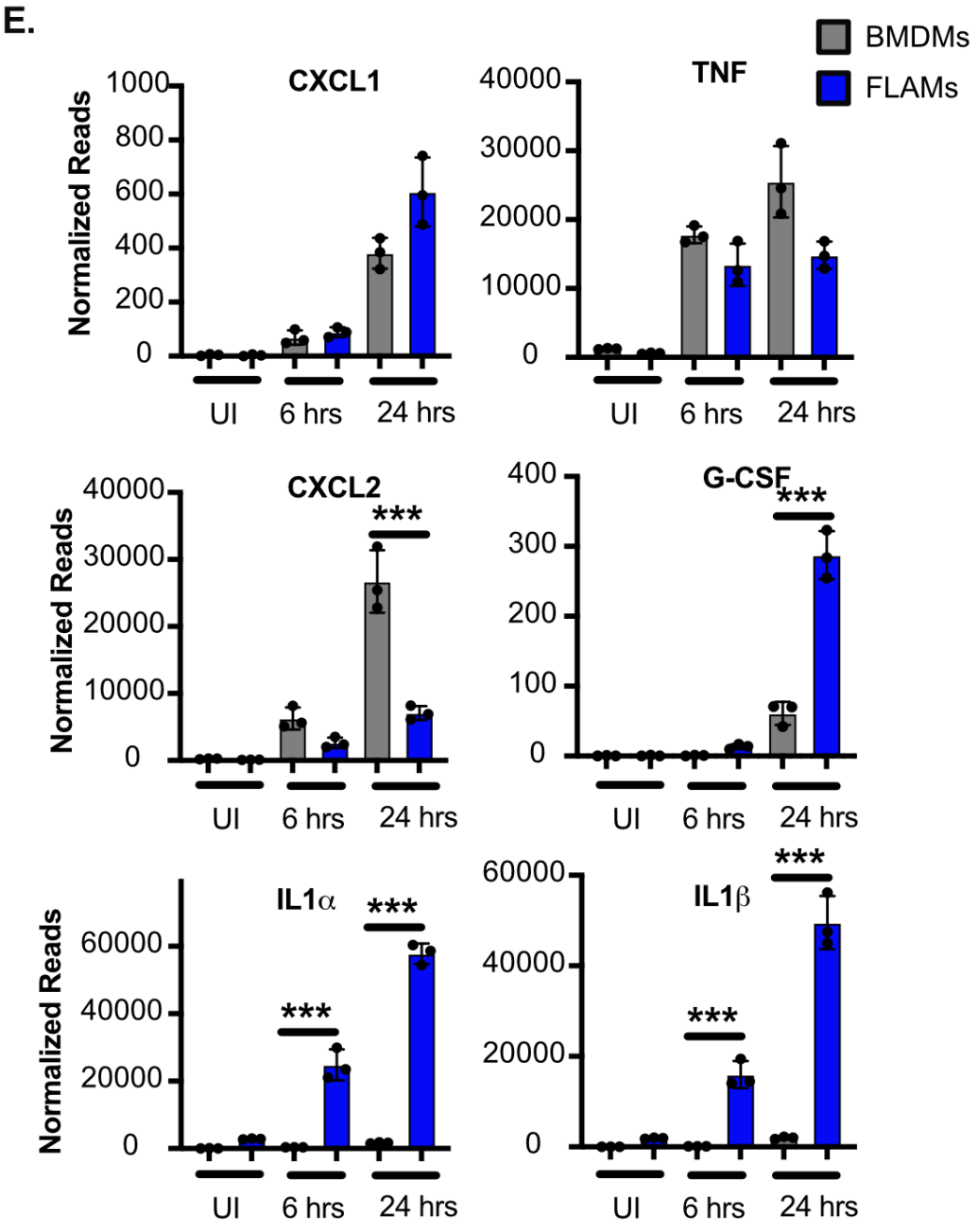

Figure 2.8. Chemical activation of HIF1α increases Nos2 expression in IFNγ-activated FLAMs following Mab infection. (A) Normalized counts of Nos2 and Ptgs2 in IFNγ-activated BMDMs (gray) and FLAMs (blue) during Mab infection. **(B)** Normalized counts of HIF1α in resting or IFNγ-activated BMDMs (gray) and FLAMs (blue) during Mab infection from the RNAseq dataset. **(C)** FLAMs were left untreated or were treated with 25ng/ml of IFNγ and/or 250μM DMOG and 12 hours later cells were infected with Mab for 4 hours. 24 hours later, RNA was isolated and qRT-PCR was used to determine the relative expression of *Nos2* compared to *B-actin* controls. **(D)** FLAMs were left untreated or were treated with 25ng/ml of IFNγ and/or 250μM DMOG and 12 hours later cells were infected with Mab for 4 hours. 24 hours later, 50μL of cell supernatants were used to measure the concentration of NO2- at each condition. Statistical significance for normalized reads was determined based on adjusted *p*-values using DeSeq2. **p<.01 ***p<.001 by two-way ANOVA with a Tukey correction for multiple comparisons.

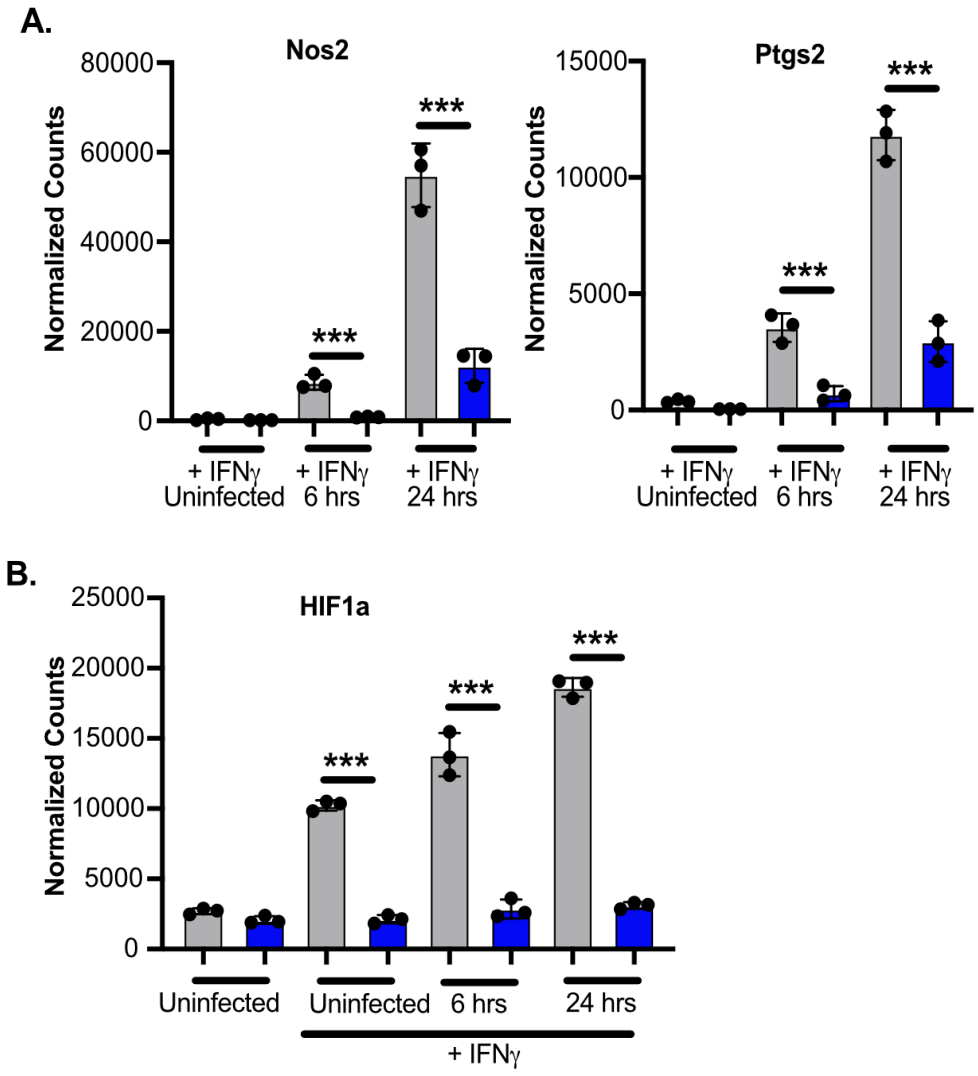

Figure 2.8 (cont'd)

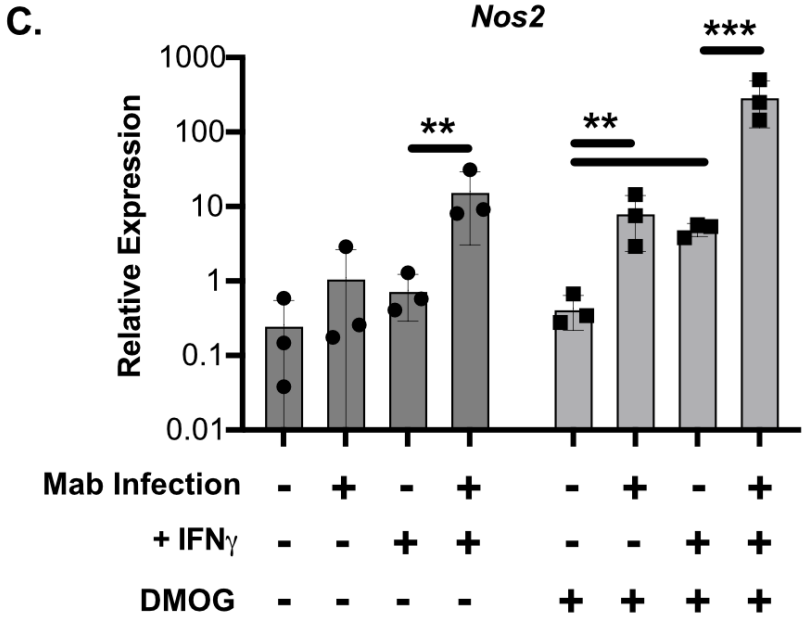

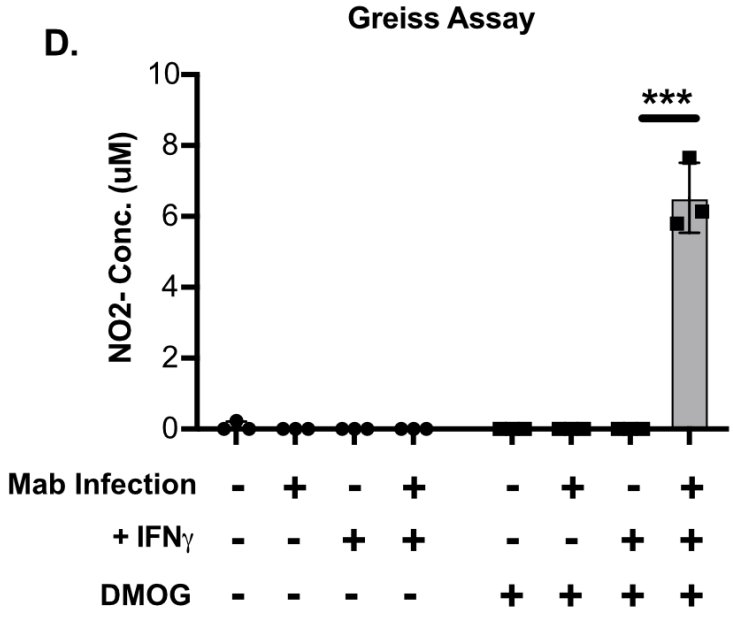

DISCUSSION

Respiratory infections with Mab are an increasing clinical concern. Given the high failures rates of antibiotic therapy and no protective host-directed therapies or vaccines available, understanding how Mab is effectively controlled in some hosts and not in others is critically important. Here, we leveraged new *ex vivo* models of lung-specific alveolar macrophages to better understand key differences in the innate response during Mab infection between distinct macrophage subtypes. Our data suggest that while both BMDMs and FLAMs control Mab infection independently of IFNγ-activation, they sense and respond to Mab infection in distinct ways. Myeloid-derived BMDMs were more inflammatory driving higher levels of cytokines, chemokines, and activated markers, in contrast FLAMs were less inflammatory with lower expression of inflammatory genes. Our findings highlight the importance of defining host-pathogen interactions in a range of tissue relevant immune cells to better identify mechanisms that contribute to control of Mab and other respiratory infections.

Mab infects macrophages which serve as a key intracellular niche throughout infection [53, 54]. The intracellular dynamics of Mab however, remain relatively uncharacterized. In contrast to other studies, our findings using an array of readouts including bulk CFU counts as well as single cell flow cytometry approaches suggest that Mab does not replicate to high levels in either BMDMs or FLAMs. Instead, intracellular Mab is maintained at a steady state over the first 2 days of infection while not inducing high levels of cell death. Whether this steady state is indicative of static growth, or equivalent rates of growth and death remains to be determined but will be important to better understand the mechanisms controlling early Mab interactions with macrophages. Given the importance of IFNγ in controlling mycobacterial infections and the inflammatory environment seen in patients susceptible to Mab infection, it was surprising that

we found very little effect of IFNγ-activation on intracellular dynamics of Mab infection. This is in contrast to *Mycobacterium tuberculosis,* which is readily restricted in IFNγ-activated BMDMs. It is possible that Mab is more resistant than Mtb to intracellular antimicrobial poisons. Alternatively, Mab may be maintained in a distinct intracellular compartment that is resistant to IFNγ-inducible effectors. Future work will be needed to better understand the intracellular dynamics of Mab infections, with particular focus on important macrophage pathways that control the replication of this opportunistic pathogen.

A key finding throughout our study was the distinct inflammatory responses that Mab activated in FLAMs and BMDMs. In general, BMDMs were more hyper-inflammatory, producing higher levels of chemokines like CXLC1 and CXCL2 and cytokines like TNF and G-CSF in both the presence and absence of IFNγ activation. One possible mechanism driving inflammatory differences is the activity of transcriptions factors, such as Nrf2 and NF-κB. Our data suggests that while loss of Nrf2 results in increased basal inflammation, it does not alter Mab dependent inflammatory responses in FLAMs. In contrast, we found that NF-κB was driving high expression of a subset of cytokines including TNF and CXCL10 in BMDMs and that NF-κB was not robustly induced in FLAMs. While IFNγ activation drove more NF-κB activation in FLAMs, many key genes remained lower than BMDMs. This included *Nos2*, which we found could be increased in FLAMs treated with IFNγ and the HIF1α activator DMOG. HIF1α is known to be interlinked with the shift of IFNγ-activated cells towards aerobic glycolysis [51, 52]. Thus, taken together we speculate that one key driver of the distinct activation of NF-κB and HIF1α in FLAMs and BMDMs during Mab infection is metabolic differences. Understanding how metabolism drives differences between FLAMs and BMDMs and manipulating these pathways genetically or chemically in resting, activated and infected

conditions will be an important next step to define the underlying mechanisms of inflammatory regulation in distinct macrophage subsets.

Mab respiratory infections are cleared by the majority of immunocompetent patients, yet the mechanisms mediating this control remain unclear. AMs are the first line of immune defense and our results using FLAMs as a model for AMs suggests these cells control Mab infection without driving a severe inflammatory response. Patients who are susceptible to Mab have pre-existing lung conditions that disrupt the normal state of alveolar macrophages through activation, including IFNγ-stimulation, and the recruitment of myeloid-derived macrophages. The inflammatory environment in the lungs and the ontogeny of airway macrophages during Mab infection may further contribute to inflammation, driving more tissue damage and increasing the severity of respiratory disease. Continuing to dissect how ongoing inflammation in susceptible patients dampens pathogen control without driving lung disease will aid in the identification of new therapeutic opportunities that could be used synergistically with antibiotic therapy.

One important shortcoming of our study is the Mab strain used is a smooth colony variant. It is well known that Mab isolates can present as smooth variants through the expression of GPLs, with the loss of these GPLs resulting in rough colony variants [54-56]. In clinical studies, both smooth and rough variants are isolated from patients, with data suggesting the host environment drives increased transition from the smooth to rough variant during infection [54, 57]. Rough Mab drives more inflammatory cytokines, such as TNF, compared to smooth Mab when infecting BMDMs [53, 58]. Rough isolates are also suggested to result in bacterial cording phenotypes that further drive inflammatory responses [37, 55]. Whether other bacterial factors in addition to GPL expression drive inflammation in macrophages remains to be fully understood. Furthermore, how AMs or FLAMs differentially sense and induce inflammation against rough

and smooth Mab isolates and other bacterial factors that modulate host inflammation remains to be tested.

Taken together our study identified many key differences in the inflammatory response of distinct macrophage subsets following infection with Mab. These differences in the innate immune response occurred independently of differences in bacterial control or cell death. Thus, the innate immune wiring of distinct macrophage subsets is unique. These results can now be used to identify the importance of distinct innate sensing pathways during infection with Mab and other respiratory pathogens to develop new host-directed therapies that prevent infection while limiting inflammatory damage to the lungs.

MATERIALS AND METHODS

Mab culture conditions.

mEmerald GFP-expressing Mab (ATCC 19977) strains were generated as previously described [31]. All mEmerald GFP-expressing Mab cultures were grown aerobically at 37°C in Middlebrook 7H9 medium supplemented with 1% glycerol, 0.05% tween80 and 10% Middlebrook OADC (oleic acid, dextrose, catalase, and bovine albumin). To select for mEmerald GFP-expressing Mab, zeocin (Invivogen) was included at a final concentration of 5μg/mL.

Animal experiments.

All cell isolation involving live mice was performed in accordance with the recommendations from the Guide for the Care and Use of Laboratory Animals of the National Institutes of Health and the Office of Laboratory Animal Welfare. Mouse studies were performed using protocols approved by the Institutional Animal Care and Use Committee (IACUC). All mice were housed and bred under specific pathogen-free conditions and in accordance with Michigan State University (PROTO202200127) IACUC guidelines. All mice were monitored and weighed regularly. C57BL6/J mice (# 000664) were purchased from The Jackson Laboratory.

BMDM and FLAM cell isolation, maintenance, and culture conditions.

HoxB8-conditionally immortalized macrophages from C57BL6/J mice were maintained in media containing 30ng/mL recombinant mGM-CSF (Peprotech), 10% fetal bovine serum (FBS) and 0.5μM β-Estradiol as previously described [59-61]. To generate BMDMs, cells were washed in PBS to remove estradiol, then plated in DMEM containing 25ng/ml M-CSF (Peprotech) and 10% FBS. Five to seven days later, cells were plated for experiments as described in figure legends. For FLAMs, C57BL/6J pregnant dam mice were euthanized by CO_2

prior to cervical dislocation and fetal liver derived cells were obtained as previously described [38]. Cells were cultured in complete Roswell Park Memorial Institute medium (RPMI; Thermo Fisher) containing 10% FBS, 30ng/ml recombinant mGM-CSF (Peprotech), and 20ng/mL recombinant hTGF-β1 (Peprotech). All macrophages were incubated in 5% CO_2 at 37°C. FLAMs were monitored regularly by flow cytometry for the continued expression of alveolar macrophage markers.

Macrophage infections.

Single cell Mab suspensions were prepared by resuspending logarithmic phase bacteria in the appropriate macrophage cell culture media followed by a soft spin at 58 xg to pellet large bacterial clumps. Macrophages were seeded at $5x10^5$/well in a 12-well and single cell Mab supernatants were used for macrophage spinfections (spun at 58xg for 5 minutes) at the indicated MOIs. Four hours later, infection media was removed and media containing 64μg/mL Amikacin was added for the remainder of the experiment. At each indicated timepoint (4 to 48 hours), macrophages were washed with PBS, lifted from plates by scrapping or Accutase™ (BioLegend) treatment, then fixed in 4% paraformaldehyde. Infected macrophages were quantified using the BD LSR II (BD Biosciences) or Attune CytPix Flow Cytometer (Thermo Fisher Scientific) at the Michigan State University Flow Cytometry Core. Live and single macrophages were identified using forward and side scatter and the mean fluorescent intensity of infected cells was determined by the fluorescence in the GFP channel. All experiments included uninfected and unstained controls to set gates for infected macrophage quantification. Analysis was performed using FlowJo V10.

For IFNγ activated macrophage experiments, cells were treated with 25ng/mL IFNγ (Peprotech) for 16-20 hours. Following macrophage activation, IFNγ containing media was

removed and infection media was added as described above. Four hours later, infection media was removed and media containing 64μg/mL Amikacin and 25ng/mL IFNγ was added for the remainder of the experiment. Cells were lifted and analyzed by Flow Cytometry as described above.

For intracellular growth experiments, macrophages were lysed at the indicated time points (12, 24 and 48 hours) with sterile cold distilled water. Following 10-fold serial dilutions on Middlebrook 7H10 agar supplemented with Middlebrook OADC and 5 μg/mL zeocin, samples were plated to perform colony forming unit (CFU) counts. Colonies were enumerated after 4-5 days of incubation at 37°C.

For flow cytometry cell death experiments, macrophages were lifted at the indicated time points (4 to 48 hours), then stained with Zombie Red Live/Dead stain (Biolegend). Once stained, cells were washed with PBS and fixed in 4% paraformaldehyde before being analyzed by Flow cytometry. For CellTiter Glo Cells were seeded in 96-well opaque plates the day prior to the experiment and stimulated with 25ng/mL of IFNγ (Prepotech) overnight. The following day, macrophages were infected as described above. At the indicated time points, viability measurements were performed following CellTiter Glo manufacture instructions. Briefly, 100μL of CellTiter Glo® Reagent was added directly to each well and plates were incubated for two minutes with shaking to induce cell lysis. Plates were then incubated for 10 more minutes at room temperature to stabilize luminescent signal and luminescence was measured on a Spark® multimode microplate reader (Tecan). Luminescence signal was normalized to uninfected cells.

Griess Assay.

The quantity of nitric oxide production by macrophages was determined by measuring its stable end product nitrite (Griess Assay, Promega). Briefly, 50uL of supernatant was transferred

to a 96-well plate, followed by 50μL of sulphanilamide and 50μL of N-1-napthylethylenediamine dihydrochloride (NED) under acidic conditions. Following incubation, absorbance was measured at 540nm on a Tecan Spark 20M plate reader and nitrite concentrations were calculated using a standard nitrite curve per manufacture instructions.

RNA isolation and qRT-PCR.

At the indicated time points (6 and 24 hours) macrophages from 6-well plates were resuspended in 1000 μL of TRIzol reagent (Life Technologies) and incubated for 5 minutes at room temperature. 200μL of chloroform was added to the homogenate, vortexed and centrifuged at 10,000 x g for 18 min at 4°C to separate nucleic acids. The upper aqueous phase was removed and combined with equal parts ethanol. This mixture was placed into a collection tube and protocols provided by the Zymo Research Direct-zol RNA extraction kit were followed. Quantity and purity of the RNA were checked using a NanoDrop and diluted to 5 ng/mL in nuclease-free water. The one-step Syber Green RT-PCR kit (Qiagen) reagents were used to amplify RNA according to manufacture instructions. Amplifications were monitored using the QuantStudio3 (ThermoFisher). Relative mRNA expression levels were calculated after normalization to β-actin.

Cytokine analysis.

Where indicated, supernatants were filter sterilized before cytokines were quantified by a Luminex multiplex assay (Eve Technology). In addition, filter sterilized supernatants from Mab-challenged and control macrophages were harvested and the indicated cytokine proteins levels were determined using CXCL10, TNF or IL1α DuoSet ELISA kits (R&D Systems) following manufacture instructions. Absorbance (450nm) was detected on a Spark® multimode microplate reader (Tecan).

RNA Sequencing and Analysis.

This work was supported in part by Michigan State University through computational resources provided by the Institute for Cyber-Enabled Research. RNASeq read quality assessment, mapping, and counting were performed using a custom pipeline built in Snakemake version 7.32.4 (https://github.com/kaylaconner/olivelab-rnaseq/tree/main) [62]. Read quality was assessed using FastQC version 0.12.1 [63] . Read mapping was performed against the GRCm39 mouse reference genome using Bowtie2 version 2.5.1 [64]. Aligned reads counts were assessed using the featurecounts function from the Subread package version 2.0.6 [65]. Differential gene expression analysis was conducted using the DESeq2 package version 1.42.0 in R version 4.3.2 [66]. Pre-filtering was performed to keep only genes that had >10 counts in 3 or more samples.

Principal component analyses (PCA) were performed using the prcomp function with scaling on normalized count matrices of all genes in R version 4.3.2, and PCA visualization was done using the autoplot function in ggplot2 version 3.4.4 [67]. Magnitude/Amplitude (MA) plots were produced by plotting Log2(Fold Change) and Log2(Base Mean) values from DESeq2 in ggplot2 version 3.4.4 [67]. Heatmaps were produced in GraphPad Prism version 9.4.1 using normalized counts data from DESeq2. Venn diagrams were produced using the VennDiagram package version 1.7.3 in R version 4.3.2 [68]. Gene clustering analysis was performed using Clust 1.18.0 [69]. All gene ontology analysis was performed using the g:OSt functional profiling tool from the g:Profiler web server version *e111_eg58_p18_30541362* (database last updated on 25/01/2024) [70].

Statistical analysis and data visualization.

Statistical analysis was performed using Prism Version 10 (GraphPad) as indicated in the Figure Legends. Data are presented, unless otherwise indicated, as mean ± standard deviation.

One-way or two-way ANOVA followed by Tukey's post hoc test was used to identify significant differences between multiple groups, and Student's t-tests were used to compare 2 groups.

REFERENCES

1. Johansen, M.D., J.L. Herrmann, and L. Kremer, *Non-tuberculous mycobacteria and the rise of Mycobacterium abscessus.* Nat Rev Microbiol, 2020. **18**(7): p. 392-407.

2. Sharma, S.K. and V. Upadhyay, *Epidemiology, diagnosis & treatment of non-tuberculous mycobacterial diseases.* Indian J Med Res, 2020. **152**(3): p. 185-226.

3. Prevots, D.R., et al., *Nontuberculous mycobacterial lung disease prevalence at four integrated health care delivery systems.* Am J Respir Crit Care Med, 2010. **182**(7): p. 970-6.

4. Victoria, L., et al., *Mycobacterium abscessus complex: A Review of Recent Developments in an Emerging Pathogen.* Front Cell Infect Microbiol, 2021. **11**: p. 659997.

5. Roux, A.L., et al., *Multicenter study of prevalence of nontuberculous mycobacteria in patients with cystic fibrosis in france.* J Clin Microbiol, 2009. **47**(12): p. 4124-8.

6. Olivier, K.N., et al., *Nontuberculous mycobacteria. I: multicenter prevalence study in cystic fibrosis.* Am J Respir Crit Care Med, 2003. **167**(6): p. 828-34.

7. De Rose, V., et al., *Airway Epithelium Dysfunction in Cystic Fibrosis and COPD.* Mediators Inflamm, 2018. **2018**: p. 1309746.

8. Fahy, J.V. and B.F. Dickey, *Airway mucus function and dysfunction.* N Engl J Med, 2010. **363**(23): p. 2233-47.

9. Daley, C.L., et al., *Treatment of Nontuberculous Mycobacterial Pulmonary Disease: An Official ATS/ERS/ESCMID/IDSA Clinical Practice Guideline.* Clin Infect Dis, 2020. **71**(4): p. 905-913.

10. Nessar, R., et al., *Mycobacterium abscessus: a new antibiotic nightmare.* J Antimicrob Chemother, 2012. **67**(4): p. 810-8.

11. Jarand, J., et al., *Clinical and microbiologic outcomes in patients receiving treatment for Mycobacterium abscessus pulmonary disease.* Clin Infect Dis, 2011. **52**(5): p. 565-71.

12. Kreda, S.M., C.W. Davis, and M.C. Rose, *CFTR, mucins, and mucus obstruction in cystic fibrosis.* Cold Spring Harb Perspect Med, 2012. **2**(9): p. a009589.

13. Moni, S.S. and A. Al Basheer, *Molecular targets for cystic fibrosis and therapeutic potential of monoclonal antibodies.* Saudi Pharm J, 2022. **30**(12): p. 1736-1747.

14. Murray, P.J. and T.A. Wynn, *Protective and pathogenic functions of macrophage subsets.* Nat Rev Immunol, 2011. **11**(11): p. 723-37.

15. Byrne, A.J., et al., *Pulmonary macrophages: key players in the innate defence of the airways.* Thorax, 2015. **70**(12): p. 1189-96.

16. Croasdell, A., et al., *PPARgamma and the Innate Immune System Mediate the Resolution of Inflammation.* PPAR Res, 2015. **2015**: p. 549691.

17. McQuattie-Pimentel, A.C., et al., *The lung microenvironment shapes a dysfunctional response of alveolar macrophages in aging.* J Clin Invest, 2021. **131**(4).

18. Ankley LM, C.K., Vielma TE, Godfrey JJ, Thapa M, Olive AJ., *GSK3α/β Restrain IFN-γ-Inducible Costimulatory Molecule Expression in Alveolar Macrophages, Limiting CD4+ T Cell Activation.* Immunohorizons, 2024. **8**(2): p. 147-162.

19. Srivastava, S. and J.D. Ernst, *Cutting edge: Direct recognition of infected cells by CD4 T cells is required for control of intracellular Mycobacterium tuberculosis in vivo.* J Immunol, 2013. **191**(3): p. 1016-20.

20. Huang, L., et al., *Growth of Mycobacterium tuberculosis in vivo segregates with host macrophage metabolism and ontogeny.* J Exp Med, 2018. **215**(4): p. 1135-1152.

21. Pisu, D., et al., *Dual RNA-Seq of Mtb-Infected Macrophages In Vivo Reveals Ontologically Distinct Host-Pathogen Interactions.* Cell Rep, 2020. **30**(2): p. 335-350 e4.

22. Goulding, J., et al., *Respiratory infections: do we ever recover?* Proc Am Thorac Soc, 2007. **4**(8): p. 618-25.

23. Walzl, G., Taguro, S., Moss, P., Openshaw, P., Hussell. T, *Influenza Virus Lung Infection Protects from Respiratory Syncytial Virus-induced Immunopathology.* JEM, 2000. **192**(9): p. 1317-1326.

24. Walzl, G., Humphreys, I.R., Marshall, B.G., Eswards, L., Openshaw P., Shaw, R., Hussell, T., *Prior Exposure to Live Mycobacterium bovis BCG Decreases Cryptococcus neoformans-Induced Lung Eosinophilia in a Gamma Interferon-Dependent Manner.* Infect Immun, 2003. **71**(6).

25. Schneider, W.M., M.D. Chevillotte, and C.M. Rice, *Interferon-stimulated genes: a complex web of host defenses.* Annu Rev Immunol, 2014. **32**: p. 513-45.

26. Rosain, J., et al., *Mendelian susceptibility to mycobacterial disease: 2014-2018 update.* Immunol Cell Biol, 2019. **97**(4): p. 360-367.

27. Rothman, G.T.a.P., *Biological functions of the IFN-γ receptors.* Allergy, 1999. **54**(12): p. 1233-1251.

28. Kak, G., M. Raza, and B.K. Tiwari, *Interferon-gamma (IFN-gamma): Exploring its implications in infectious diseases.* Biomol Concepts, 2018. **9**(1): p. 64-79.

29. Thiel, B.A., et al., *Human alveolar macrophages display marked hypo-responsiveness to IFN-gamma in both proteomic and gene expression analysis.* PLoS One, 2024. **19**(2): p. e0295312.

30. Ahn, J.H., et al., *Type I Interferons Are Involved in the Intracellular Growth Control of Mycobacterium abscessus by Mediating NOD2-Induced Production of Nitric Oxide in Macrophages.* Front Immunol, 2021. **12**: p. 738070.

31. Gilliland HN., B.O., Olive AJ *A Genome-Wide Screen in Macrophages Defines Host Genes Regulating the Uptake of Mycobacteirum abscessus.* mSphere, 2023. **8**(2): p. e0066322.

32. Laencina, L., et al., *Identification of genes required for Mycobacterium abscessus growth in vivo with a prominent role of the ESX-4 locus.* Proc Natl Acad Sci U S A, 2018. **115**(5): p. E1002-E1011.

33. Le Moigne, V., et al., *MgtC as a Host-Induced Factor and Vaccine Candidate against Mycobacterium abscessus Infection.* Infect Immun, 2016. **84**(10): p. 2895-903.

34. Means, T.K., et al., *Differential effects of a Toll-like receptor antagonist on Mycobacterium tuberculosis-induced macrophage responses.* J Immunol, 2001. **166**(6): p. 4074-82.

35. Shin, D.M., et al., *Mycobacterium abscessus activates the macrophage innate immune response via a physical and functional interaction between TLR2 and dectin-1.* Cell Microbiol, 2008. **10**(8): p. 1608-21.

36. Bernut, A., et al., *Mycobacterium abscessus-Induced Granuloma Formation Is Strictly Dependent on TNF Signaling and Neutrophil Trafficking.* PLoS Pathog, 2016. **12**(11): p. e1005986.

37. Bernut, A., et al., *Mycobacterium abscessus cording prevents phagocytosis and promotes abscess formation.* Proc Natl Acad Sci U S A, 2014. **111**(10): p. E943-52.

38. Thomas, S.T., et al., *Fetal Liver-Derived Alveolar-like Macrophages: A Self-Replicating Ex Vivo Model of Alveolar Macrophages for Functional Genetic Studies.* Immunohorizons, 2022. **6**(2): p. 156-169.

39. Fejer, G., et al., *Nontransformed, GM-CSF-dependent macrophage lines are a unique model to study tissue macrophage functions.* Proc Natl Acad Sci U S A, 2013. **110**(24): p. E2191-8.

40. Luo, M., et al., *Development of an Optimized Culture System for Generating Mouse Alveolar Macrophage-like Cells.* J Immunol, 2021. **207**(6): p. 1683-1693.

41. Guilliams, M., et al., *Alveolar macrophages develop from fetal monocytes that differentiate into long-lived cells in the first week of life via GM-CSF.* J Exp Med, 2013. **210**(10): p. 1977-92.

42. Yu, X., et al., *The Cytokine TGF-beta Promotes the Development and Homeostasis of Alveolar Macrophages.* Immunity, 2017. **47**(5): p. 903-912 e4.

43. Rothchild, A.C., et al., *Alveolar macrophages generate a noncanonical NRF2-driven transcriptional response to Mycobacterium tuberculosis in vivo.* Sci Immunol, 2019. **4**(37).

44. Mai, D., et al., *Exposure to Mycobacterium remodels alveolar macrophages and the early innate response to Mycobacterium tuberculosis infection.* PLoS Pathog, 2024. **20**(1): p. e1011871.

45. Bai, X., et al., *Inhibition of nuclear factor-kappa B activation decreases survival of Mycobacterium tuberculosis in human macrophages.* PLoS One, 2013. **8**(4): p. e61925.

46. Abdelaal, H.F.M., et al., *Mycobacterium abscessus: It's Complex.* Microorganisms, 2022. **10**(7).

47. Braverman, J. and S.A. Stanley, *Nitric Oxide Modulates Macrophage Responses to Mycobacterium tuberculosis Infection through Activation of HIF-1alpha and Repression of NF-kappaB.* J Immunol, 2017. **199**(5): p. 1805-1816.

48. Braverman, J., et al., *HIF-1alpha Is an Essential Mediator of IFN-gamma-Dependent Immunity to Mycobacterium tuberculosis.* J Immunol, 2016. **197**(4): p. 1287-97.

49. Mishra, B.B., et al., *Nitric oxide prevents a pathogen-permissive granulocytic inflammation during tuberculosis.* Nat Microbiol, 2017. **2**: p. 17072.

50. Jantsch, J., et al., *Toll-like receptor activation and hypoxia use distinct signaling pathways to stabilize hypoxia-inducible factor 1alpha (HIF1A) and result in differential HIF1A-dependent gene expression.* J Leukoc Biol, 2011. **90**(3): p. 551-62.

51. Li, C., et al., *HIF1alpha-dependent glycolysis promotes macrophage functional activities in protecting against bacterial and fungal infection.* Sci Rep, 2018. **8**(1): p. 3603.

52. Wang, T., et al., *HIF1alpha-Induced Glycolysis Metabolism Is Essential to the Activation of Inflammatory Macrophages.* Mediators Inflamm, 2017. **2017**: p. 9029327.

53. Roux, A.L., et al., *The distinct fate of smooth and rough Mycobacterium abscessus variants inside macrophages.* Open Biol, 2016. **6**(11).

54. Kim, B.R., et al., *Phagosome Escape of Rough Mycobacterium abscessus Strains in Murine Macrophage via Phagosomal Rupture Can Lead to Type I Interferon Production and Their Cell-To-Cell Spread.* Front Immunol, 2019. **10**: p. 125.

55. Gutierrez, A.V., et al., *Glycopeptidolipids, a Double-Edged Sword of the Mycobacterium abscessus Complex.* Front Microbiol, 2018. **9**: p. 1145.

56. Howard, S.T., et al., *Spontaneous reversion of Mycobacterium abscessus from a smooth to a rough morphotype is associated with reduced expression of glycopeptidolipid and reacquisition of an invasive phenotype.* Microbiology (Reading), 2006. **152**(Pt 6): p. 1581-1590.

57. Bernut, A., et al., *CFTR Protects against Mycobacterium abscessus Infection by Fine-Tuning Host Oxidative Defenses.* Cell Rep, 2019. **26**(7): p. 1828-1840 e4.

58. Rhoades, E.R., et al., *Mycobacterium abscessus Glycopeptidolipids mask underlying cell wall phosphatidyl-myo-inositol mannosides blocking induction of human macrophage TNF-alpha by preventing interaction with TLR2.* J Immunol, 2009. **183**(3): p. 1997-2007.

59. Kiritsy, M.C., et al., *A genetic screen in macrophages identifies new regulators of IFNgamma-inducible MHCII that contribute to T cell activation.* Elife, 2021. **10**.

60. Roberts, A.W., et al., *Cas9(+) conditionally-immortalized macrophages as a tool for bacterial pathogenesis and beyond.* Elife, 2019. **8**.

61. Johnson BK, T.S., Olive AJ, Abramovitch RB, *Macrophage Infection Models for Mycobacterium tuberculosis.* Methods in Molecular Biology, 2021. **2314**: p. 167-182.

62. Köster, J. and S. Rahmann, *Snakemake--a scalable bioinformatics workflow engine.* Bioinformatics, 2012. **28**(19): p. 2520-2.

63. Andrews, S. *FastQC: A Quality Control Tool for High Throughput Sequence Data*. 2010; Available from: http://www.bioinformatics.babraham.ac.uk/projects/fastqc/.

64. Langmead, B. and S.L. Salzberg, *Fast gapped-read alignment with Bowtie 2.* Nat Methods, 2012. **9**(4): p. 357-9.

65. Liao, Y., G.K. Smyth, and W. Shi, *featureCounts: an efficient general purpose program for assigning sequence reads to genomic features.* Bioinformatics, 2014. **30**(7): p. 923-30.

66. Love, M.I., W. Huber, and S. Anders, *Moderated estimation of fold change and dispersion for RNA-seq data with DESeq2.* Genome Biol, 2014. **15**(12): p. 550.

67. H, W., *ggplot2: Elegant Graphics for Data Analysis*. 2016, New York: Springer-Verlag.

68. Chen, H.a.B., P.C., *VennDiagram: a package for the generation of highly-customizable Venn and Euler diagrams in R.* BMC Bioinformatics, 2011. **12**(35).

69. Abu-Jamous, B. and S. Kelly, *Clust: automatic extraction of optimal co-expressed gene clusters from gene expression data.* Genome Biol, 2018. **19**(1): p. 172.

70. Reimand, J., et al., *g:Profiler--a web-based toolset for functional profiling of gene lists from large-scale experiments.* Nucleic Acids Res, 2007. **35**(Web Server issue): p. W193-200.

CHAPTER 4: Concluding Remarks and Future Directions.

The increasing prevalence of *Mycobacterium abscessus* (Mab) infections seen in patients with acquired or chronic lung disease is concerning [1-3]. These infections are complicated by Mab's natural recalcitrance to antibiotics, directly increasing treatment timelines and worsening patient compliance [1, 4, 5]. In response, the research community began dissecting Mab virulence factors, Mab antibiotic resistance mechanisms, additional drug options, and host-Mab interactions in the hopes of improving available treatment options [6-10]. Yet, a key question regarding Mab lung infections remains unanswered: Why is Mab cleared by healthy lungs with relative ease? In this dissertation, I started answering this complex question by leveraging distinct macrophage models to begin understanding how these important intracellular niches interact with and respond to Mab during infection.

I began by looking at early macrophage interactions with Mab. Macrophages are the first immune cells Mab encounters during infection and represent an important intracellular niche for this opportunistic pathogen. By defining unique interactions occurring at this early macrophage-Mab interface, we can better understand how Mab may be leveraging its interactions with macrophages to gain an advantage. To do this I used our loss-of-function (LOF) macrophage library to screen for macrophage genes required to initiate Mab uptake. In addition to known uptake receptors, I identified a unique requirement for sulfated glycosaminoglycan (sGAG) synthesis in Mab uptake by macrophages. Downstream mechanistic experiments showed a novel mechanism where sGAGs are required to maintain known uptake receptors on the surface of the macrophage.

Then, in Chapter 3 we began to explore how unique macrophage subsets respond to Mab infection. Alveolar macrophages are the native macrophage subset populating the lung environment from birth. However, in patients with acquired or chronic lung disease, where

chronic inflammation and tissue damage are present, there is a rapid decline in alveolar macrophage populations seen in the lungs [11, 12]. As a result, resident alveolar macrophages are replaced by recruited myeloid derived macrophages that help aide in infection control [11, 12]. As such, it is important to consider the possibility of each subset being present during Mab infection. In chapter 3, we leverage our fetal liver derived alveolar macrophage (FLAM) and bone-marrow derived macrophage (BMDM) models to determine global differences in macrophage responses to Mab infection. Although we find minimal changes in Mab intracellular levels and macrophage cell death over the first few days of infection, global transcriptional and cytokine profile analysis reveal Mab infected FLAMs and BMDMs have significant differences in upregulated innate responses in both resting and IFNγ-activated states. Notably, NF-kB, a global transcription factor known to regulate inflammatory responses in macrophages, was not upregulated following Mab infection in FLAMs. Although activation of FLAMs with IFNγ prior to Mab infection led to increased NF-κB expression, there remains important global differences between FLAMs and BMDMs. For example, IFNγ-activated FLAMs did not induce high levels of the inducible nitric oxide synthase (iNOS). Mechanistic studies saw this phenotype reversed upon activation of HIF1α. Together, this chapter highlights the hypoinflammatory nature of FLAMs during Mab infection and defines global differences in innate immune responses between FLAMs and BMDMs following Mab exposure. Broadly, this study emphasizes the continued need for research defining how these global differences impact immune control.

Alveolar macrophages are essential to maintaining lung homeostasis, independent of lung infections [13, 14]. In patients with acquired lung disease, a decline in alveolar macrophage populations is often the result of off-target tissue damage and changes in cell activation states that result from chronic airway inflammation [12, 15]. Consequently, recruited myeloid derived

macrophages are leveraged to help maintain lung homeostasis [13, 15, 16]. As such, it is important to consider the biology of each macrophage subset, independent of infection, to gain insight into how alveolar macrophage biology differs from recruited myeloid derived macrophages. For example, alveolar macrophages primarily use fatty acid metabolism and oxidative phosphorylation to generate energy [17-19]. Whereas recruited myeloid derived macrophages primarily use glycolysis [20-22]. It is tempting to consider the significant impact this metabolic distinction can have on macrophage biology. The FLAM model has allowed our group to start exploring these mechanistic differences [23, 24]. Specifically, our initial studies characterizing FLAMs highlighted oxidative phosphorylation as a necessary pathway in maintaining known alveolar macrophage surface markers, like SiglecF [23]. Downstream comparative studies confirmed both alveolar macrophages and FLAMs rely on fatty acid metabolism and mitochondrial respiration to maintain AM-like qualities [24]. Expanding these studies to compare FLAM and BMDM immune activation, we found global differences in upregulated immune pathways and cytokine responses following IFNγ stimulus in BMDMs compared to FLAMs [24]. Further studies exploring alveolar macrophage metabolism and how this may impact immune activation are necessary. Beyond this, the FLAM cell model is currently being used to study differences in macrophage responses during bacterial and fungal lung infections, including Mab infection as previously described in this manuscript. With the scale and efficiency of these two models, we can further define alveolar macrophage immune regulation compared to other macrophage subsets as it pertains to macrophage biology and lung homeostasis prior to pathogen exposure.

Given the global differences in Mab control by FLAMs compared to BMDMs, future endeavors should focus on defining key pathways required for Mab uptake in FLAMs. In chapter

2, we identify sGAG synthesis as a key modulator for maintaining integrins on the surface of BMDMs to facilitate successful engulfment of Mab. It would be interesting to expand this study to define the requirement of sGAG synthesis in FLAM-Mab interactions during early infection as well. If sGAG synthesis is not important for FLAM uptake, these studies should consider global differences between BMDM and FLAM surface pattern recognition receptors. For example, CD14 is highly expressed on BMDMs, while MARCO is largely associated with alveolar macrophages [25]. Relative expression of these known pattern recognition receptors can influence upregulated antimicrobial responses, including inflammatory cytokine release and intracellular restriction mechanisms [26, 27]. It would be interesting to conduct a CRISPR-Cas9 LOF macrophage screen within CD14 knockout BMDMs or MARCO knockout FLAMs to identify host pathways with decreased Mab intracellular levels. In doing so, we would get critical insight into the role specific pattern recognition receptor expression has in mediating Mab control following infection.

Once Mab establishes infection, it is currently unclear how healthy lung environments efficiently contain infection. The current dogma suggests resident alveolar macrophages take-up Mab following exposure. These macrophages will then upregulate several intracellular antimicrobial responses, including increased phagosome-lysosome fusion events, induced ROS and NO expression and inflammatory cytokine release [28-33]. However, our data suggest alveolar macrophage control is not this simple. RNAseq and multiplex data from Chapter 3 show largely unaltered and hypoinflammatory responses in Mab infected FLAMs compared to BMDMs. This suggests a mechanism in which host alveolar macrophages are either innately primed against antimicrobial immune responses or that Mab is directly restricting these immune mechanisms. Xin et al. has recently shown that cross talk between alveolar macrophages and

alveolar epithelium cells during Legionella infection is critical to promote host defense mechanisms [34]. In this study, alveolar epithelium cells serve as a middleman between alveolar macrophages and circulating monocytes [34]. Mechanistic studies found this to be an IL-1 and GM-CSF dependent communication loop that led to the metabolic reprograming of circulating monocytes, allowing them to aid alveolar macrophages by mounting antimicrobial defenses against Legionella infection [34]. Notably, multiplex data from Chapter 3 shows significantly higher IL-1 cytokine production profiles in Mab infected FLAMs compared to BMDMs. Combined, it is tempting to hypothesize a similar forward feedback loop between alveolar macrophages, alveolar epithelial cells and circulating monocytes is also important during Mab pulmonary infection. Furthermore, mouse studies conducted by Rottman et al. have shown significant Mab survival rates in mice lacking TNF, suggesting it plays a crucial role in Mab containment [35]. We find TNF expression levels are low in FLAMs compared to BMDMs following infection. It is possible FLAMs are innately wired against TNF expression and instead favor crosstalk interactions with neighboring cells to induce the expression of TNF. This line of thinking makes sense when considering the lung environments in patients who are at-risk for Mab infection. In these lungs, chronic inflammation and mucus buildup may interfere with appropriate immune cell function as well as subsequent cell-to-cell interactions. Mechanistically, this would prevent appropriate immune responses from being initiated and permit Mab persistence. To determine if a three-way cell crosstalk mechanism is required for Mab control by alveolar macrophages, future studies should leverage genetically engineered mouse models, such as Cre/lox mice lacking alveolar epithelial cells, to identify unique cell subsets required for upregulating appropriate antimicrobial defense mechanisms against Mab infection [34]. Once identified, defining the cytokines driving these interactions should be explored, with particular

focus on IL-1, GM-CSF, and TNF as potential contributors that prime macrophage responses against Mab. Taken together, these studies would give insight into the immune mechanisms required for Mab control by alveolar macrophages.

In vivo studies using Rag2 and CD3ε deficient mice have implicated the importance of T-cells in Mab control [35, 36]. T-cells require three distinct signals to be activated by macrophages. The first signal is between antigen specific T-cell receptors (TCRs) and pathogen specific peptides loaded onto major histocompatibility complex class II (MHCII) on the macrophage membrane. The second signal is the binding of costimulatory molecules, including CD40, CD80 and CD86, on the macrophage membrane to their corresponding ligand on the T-cell. The third signal is driven by cytokines, including IFNγ and TNFα. Deficient Th1 responses, including IFNγ and TNFα cytokine production, are considered risk factors for Mab infection and impaired disease control [35, 36]. Notably, mechanistic interactions between macrophages and T-cell activation have yet to be explored following Mab infection. However, differential expression of macrophage costimulatory molecules is known to directly impact T-cell mediated control following Mtb infection [37]. It is tempting to hypothesize that the chronically inflamed lung environments seen in patients most at risk for Mab infection result in macrophage populations primed against T-cell activation in a bid to prevent excess inflammation and off target tissue damage. In a comparative study between BMDMs and FLAMs, we have shown both resting and IFNγ-activated FLAMs favor high expression of T-cell co-inhibitory molecules, PDL1 and PDL2 relative to costimulatory molecules, CD40, CD80 and CD86 [24]. It would be interesting to define the expression of these costimulatory molecules over the course of Mab infection with the goal of determining signatures for improved T-cell mediated Mab control. By expanding these

studies to include interactions between T-cells and macrophages, we gain a more well-rounded picture for immune responses required for control following Mab pulmonary infection.

Independent of macrophage biology and the global differences between macrophage subsets, Mab-macrophage interactions can be leveraged to further understand Mab pathogenesis. Mab has two morphotypes [38-42]. The smooth morphotype is considered the variant that establishes infection in the host and is characterized by the presence of a glycopeptidolipid (GPL) layer on Mab's membrane [33, 38]. The rough variant is associated with more progressive disease states and is noticeably missing the GPL layer seen on its smooth variant counterpart [30, 33]. A research concentration for many has focused on defining distinct morphotype characteristics during infection. For example, smooth Mab variants are found tightly encased in phagosomes once engulfed and are thought to favor extracellular biofilm formation if they are not taken up by macrophages [33, 43]. Rough variants, on the other hand, are known to form looser phagosomes due to their clumping nature and often favor a cording motif if successful phagosome escape occurs [31, 33, 43]. Rough variants are also associated with higher inflammation, increasing the likelihood of more aggressive infection profiles and chronic infection [28, 29, 43]. The mechanism behind the smooth to rough morphotype switch result from indel or frameshift mutation(s) within Mab's *gpl* locus [41, 44, 45]. This locus includes genes responsible for GPL construction and transportation to the Mab membrane, making each smooth to rough morphotype transition potentially distinct [41, 44]. Neely, et al. has shown specific growth medium conditions differentially modulate smooth or rough Mab variant formation in broth culture media [46]. Interestingly, the presence of nitric oxide (NO) in broth cultures lowered GPL expression profiles, implicating the importance of environmental cues in driving the switch from a smooth to rough morphotype [46]. In chapter 3, we show NO

production in Mab infected FLAMs is significantly reduced compared to BMDMs. In addition, global multiplex and transcriptional analysis show FLAMs remain largely hypoinflammatory during the early stages of infection. Combined, it is tempting to hypothesize that the lack of NO production and inflammatory cytokine release retains Mab in the smooth variant, inhibiting the rough variant from taking hold and driving aggressive Mab infection phenotypes. Notably, cohorts at high-risk for Mab pulmonary infection have chronically inflamed, hypoxic and nutrient starved lung environments. It is easy to hypothesize that these altered lung environments increase the frequency of smooth to rough Mab morphotype transitions, inadvertently increasing Mab virulence. However, both smooth and rough Mab variants are consistently isolated from Mab infected patients at all stages of infection, suggesting more complex mechanistic interactions occurring at this host-pathogen interface [4, 47-49]. Future work should define the host environmental factors that modulate aggressive disease states with particular focus on the dynamics driving Mab phase variation.

Complicating matters, lung health, antibiotic treatment history and the persistence of additional co-infections all represent the diverse lung environments where Mab must gain an advantage to survive. To begin dissecting these complicated interfaces, researchers have started looking into co-infections between Mab and *Pseudomonas aeruginosa,* a gram-negative bacterium that often infects patients with persistent lung disease [50-53]. In these studies, the goal was to define a distinct mechanism that allows Mab to gain a pathogenic advantage. To date, these studies remain inconclusive and point to more complicated interactions between the two pathogens during infection [53]. Competition assays leveraging both pathogens *in vivo* may give clearer insight into Mab virulence mechanisms leveraged to gain a competitive advantage. Notably, a transposon mutant Mab library has already been leveraged to determine Mab

antibiotic resistance mechanisms [54]. An interesting future endeavor is one where researchers use the same Mab transposon mutant library in a head-to-head experiment with a second pathogen, such as *Pseudomonas aeruginosa*, to determine unique Mab virulence factors required during co-infection. Furthermore, the diversity of clinical isolates recovered from Mab infected patients can give additional insight into Mab pathogenesis. Our lab has made a fluorescent library of clinical isolates to examine how distinct isolates alter the host inflammatory response following infection. Preliminary experiments have confirmed rough clinical isolates drive robust inflammatory cytokine profiles compared to their smooth variant counterparts. Interestingly, one rough clinical isolate, MAB016, was found to drive even higher inflammatory cytokine release compared to other rough variants, suggesting Mab virulence mechanisms are further primed by the host environment. Future studies are focused on examining these cytokine signatures with particular focus on the clinical isolates that improve Mab virulence by driving dysregulated or heightened inflammatory cytokine release profiles. Layering these studies with a LOF CRISPR-Cas9 macrophage screen would allow the identification of host pathways required for Mab-macrophage interactions. It would also be interesting to conduct a LOF CRISPR-Cas9 macrophage screen with each Mab clinical isolate to identify both overlapping and unique macrophage restriction mechanisms required for each isolate during Mab infection. Moreover, comparing downstream mechanistic findings between macrophage subsets, such as BMDMs compared to FLAMs, would give insight into how macrophage biology influences immune responses following Mab infection. Combined, these studies would allow for the delineation of clearer Mab pathogenesis profiles, while gaining insight into key host immune responses that can be used to improve treatment options for patients in the future.

A variety of murine models are currently being leveraged to gain insight into Mab pathogenesis during chronic infection. Since Mab is easily cleared in almost all immunocompetent mouse models, these studies often rely on immunodeficient mice. Byrd and Lyons were some of the first to leverage SCID mice to study chronic Mab infection, clearly implementing the importance of the adaptive immune system in Mab control [55, 56]. Rottman et al. expanded on these findings, using Rag2, CD3ε, IFNγ receptor 1 and TFNα knockout mice to further show the importance of T-cells, IFNγ and TFNα during infection as well [35]. While these studies give valuable insight into adaptive immune responses during disseminated and chronic Mab infection, one drawback is they often rely on intravenous injection to initiate infection. Unfortunately, Mab aerosolized infections are cleared with ease, even in immunocompromised mice. Researchers are currently developing murine models that better replicate pulmonary Mab infection, which will allow for an increase in murine aerosolized infection studies in the future.

Another significant drawback to studies conducted in murine models is the lack of genetic diversity. The human population has a significant number of genetic variability and epigenetic polymorphisms that contribute to immune responses, while nearly all murine models are cloned and inbred. This has allowed researchers to gather consistent, reproducible, and statistically powerful results for their studies. However, it also prevents many findings from being readily applicable to human health and disease. To address this and create human-like randomized genetic diversity in a mouse population, the Collaborative Cross (CC) mouse model was created [57]. This model involves the randomized breeding between 8, genetically distinct founder strains, followed by multiple generations of interbreeding [57]. This strategy has resulted in hundreds of recombinant inbred mouse lines that each possess a unique allelic profile that can

be traced back to each founder strain [58-60]. The defined distribution of alleles between strains has allowed initial studies to align analyzed phenotypes with distinct allelic combinations present in specific CC mouse strains [58-60]. Leveraging this model to further understand Mab pathogenesis would give insight into unknown genetic polymorphisms influencing host control during Mab infection. While this model is a powerful tool that allows researchers to model human genetic diversity, a major limitation is the high cost of resources and time required to obtain and maintain each CC mouse strain. One way researchers have begun to offset this cost burden is by developing hox cell lines from each original founder mouse strain. These hox cells are immortalized macrophage progenitors that require estradiol to be maintained. By removing estradiol and adding M-CSF, each hox cell will terminally differentiate into macrophages [61]. In chapter 3, we leverage HoxB8 differentiated macrophages to conduct a comparative study between BMDMs and FLAMs during Mab infection. Our lab plans to expand these studies to include differentiated macrophages from immortalized macrophage progenitors initially isolated from the original founder mouse strains of the CC model. By including host variation in these studies, we are uniquely positioned to define novel host mechanisms required for Mab control. Furthermore, attempting to employ the CC model with alveolar macrophages to study lung infections would require a massive quantity of time and resources. The FLAM model can alleviate this concern. We can use a single viable breeder pair for each line to generate a large collection of FLAMs from each CC mouse strain. Combining the CC model with our newly developed FLAM cell model would allow us to identify distinct host alleles that directly contribute to Mab pathogenesis and disease. Using a genetics squared approach by layering these studies with Mab genetic diversity, such as clinical isolates or Mab Tnseq libraries, would lead to

more relevant, informative, and impactful findings that can be leveraged to improve Mab treatment options in a clinically relevant manner [62].

Mab is broadly recalcitrant to many antibiotic treatments, which directly increase treatment timelines and the requirement for multi-drug therapies. As a result, treatment costs, patient compliance and antibiotic related toxic side effects are also directly impacted, highlighting the need for new therapeutic options. In the studies described above, I illustrate an array of future directions that will further our understanding of Mab pathogenesis and the role macrophages have in disease progression. By setting out to better understand the host macrophage-Mab interface, I was able to combine our BMDM and FLAM models with iterative genetic approaches to uncover novel macrophage mechanisms required during early Mab infection. By leveraging these approaches, we aid the field in the collective goal of decreasing the prevalence of Mab pulmonary infection. In combination with others, such studies allow the collective advancement towards improved therapeutics, including potential bacterial targets for vaccine development and host responses required to protect the lung tissue from damage and chronic infection. We continue to leverage these strategies to further our understanding of this opportunistic pathogen during lung infection and contribute these findings to improve therapeutic options for at-risk patients in the future.

REFERENCES

1. Daley, C.L., et al., *Treatment of Nontuberculous Mycobacterial Pulmonary Disease: An Official ATS/ERS/ESCMID/IDSA Clinical Practice Guideline.* Clin Infect Dis, 2020. **71**(4): p. 905-913.

2. Harris, K.A. and D.T.D. Kenna, *Mycobacterium abscessus infection in cystic fibrosis: molecular typing and clinical outcomes.* J Med Microbiol, 2014. **63**(Pt 10): p. 1241-1246.

3. Sharma, S.K. and V. Upadhyay, *Epidemiology, diagnosis & treatment of non-tuberculous mycobacterial diseases.* Indian J Med Res, 2020. **152**(3): p. 185-226.

4. Griffith, D.E. and C.L. Daley, *Treatment of Mycobacterium abscessus Pulmonary Disease.* Chest, 2022. **161**(1): p. 64-75.

5. Haworth, C.S., et al., *British Thoracic Society guidelines for the management of non-tuberculous mycobacterial pulmonary disease (NTM-PD).* Thorax, 2017. **72**(Suppl 2): p. ii1-ii64.

6. Griffith, D.E., et al., *Amikacin Liposome Inhalation Suspension for Treatment-Refractory Lung Disease Caused by Mycobacterium avium Complex (CONVERT). A Prospective, Open-Label, Randomized Study.* Am J Respir Crit Care Med, 2018. **198**(12): p. 1559-1569.

7. Luthra, S., A. Rominski, and P. Sander, *The Role of Antibiotic-Target-Modifying and Antibiotic-Modifying Enzymes in Mycobacterium abscessus Drug Resistance.* Front Microbiol, 2018. **9**: p. 2179.

8. Ripoll, F., et al., *Non mycobacterial virulence genes in the genome of the emerging pathogen Mycobacterium abscessus.* PLoS One, 2009. **4**(6): p. e5660.

9. Mathias Richard, A.V.G., Laurent Kremer, *Dissecting erm(41)-Mediated Macrolide-Inducible Resistance in Mycobacterium abscessus.* Antimicrobial Agents and Chemotherapy, 2020. **64**(2): p. e01879-19.

10. Brown-Elliott, B.A., et al., *Utility of sequencing the erm(41) gene in isolates of Mycobacterium abscessus subsp. abscessus with low and intermediate clarithromycin MICs.* J Clin Microbiol, 2015. **53**(4): p. 1211-5.

11. McQuattie-Pimentel, A.C., et al., *The lung microenvironment shapes a dysfunctional response of alveolar macrophages in aging.* J Clin Invest, 2021. **131**(4).

12. Misharin, A.V., et al., *Monocyte-derived alveolar macrophages drive lung fibrosis and persist in the lung over the life span.* J Exp Med, 2017. **214**(8): p. 2387-2404.

13. Byrne, A.J., et al., *Pulmonary macrophages: key players in the innate defence of the airways.* Thorax, 2015. **70**(12): p. 1189-96.

14. Hu, G. and J.W. Christman, *Editorial: Alveolar Macrophages in Lung Inflammation and Resolution.* Front Immunol, 2019. **10**: p. 2275.

15. Hou, F., et al., *Diversity of Macrophages in Lung Homeostasis and Diseases.* Front Immunol, 2021. **12**: p. 753940.

16. Murray, P.J. and T.A. Wynn, *Protective and pathogenic functions of macrophage subsets.* Nat Rev Immunol, 2011. **11**(11): p. 723-37.

17. Woods, P.S., et al., *Tissue-Resident Alveolar Macrophages Do Not Rely on Glycolysis for LPS-induced Inflammation.* Am J Respir Cell Mol Biol, 2020. **62**(2): p. 243-255.

18. Reddy, R.C., *Immunomodulatory Role of PPAR-γ in Alveolar Macrophages.* Journal of Investigative Medicine, 2008. **56**(2): p. 552-557.

19. Croasdell, A., et al., *PPARgamma and the Innate Immune System Mediate the Resolution of Inflammation.* PPAR Res, 2015. **2015**: p. 549691.

20. Wang, T., et al., *HIF1alpha-Induced Glycolysis Metabolism Is Essential to the Activation of Inflammatory Macrophages.* Mediators Inflamm, 2017. **2017**: p. 9029327.

21. Batista-Gonzalez, A., et al., *New Insights on the Role of Lipid Metabolism in the Metabolic Reprogramming of Macrophages.* Front Immunol, 2019. **10**: p. 2993.

22. Appari, M., K.M. Channon, and E. McNeill, *Metabolic Regulation of Adipose Tissue Macrophage Function in Obesity and Diabetes.* Antioxid Redox Signal, 2018. **29**(3): p. 297-312.

23. Thomas, S.T., et al., *Fetal Liver-Derived Alveolar-like Macrophages: A Self-Replicating Ex Vivo Model of Alveolar Macrophages for Functional Genetic Studies.* Immunohorizons, 2022. **6**(2): p. 156-169.

24. Ankley LM, C.K., Vielma TE, Godfrey JJ, Thapa M, Olive AJ., *GSK3α/β Restrain IFN-γ-Inducible Costimulatory Molecule Expression in Alveolar Macrophages, Limiting CD4+ T Cell Activation.* Immunohorizons, 2024. **8**(2): p. 147-162.

25. Mould, K.J., et al., *Single cell RNA sequencing identifies unique inflammatory airspace macrophage subsets.* JCI Insight, 2019. **4**(5).

26. Lee, M.S. and Y.-J. Kim, *Pattern-Recognition Receptor Signaling Initiated From Extracellular, Membrane, and Cytoplasmic Space.* Molecules and Cells, 2007. **23**(1): p. 1-10.

27. Li, D. and M. Wu, *Pattern recognition receptors in health and diseases.* Signal Transduct Target Ther, 2021. **6**(1): p. 291.

28. Ahn, J.H., et al., *Type I Interferons Are Involved in the Intracellular Growth Control of Mycobacterium abscessus by Mediating NOD2-Induced Production of Nitric Oxide in Macrophages.* Front Immunol, 2021. **12**: p. 738070.

29. Bernut, A., et al., *CFTR Protects against Mycobacterium abscessus Infection by Fine-Tuning Host Oxidative Defenses.* Cell Rep, 2019. **26**(7): p. 1828-1840 e4.

30. Bernut, A., et al., *Mycobacterium abscessus cording prevents phagocytosis and promotes abscess formation.* Proc Natl Acad Sci U S A, 2014. **111**(10): p. E943-52.

31. Kim, B.R., et al., *Phagosome Escape of Rough Mycobacterium abscessus Strains in Murine Macrophage via Phagosomal Rupture Can Lead to Type I Interferon Production and Their Cell-To-Cell Spread.* Front Immunol, 2019. **10**: p. 125.

32. Lee, J.Y., et al., *Nucleotide-Binding Oligomerization Domain 2 Contributes to Limiting Growth of Mycobacterium abscessus in the Lung of Mice by Regulating Cytokines and Nitric Oxide Production.* Front Immunol, 2017. **8**: p. 1477.

33. Roux, A.L., et al., *The distinct fate of smooth and rough Mycobacterium abscessus variants inside macrophages.* Open Biol, 2016. **6**(11).

34. Liu, X., et al., *Legionella-Infected Macrophages Engage the Alveolar Epithelium to Metabolically Reprogram Myeloid Cells and Promote Antibacterial Inflammation.* Cell Host Microbe, 2020. **28**(5): p. 683-698 e6.

35. Rottman, M., et al., *Importance of T cells, gamma interferon, and tumor necrosis factor in immune control of the rapid grower Mycobacterium abscessus in C57BL/6 mice.* Infect Immun, 2007. **75**(12): p. 5898-907.

36. Bernut, A., et al., *Mycobacterium abscessus-Induced Granuloma Formation Is Strictly Dependent on TNF Signaling and Neutrophil Trafficking.* PLoS Pathog, 2016. **12**(11): p. e1005986.

37. Sia, J.K., et al., *Engaging the CD40-CD40L pathway augments T-helper cell responses and improves control of Mycobacterium tuberculosis infection.* PLoS Pathog, 2017. **13**(8): p. e1006530.

38. Johansen, M.D., J.L. Herrmann, and L. Kremer, *Non-tuberculous mycobacteria and the rise of Mycobacterium abscessus.* Nat Rev Microbiol, 2020. **18**(7): p. 392-407.

39. Gutierrez, A.V., et al., *Glycopeptidolipids, a Double-Edged Sword of the Mycobacterium abscessus Complex.* Front Microbiol, 2018. **9**: p. 1145.

40. Schorey, J.S. and L. Sweet, *The mycobacterial glycopeptidolipids: structure, function, and their role in pathogenesis.* Glycobiology, 2008. **18**(11): p. 832-41.

41. Pawlik, A., et al., *Identification and characterization of the genetic changes responsible for the characteristic smooth-to-rough morphotype alterations of clinically persistent Mycobacterium abscessus.* Mol Microbiol, 2013. **90**(3): p. 612-29.

42. Medjahed, H. and J.M. Reyrat, *Construction of Mycobacterium abscessus defined glycopeptidolipid mutants: comparison of genetic tools.* Appl Environ Microbiol, 2009. **75**(5): p. 1331-8.

43. Iakobachvili, N., et al., *Mycobacteria-host interactions in human bronchiolar airway organoids.* Mol Microbiol, 2022. **117**(3): p. 682-692.

44. Ripoll, F., et al., *Genomics of glycopeptidolipid biosynthesis in Mycobacterium abscessus and M. chelonae.* BMC Genomics, 2007. **8**: p. 114.

45. Howard, S.T., et al., *Spontaneous reversion of Mycobacterium abscessus from a smooth to a rough morphotype is associated with reduced expression of glycopeptidolipid and reacquisition of an invasive phenotype.* Microbiology (Reading), 2006. **152**(Pt 6): p. 1581-1590.

46. Nandanwar, N., J.E. Gibson, and M.N. Neely, *Growth medium and nitric oxide alter Mycobacterium abscessus morphotype and virulence.* Microbiol Res, 2021. **253**: p. 126887.

47. Jeon, K., et al., *Antibiotic treatment of Mycobacterium abscessus lung disease: a retrospective analysis of 65 patients.* Am J Respir Crit Care Med, 2009. **180**(9): p. 896-902.

48. Jarand, J., et al., *Clinical and microbiologic outcomes in patients receiving treatment for Mycobacterium abscessus pulmonary disease.* Clin Infect Dis, 2011. **52**(5): p. 565-71.

49. Koh, W.J., et al., *Clinical significance of differentiation of Mycobacterium massiliense from Mycobacterium abscessus.* Am J Respir Crit Care Med, 2011. **183**(3): p. 405-10.

50. Birmes, F.S., et al., *Mycobacterium abscessus subsp. abscessus Is Capable of Degrading Pseudomonas aeruginosa Quinolone Signals.* Front Microbiol, 2017. **8**: p. 339.

51. Rodriguez-Sevilla, G., et al., *Influence of three-dimensional lung epithelial cells and interspecies interactions on antibiotic efficacy against Mycobacterium abscessus and Pseudomonas aeruginosa.* Pathog Dis, 2018. **76**(4).

52. Rodriguez-Sevilla, G., et al., *Antimicrobial Treatment Provides a Competitive Advantage to Mycobacterium abscessus in a Dual-Species Biofilm with Pseudomonas aeruginosa.* Antimicrob Agents Chemother, 2019. **63**(11).

53. Ayantu W. Idosa, D.J.W., Luanne Hall-Stoodley, *Surface Dependent Inhibition of Mycobacteirum abscessus by Diverse Pseudomonas aeruginosa Strains.* Microbiol Spectrum, 2022. **10**(6): p. e02471-22.

54. Akusobi, C., et al., *Transposon mutagenesis in Mycobacterium abscessus identifies an essential penicillin-binding protein involved in septal peptidoglycan synthesis and antibiotic sensitivity.* Elife, 2022. **11**.

55. Lyons, T.F.B.a.C.R., *Preliminary Characterization of a Mycobacterium abscessus Mutant in Human and Murine Models of Infection.* Infection and Immunity, 1999. **67**(9): p. 4700-4707.

56. Obregon-Henao, A., et al., *Susceptibility of Mycobacterium abscessus to antimycobacterial drugs in preclinical models.* Antimicrob Agents Chemother, 2015. **59**(11): p. 6904-12.

57. Chesler, E.J., et al., *The Collaborative Cross at Oak Ridge National Laboratory: developing a powerful resource for systems genetics.* Mamm Genome, 2008. **19**(6): p. 382-9.

58. Threadgill, D.W., Miller, D.R., Churchill, G.A., Pardo-Manuel de Villena, F., *The Collaborative Cross: A Recombinant Inbred Mouse Population for the Systems Genetic Era.* ILAR J., 2011. **52**(1): p. 24-31.

59. Noll, K.E., M.T. Ferris, and M.T. Heise, *The Collaborative Cross: A Systems Genetics Resource for Studying Host-Pathogen Interactions.* Cell Host Microbe, 2019. **25**(4): p. 484-498.

60. Smith, C.M., et al., *Host-pathogen genetic interactions underlie tuberculosis susceptibility in genetically diverse mice.* Elife, 2022. **11**.

61. Wang, G.G., et al., *Quantitative production of macrophages or neutrophils ex vivo using conditional Hoxb8.* Nat Methods, 2006. **3**(4): p. 287-93.

62. Persson, J. and R.E. Vance, *Genetics-squared: combining host and pathogen genetics in the analysis of innate immunity and bacterial virulence.* Immunogenetics, 2007. **59**(10): p. 761-78.

APPENDIX

DECLARATIONS

Authors

Haleigh N. Gilliland[1] and Andrew J. Olive[1]

1 Michigan State University

Contributions

HG and AO designed the studies. HG investigated macrophage restriction mechanisms during Mab infection following Linezolid treatment. HG and AO wrote and reviewed the chapter.

ABSTRACT

A macrophage's ability to sense and appropriately respond to invading pathogens is critical to preventing disease progression. *Mycobacterium abscessus* (Mab), is a highly drug resistant, rapidly growing non-tuberculous mycobacterium (NTM) that causes opportunistic infections in patients with acquired or chronic lung diseases. Macrophages are one of the first immune cells Mab encounters during infection, making their interactions a critical determinant in Mab pathogenesis. However, our understanding on how the macrophage environment interacts with antibiotic treatment to mediate intracellular control of Mab remains unknown. Here, we conduct a forward genetic screen in immortalized bone marrow derived macrophages (iBMDMs) to identify host genes that are required for macrophage control of Mab in the presence of Linezolid. Our screen identified pathways such as oxidative phosphorylation contribute to macrophage control of Mab in antibiotic treated macrophages. Validation of a subset of candidates including Citrate synthase, however found that many identified genes control Mab growth independently of Linezolid treatment. These data suggest that baseline replication and survival of Mab is a key variable in intracellular antibiotic control and highlight a key need to better define cell autonomous mechanisms of host-Mab interactions to develop new effective host-directed therapies.

INTRODUCTION

Mycobacterium abscessus (Mab) is a rapidly growing nontuberculous mycobacterium (NTM) that has been increasing in prevalence since it was recognized as an independent pathogen in 1992 [1, 2]. This opportunistic pathogen primarily infects patients with acquired or chronic lung disease, including patients with cystic fibrosis, bronchiectasis, or chronic obstructive pulmonary disease (COPD) [3-5]. A closer look at these lung environments shows key overlapping risk factors, including excess mucus build-up and prolonged airway inflammation. As a result, regulation of appropriate immune responses following pathogen exposure are impaired. Complicating matters, Mab is intrinsically resistant to many of the common antibiotics prescribed to patients [6-8]. Long treatment time frames, adverse side effects to antibiotics and patient compliance result in treatment failure or regimen alterations in nearly half (48.3%) of patients prior to treatment completion [8, 9]. Thus, Mab is an emerging pathogen of clinical importance with a critical need to develop more effective treatment options that prevent the rising prevalence of Mab in at-risk cohorts.

One interaction that inadvertently alters appropriate immune responses is antibiotic treatment. Antibiotics can interfere with the immune system either indirectly by disrupting the body's microbiota, or directly by modulating appropriate immune cell function [10, 11]. Such interactions can impact treatment efficacy and increase host susceptibility to reoccurring infection. Although an FDA approved drug regimen for Mab pulmonary infection does not exist, patients are often treated with two or more intravenous drugs (amikacin, tigecycline, imipenem and/or cefoxitin) and one or two oral antimicrobials (clofazimine, linezolid and/or azithromycin) for 3 months following diagnosis [8, 9]. However, these treatment timelines are frequently adjusted prior to treatment completion, with almost 80% of patients reporting adverse side

effects that result from their treatment regimens [9]. Therefore, research focused on understanding altered host responses during Mab infection throughout antibiotic treatment are required to develop more effective treatment strategies. How traditional antibiotic treatment during *Mycobacterium tuberculosis* (Mtb) infection alters host responses, has recently started to be examined. For example, one study found host cells aid in the localization of antibiotics to pathogen containing vacuoles, directly modulating antibiotic mediated control of infection [12]. Additionally, long-term Linezolid treatment has been shown to directly alter macrophage physiological responses by decreasing mitochondrial mass over time [13]. Combined, these studies highlight the importance of understanding host pathways modulating antibiotic efficacy during infection that may contribute to pathogen clearance in the lungs.

Macrophages are the first immune cells Mab encounters during infection, making Mab-macrophage interactions critical to understanding disease progression. Upon exposure, Mab is recognized by macrophage pattern recognition receptors (PRRs), including toll-like receptors, Dectin receptors and scavenger receptors [14, 15]. These initial interactions are complicated by the ability of Mab to transition from a smooth to rough variant. For example, toll-like receptor 2 (TLR2) seems to favor interactions with rough Mab variants prior to uptake [14]. Following adherence, phagocytosis or receptor mediated endocytosis facilitate pathogen internalization [16-18]. While pathogen uptake can be initiated by multiple receptors, the downstream phagosome maturation process remains well conserved. In general, reorganization of the actin cytoskeleton and progressive engagement of additional receptors around the pathogen initiates nascent phagosome formation [18, 19]. During Mab infection, rough Mab variants favor the formation of a loose phagosome compared to their tightly encased smooth counterparts [20]. From here, downstream phagosome maturation is characterized by compartment acidification by vacuolar-

ATPases, production of reaction oxygen (ROS) and nitrogen species (RNS) and delivery of recruited cathepsins and hydrolases to the maturing phagosome [19, 21, 22]. The matured phagosome then fuses with the lysosome, a compartment containing numerous anti-microbial acid-activated hydrolytic enzymes, creating the phagolysosome [23]. Recent research shows Mab leverages a variety of virulence factors to subvert phagosome maturation and macrophage antimicrobial defense mechanisms. For example, Mab upregulates ESX-IV, a type VII secretion system, to access essential nutrients being quenched by the maturing phagosome and to subvert phagolysosome formation [24]. Transposon mutagenesis studies have shown an ATPase gene, *eccB4*, in the ESX-IV secretion system is specifically required to disrupt phagosome acidification [24]. However, if these attempts are unsuccessful, Mab relies on microbial membrane protein large 8 (MmpL8) to facilitate phagosomal escape [25]. Although many studies have focused on Mab virulence factors used to subvert macrophage restriction, the requirement of each intracellular restriction pathway throughout the course of Mab infection remains largely unexplored.

Here, we set out to define host genes required for improved control of Mab during antibiotic treatment. The antibiotic Linezolid was chosen for this study as it is an antibiotic commonly used to treat Mab pulmonary infection with known off target effects on the host [8, 13]. To define host pathways differentially modulating Linezolid efficacy during Mab infection, we coupled a fluorescent Mab reporter strain with a genome-wide CRISPR-Cas9-mediated macrophage knockout library in iBMDMs to perform a forward genetic screen to identify host genes that alter intracellular Mab levels during Linezolid treatment. Pathway analysis of screen results show Linezolid efficacy in Mab infected macrophages requires oxidative phosphorylation. However, follow-up experiments with macrophage top screen hits show

targeted knockouts are required for controlling intracellular Mab levels independent of antibiotic treatment. Taken together, these data reveal novel macrophage intracellular restriction mechanisms leveraged during Mab infection, while highlighting the need for continued research on cell-autonomous control of Mab during infection.

RESULTS

Optimized screening platform allows the identification of host pathways modulating Mab intracellular burden.

Mab pathogenesis relies on its ability to subvert macrophage intracellular restriction mechanisms during prolonged antibiotic treatment. Yet our understanding of how these antibiotics may be modulating intracellular macrophage control of Mab remains limited. To help fill this gap in knowledge, we leveraged an mEmerald GFP-expressing Mab (ATCC 19977) strain. In a previous study, this fluorescent reporter strain enabled the dissection of macrophage-Mab interactions 4 hours post-infection [26]. We hypothesized that this same reporter strain used at later timepoints, would distinguish novel intracellular restriction mechanisms by macrophages during Linezolid treatment. We chose the antibiotic Linezolid for this study as it has known off target effects on the host yet continues to be to be commonly used to treat pulmonary Mab infection [8, 13]. As a first step, we measured mEmerald fluorescence and optical density of *in vitro* liquid cultures at increasing concentrations of Linezolid over time (Figure 3.1A – 3.1B). We observed that bacterial growth and antibiotic mediated killing with Linezolid was reliably measured by mEmerald fluorescence. We next examined the ability of the fluorescent Mab strain as a tool to dissect macrophage-Mab interactions during Linezolid treatment. We infected immortalized bone marrow-derived macrophages (iBMDMs) with fluorescent Mab at a multiplicity of infection (MOI) of five. After four hours, infection media was removed and

replaced with cell culture media containing increasing concentrations of Linezolid for three days. The mean fluorescent intensity (MFI) of mEmerald+ cells was then quantified by flow cytometry. Notably, we saw a distinct decrease in MFI in infected cells as antibiotic concentrations increased (Figure 3.1C- 3.1D), allowing the identification of antibiotic concentrations that modulate intracellular restriction of Mab by macrophages. We have previously confirmed that intracellular mEmerald fluorescence correlates with bacterial survival (See Chapter 3 Figure 2.1). We next wanted to confirm that the decrease in mEmerald fluorescence observed at higher antibiotic concentrations correlated with lower bacterial survival. To test this, iBMDMs were infected with fluorescent Mab. After 4 hours, infected media was removed and replaced with low (4 μg/mL) or high (32 μg/mL) concentrations of Linezolid for three days. Fluorescence activated cell sorting (FACS) was used to sort 100,000 infected macrophages that were mEmerald positive in each condition. Cells were then lysed and plated for colony forming units (CFU) (Figure 3.1E). We observed a decrease in total CFU counts per 100,000 cells in both low and high Linezolid treatment that correlated with a drop in intracellular mEmerald fluorescence. Importantly, we observed that high concentrations of linezolid more strongly restricted Mab than low levels of antibiotics. Taken together, these data highlight the sensitivity of the mEmerald GFP reporter strain and flow cytometry as an approach to measure intracellular Mab levels at a single cell level during antibiotic treatment.

Genome-wide screen identify macrophage genes required to restrict Mab during antibiotic treatment.

Given that host pathways must synergize with antibiotics to drive intracellular control, we wondered if we could identify new pathways that contribute to host-pathogen-antibiotic

interactions in Mab infected macrophages. Thus, we conducted a genome-wide loss-of-function screen to identify host genes that when disrupted result in less effective antibiotic control (Figure 3.2A). We previously optimized a pooled genome-wide loss-of-function library in Cas9+ iBMDMs to globally identify host pathways required for Mab uptake [27]. We next used this library to identify intracellular restriction mechanisms modulated by antibiotic treatment during Mab infection. The loss-of-function macrophage library was infected with mEmerald Mab at an MOI of five. Four hours later, we removed infection media and replaced with 4μg/mL Linezolid containing media for three days. We then used FACS to isolate over 100x sgRNA coverage of the library from mEmerald^{hi} cells and mEmerald^{low} cells. Following genomic DNA extraction, the abundance of sgRNAs from each of the sorted bins were quantified by Illumina sequencing. Then, we used the Model-based Analysis of Genome-wide CRISPR/Cas9 Knockout (MAGeCK) robust rank algorithm (α-RRA) to test for statistical enrichment of sgRNAs and genes. To identify macrophage genes required for Mab restriction during antibiotic treatment, we compared the enrichment of sgRNAs in the mEmerald^{low} directly to the mEmerald^{hi} population three days post-infection. We predicted genes significantly enriched in mEmerald^{hi} would be host genes that cannot effectively control Mab during Linezolid treatment. The α-RRA analysis identified over 250 genes with a p-value <0.01 and a fold change of 2 with at least 3 independent sgRNAs. Among the top 100 candidates, we identified known modulators of pathogen restriction by macrophages including GPS1, Ndufaf1, Ndufa2, Ndufa3, Ndufa8 and Irf8 with each gene showing enrichment in the mEmerald^{hi} population (Figure 3.2B). Analysis of individual guides showed agreement with three sgRNAs targeting these genes, signifying a robust screen and candidate list (Figure 3.2C – 3.2G).

Top screen hits, CS, Furin and Wdr81, are required for Mab control by iBMDMs independent of Linezolid treatment.

Stringent analysis of screen results revealed an enrichment of genes with no previously described role in Mab restriction by macrophages, including CS, Furin and Wdr81 (Figure 3.3A-3.3C). To identify pathways that were associated with these genes, we filtered the ranked list to include genes that had a gold change of >2 with at least 2 sgRNAs and used DAVID analysis to identify pathways and functions that were enriched in our dataset. Among the top enriched KEGG pathways was oxidative phosphorylation, with many core components of its regulation identified as key components in Mab control by macrophages during Linezolid treatment. KEGG analysis also found a significant enrichment of pathways required following pathogen exposure, including several genes associated with phagocytosis and NF-κB upregulation. Both of which are known modulators for macrophage control following pathogen exposure. Thus, bioinformatic analysis of top screen candidates identified pathways needed for improved intracellular control of Mab following infection.

To discover novel pathways required for Mab restriction by macrophages, we validated the role of a subset of candidate genes in our screen hit list to identify their requirement in restricting Mab during antibiotic treatment. These genes included CS, Furin and Wdr81 that we predicted may directly alter host-Mab-antibiotic interactions. Knockout iBMDM cell lines were first made using ribonucleoprotein (RNP) nucleofections to target unique sgRNAs for each gene. After knockout line construction and validation by sequencing, we then infected each knockout macrophage cell line with fluorescent Mab and monitored mEmerald fluorescence in macrophages three days post-infection. Interestingly, in the absence of antibiotic treatment, loss of CS, Furin or Wdr81 resulted in a significant increase in mEmerald^{hi} iBMDMs compared to

wild-type controls (Figure 3.3D-3.3E). However, this change in intracellular Mab levels was no longer present in cells treated with Linezolid. These data suggest that many of the top candidates from the screen do not alter antibiotic efficacy but rather alter baseline Mab survival and replication in BMDMs.

FIGURES

Figure 3.1 Optimization of screening platform to identify host genes controlling *Mycobacterium abscessus* intracellular levels. (A-B) The optical density and mEmerald fluorescent intensity of fluorescent *Mycobacterium abscessus* (Mab) was monitored over 48 hours in 7h9 broth at increasing concentrations of Linezolid antibiotic treatment. **(C)** A schematic of the infection assay used to optimize the forward genetic screening pipeline. Figure made in Biorender. **(C-D)** iBMDMs from C57BL6J mice were infected at a MOI of 5 for four hours. Infection media was then removed and replaced with the indicated Linezolid antibiotic concentrations for three days. **(D)** Flow cytometry was used to measure the percent of infected cells that were infected (mEmerald+). Shown are representative flow cytometry plots gated on live and single cells for each condition. **(E)** iBMDMs from C57BL6J mice were infected with Mab at a MOI of 5 for four hours, before infection media was removed and replaced with cell culture media containing Low (4 µg/mL) or High (32 µg/mL) Linezolid concentrations. Three days post-infection, FACS was used to sort mEmerald+ cells, then macrophages were lysed and plated for CFU. A representative bar graph of CFU counts from each sorted population are shown. Results are representative of three experimental replicates. ***p<.001 by one-way ANOVA with Tukey's multiple comparison test.

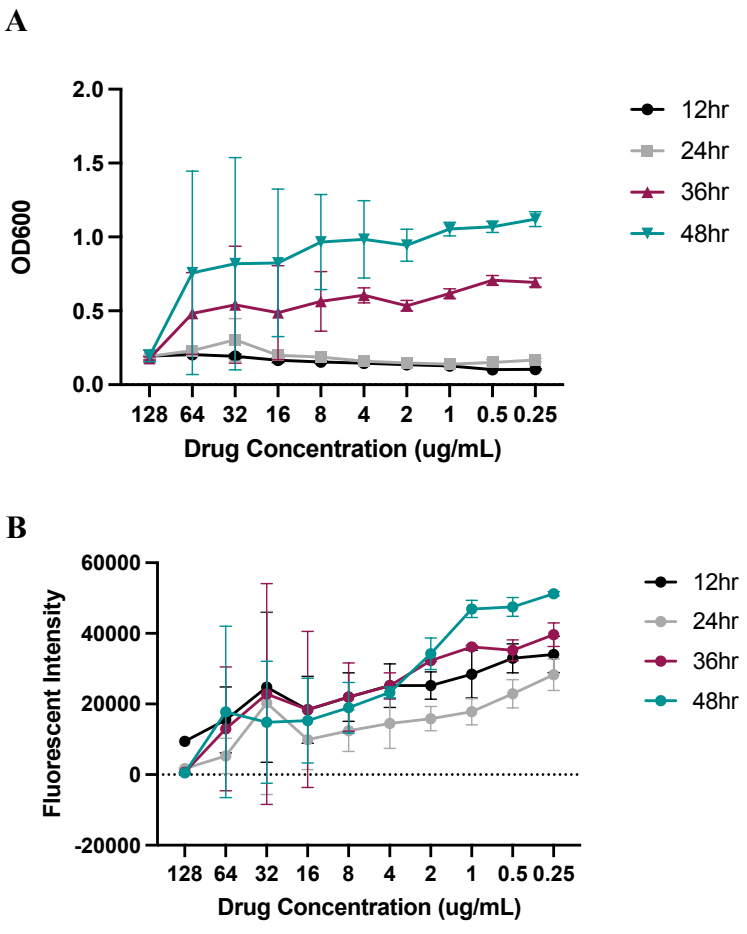

Figure 3.1 (cont'd)

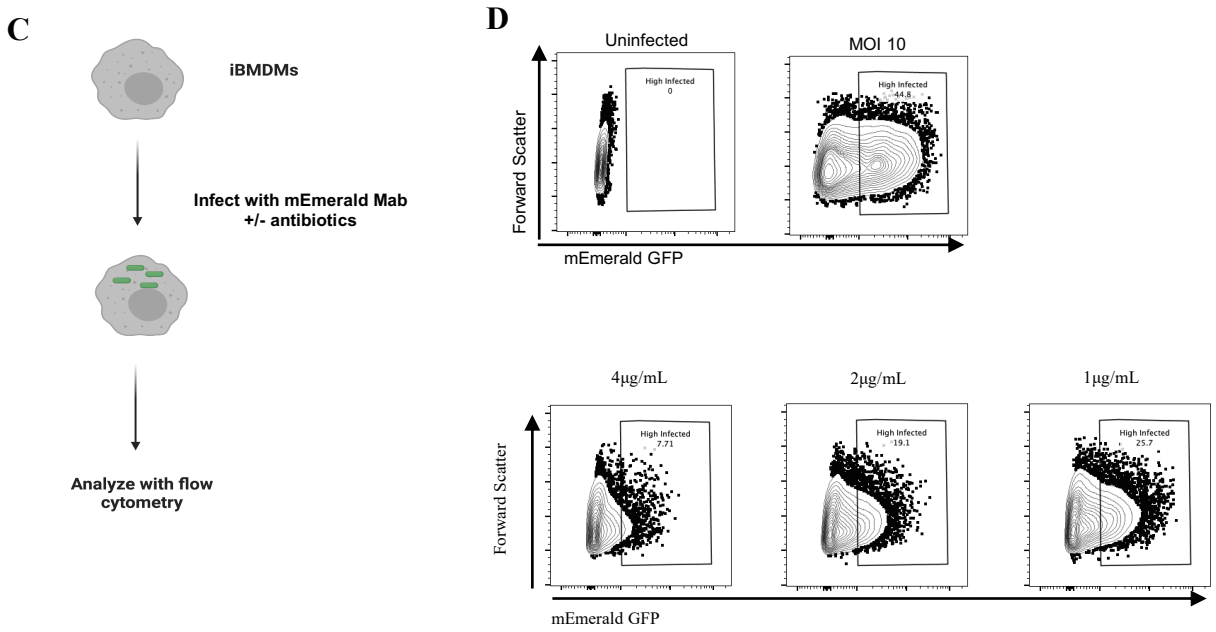

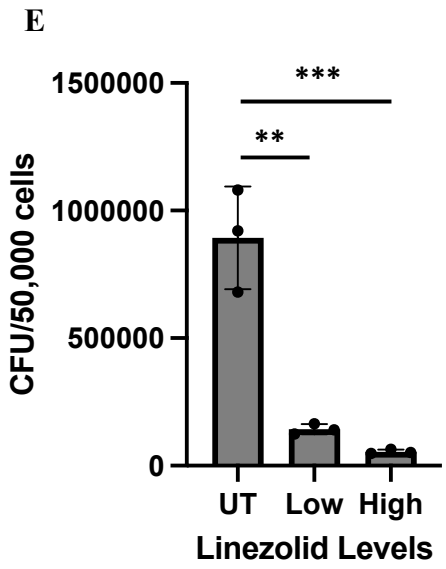

Figure 3.2 Genome-wide screens identify host genes that result in increased *Mycobacterium abscessus* intracellular burden during antibiotic treatment. (A) A schematic of the genome-wide screen used to identify host pathway required for intracellular control of *Mycobacterium abscessus* (Mab) during Linezolid treatment. A loss-of-function genome wide library created in Cas9+ iBMDMs with 4 sgRNAs per genes from the Brie library was infected with mEmerald Mab at a MOI of 5 for four hours. Infection media was removed and then replaced with 4 µg/mL Linezolid for three days. Cells were fixed and mEmerald^{hi} and mEmerald^{low} cells were isolated by FACS. Deep sequencing was used to determine sgRNA abundance in sorted populations. Figure made in Biorender. **(B)** Shown is alpha-robust ranking algorithm (α-RRA) score determined in MAGeCK for each gene in the iBMDM loss-of-function CRISPR-Cas9 library that passed filtering metrics from two independent screen replicates. Highlighted genes represent known host factors that contribute to pathogen restriction by macrophages. **(C-G)** Normalized sg*GPS1*, sg*Ndufaf1*, sg*Ndufa3*, sg*Ndufa8* and sg*Irf8* counts for each sgRNA found in both the mEmerald^{hi} and mEmerald^{low} sorted populations as shown.

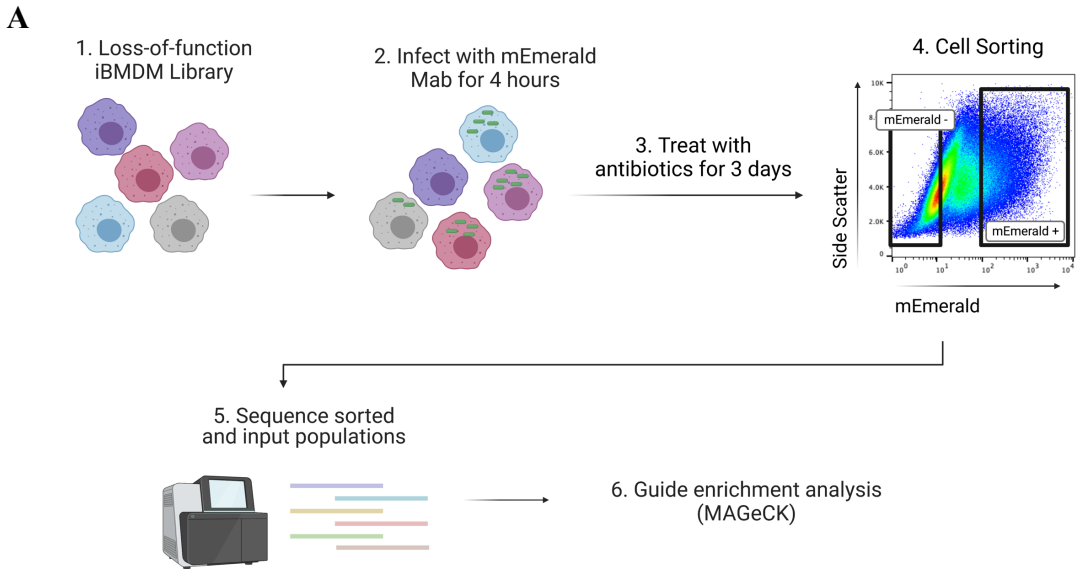

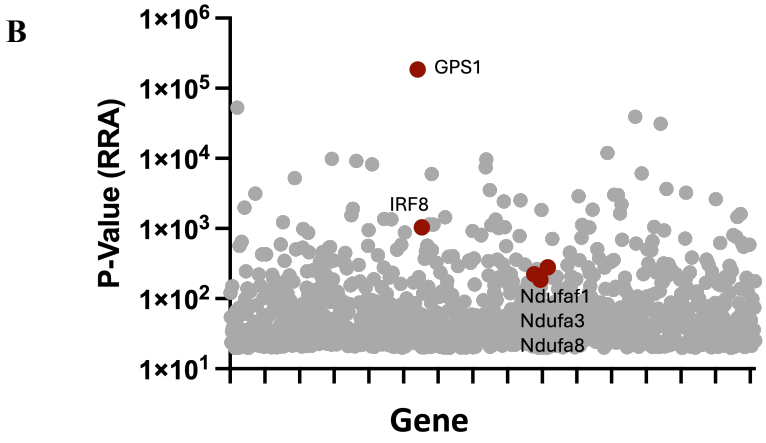

Figure 3.2 (cont'd)

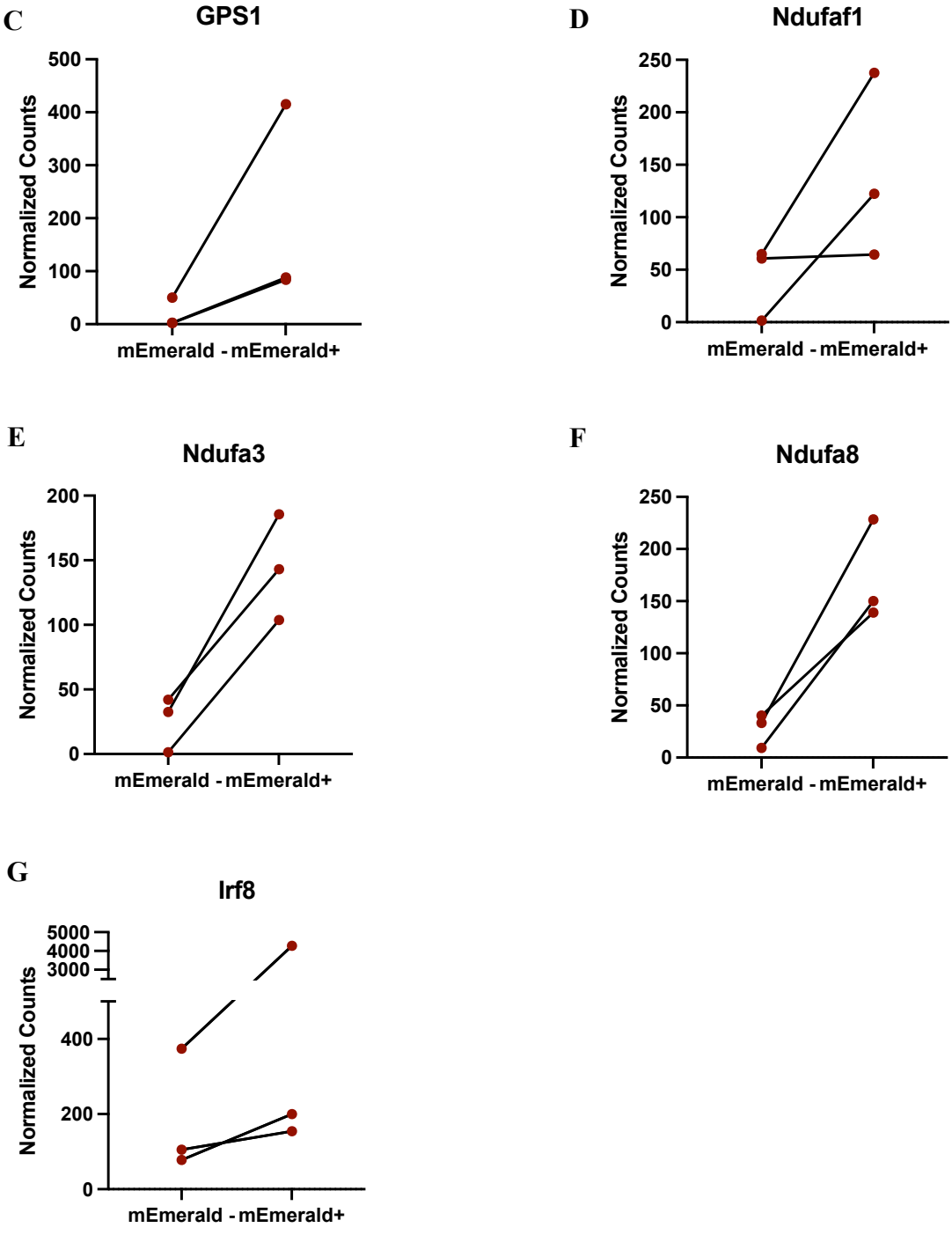

Figure 3.3 Macrophages deficient in CS, Furin or Wdr81 show increased *Mycobacterium abscessus* intracellular burden independent of antibiotic treatment. (A-C) Normalized sg*CS*, sg*Furin* and sg*Wdr81* counts for 3 sgRNAs found in both the mEmerald^{low} and mEmerald^{high} sorted populations as shown. **(D-E)** Wild-type, CS, Furin and Wdr81 deficient iBMDMs were infected with fluorescent Mab for four hours before infection media was removed and replaced with cell culture media containing 4µg/mL Linezolid. After three days, the percent uptake **(D)** and mean fluorescent intensity **(E)** was quantified by flow cytometry. Results are representative of three experimental replicates. ****p<.0001 ***p<.001 **p<.001 *p<.01 by two-way ANOVA with Tukey's multiple comparison test.

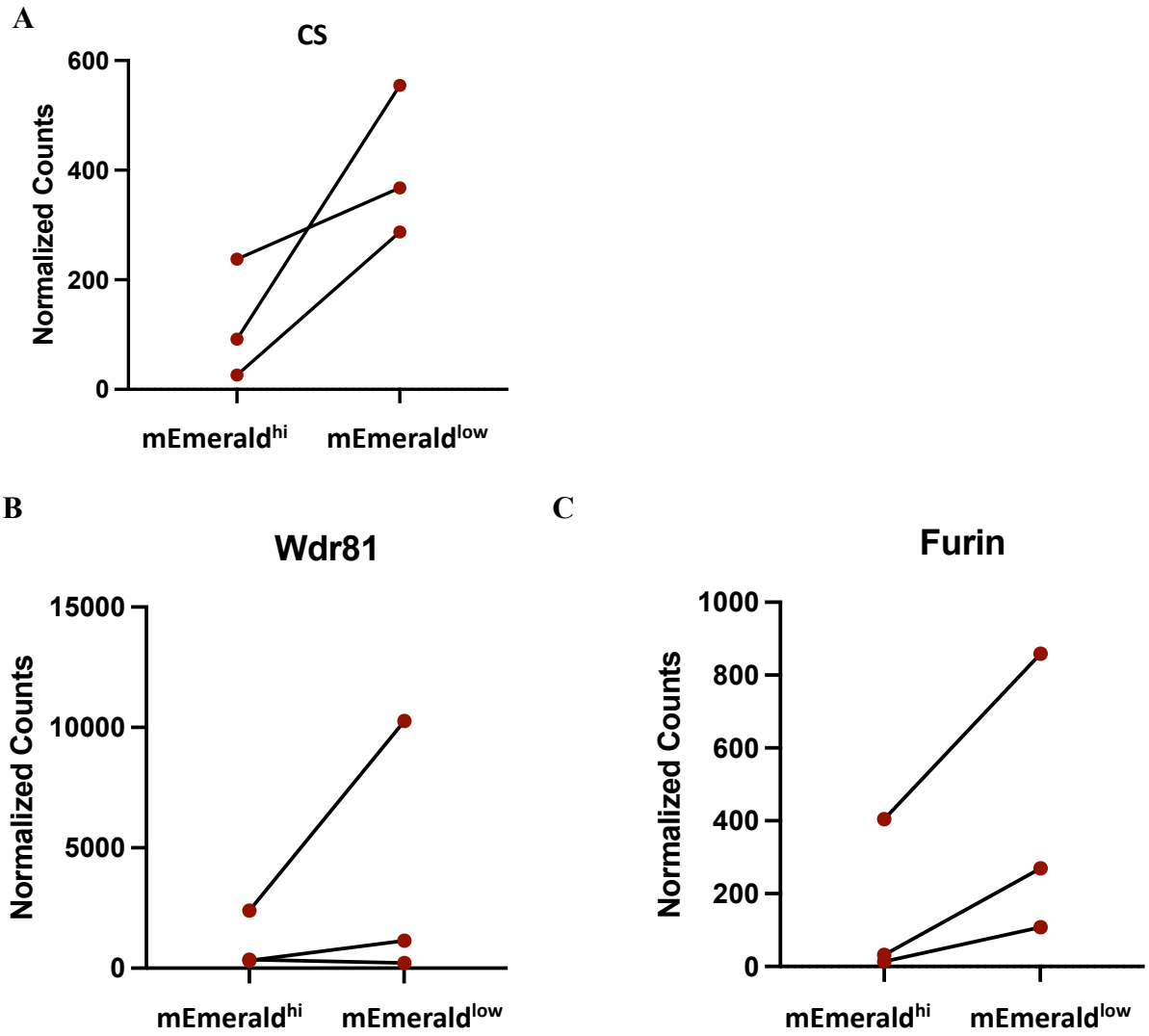

Figure 3.3 (cont'd)

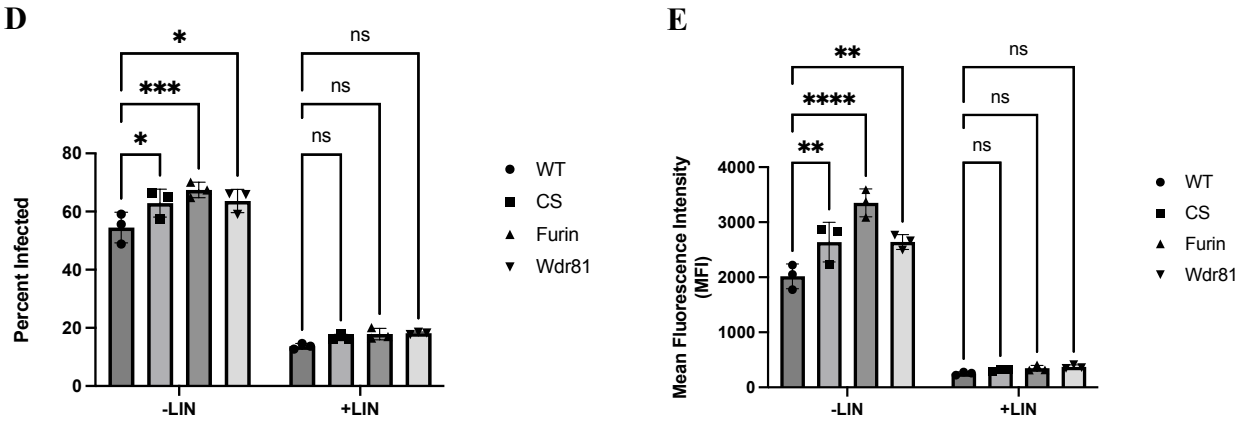

DISCUSSION

Pulmonary infections with *Mycobacterium abscessus* (Mab) are increasing in prevalence, with their intrinsic resistance to antibiotic therapy driving higher chronic infection percentages in at risk cohorts. Combating this opportunistic pathogen requires a deeper understanding of disease progression at the host-pathogen interface during antibiotic treatment. Here, we leveraged our fluorescent Mab reporter strain to conduct a forward genetic screen in the presence of Linezolid to globally identify host genes required to control intracellular Mab levels. While our initial screen analysis identified pathways such as oxidative phosphorylation as important for Linezolid-mediated control, our validation suggests many candidates directly alter macrophage-Mab interactions instead. Our study highlights our continued lack of understanding of how Mab is controlled by macrophages and emphasizes the need for continued research on cell-autonomous mechanisms of control in order to improve host-directed therapies against Mab pulmonary infection.

In general, intracellular macrophage restriction mechanisms are well known. This process is initiated by phagocytosis or receptor mediated endocytosis of pathogens. Although each phagocytic cargo has its own unique components, the downstream phagosome maturation process remains well conserved. Briefly, phagosome maturation is characterized by highly regulated interactions with various endosomal compartments [21, 28, 29]. These interactions lead to the progressive acidification of the pathogen containing vacuole, upregulation of reactive oxygen (ROS) and nitrogen (RNS) species and eventual fusion with the lysosome, creating the phagolysosome [23]. Although studies have started to define Mab virulence factors required to subvert macrophage restriction mechanisms, the requirement of key intracellular host restriction mechanisms for Mab control remain largely unexplored. Our study identified a novel

requirement for oxidative phosphorylation in Mab control by macrophages. This is interesting because Mab has been suggested to directly alter oxidative phosphorylation in cells to survive [30]. Both validated candidates CS and WDR81 play important roles at the mitochondria and suggest that Mab may be exquisitely tuned to modulate host respiratory capacity. Our other top hit FURIN was also found to be required for Mab control by macrophages. Interestingly, Furin is required for processing key secretory pathway precursors, including TGFβ. Its mechanistic involvement in macrophage restriction of pathogens remains unexplored, making its identification in our screen and involvement in Mab control intriguing. Given our validated candidates modulated Mab intracellular control independently of antibiotic treatment it is surprising that our study failed to define previously described trafficking genes involved in regulating autophagy and lysosomal control of Mab. This suggests that either our screen was not sensitive enough to define these pathways due to redundancy or perhaps that Mab manipulates host macrophages to avoid destruction. Future studies will be required to determine what steps of intracellular Mab trafficking are required for control or persistence in macrophages. This could be done by knocking out essential components of distinct trafficking pathways and determining the growth kinetics and intracellular survival of Mab over time. Combined, these assays would allow researchers to gain a better understanding of cell-autonomous mediated restriction of Mab following infection.

One drawback of this study is that it failed to identify macrophage genes that directly improve Linezolid efficacy during Mab infection. The minimum inhibitory concentration 90 (MIC_{90}) of Linezolid targeting Mab in broth cultures is 32μg/mL, yet our screen was performed following a three-day 4μg/mL treatment with Linezolid [31, 32]. Although this subinhibitory antibiotic concentration was deliberately chosen following a series of optimization experiments,

it is possible that this concentration is too low to properly define host pathways required for modulating antibiotic efficacy during infection. Furthermore, it is possible that the chosen antibiotic concentration was not consistently present within the macrophage over time, therefore permitting differential intracellular Mab survival percentages. Together, these variables may have impacted the sensitivity of our assay to identify host genes modulating antibiotic efficacy during Mab infection at a population level. Future studies should conduct mass spectrometry to examine the variability of antibiotic concentrations overtime to more thoroughly define these complex interactions. Given Linezolid is known to have off-target effects on host mitochondrial function, a clearer understanding of how Linezolid directly alters macrophages should be a priority. These studies will define new candidate pathways that may play an important role in regulating the host-pathogen-antibiotic landscape during Mab infection.

A variety of *in vivo* Mab studies have been conducted to gain insight into global immune control during chronic Mab infection. Notably, studies conducted with immunocompetent murine models, including C57BL/6 and leptin-deficient (Ob/Ob) mice, found Mab infection was cleared with relative ease [33-35]. These studies mirror clinical data, where the prevalence of chronic Mab infection is largely seen in patients with abnormal lung environments. In these cohorts, excess mucus and chronic inflammation are known to interfere with appropriate lung function, including immune responses following pathogen exposure [3, 36, 37]. As such, it is tempting to consider that Mab restriction mechanisms rely on cell-to-cell cross talk mechanisms to upregulate appropriate immune responses, making a large part of infection control independent of cell autonomous mediated restriction. Other researchers have considered the importance of immune feedback loops as essential mechanisms for pathogen control. For example, research conducted by Xin et al. leveraged Legionella infection to dissect an interesting crosstalk

mechanism used by alveolar macrophages and surrounding alveolar epithelium cells to prime circulating monocytes prior to entering the pulmonary space [38]. In short, Legionella was found to block appropriate alveolar macrophage restriction mechanisms. In response, IL-1 released by infected alveolar macrophages induced the production of GM-CSF from surrounding alveolar epithelium cells [38]. The presence of increased GM-CSF levels aided in upregulating appropriate inflammatory responses in recruited circulating monocytes to improve host-control of infection [38]. Future studies should focus on improving *in vivo* murine models that better replicate lung environments most at risk for Mab pulmonary infection. Combined, these research tools would permit studies that better define key host-pathogen interactions required for Mab control during pulmonary infection.

Altogether, we optimized a host genetic screening platform to identify macrophage restriction pathways required during Mab infection. Here, we attempted to leverage this approach to identify host requirements for intracellular antibiotic control, yet instead we found a new subset of host genes that directly modulate Mab control independently of antibiotic therapy. Our data suggest a key requirement for host mitochondrial function in controlling intracellular Mab independently of Linezolid. Thus, continuing to leverage genome-wide genetic approaches is key to defining new intracellular macrophage restriction mechanisms used throughout the course of Mab infection. These findings will help with the overall goal of improving host-directed therapies for at-risk patients.

MATERIALS AND METHODS

Mab culture conditions and antibiotic growth assays

The mEmerald GFP-expressing Mab (ATCC 19977) strain was generated as previously described [26]. To select for mEmerald GFP-expressing, all mEmerald GFP-expressing cultures were selected in zeocin (Invivogen) at a final concentration of 5μg/mL and grown aerobically at 37°C in Middlebrook 7H9 medium supplemented with 1% glycerol, 0.05% tween80 and 10% Middlebrook OADC (oleic acid, dextrose, catalase, and bovine albumin).

To quantify bacterial growth at different Linezolid antibiotic concentrations, mEmerald GFP-Mab single cell suspensions were inoculated in the presence of antibiotic at the indicated concentrations at $5x10^5$ bacteria/mL in 7H9 broth media. Optical density was quantified by measuring the absorbance at 600nm on a Tecan Spark 20M plate reader at the indicated timepoints.

Cell culture.

J2-virus immortalized murine bone marrow derived macrophages (iBMDMs) were maintained in Dulbecco's Modified Eagle Medium (DMEM; Hyclone) supplemented with 10% heat inactivated fetal bovine serum (FBS; Seradigm) as previously described [26]. All macrophages were incubated in 5% CO_2 at 37°C.

Macrophage infections.

Single cell Mab suspensions were prepared by resuspending logarithmic phase bacteria in the appropriate cell culture media followed by a soft spin (58xg) to pellet large bacterial clumps. The supernatant was then used to infect macrophages, seeded at $5x10^5$ /well in a 12-well plate, at the indicated MOIs for the indicated time points (4-48 hours). Following the initial 4-hour infection, infection media was removed and replaced with the indicated antibiotic concentration

for the remainder of the experiment. At the indicated timepoints, macrophages were then washed with PBS, lifted from plates by scrapping, then fixed in 4% paraformaldehyde. Infected macrophages were quantified using the Attune CytPix Flow Cytometer (Thermo Fisher Scientific) at the Michigan State University Flow Cytometry Core. Live and single macrophages were identified using forward and side scatter. Then, the mean fluorescent intensity of infected cells or percentage of infected cells was determined by the fluorescence in the GFP channel. All experiments include an uninfected control to gate for uptake quantification during analysis that was performed using FlowJo v10.

For colony forming unit (CFU) assays, cells were lysed at the indicated time points with sterile cold distilled water and 10-fold serial dilutions were plated on Midllebrook 7H10 agar supplemented with Middlebrook OADC (oleic acid, dextrose, catalase, and bovine albumin) and 5μg/mL zeocin (Invivogen). Plates were incubated for 5 days at 37°C, then colonies were enumerated.

CRISPR screen and analysis.

Mouse Brie CRISPR knockout pooled library was a gift from David Root and John Doench (Addgene #73633) [39] and infected with our smooth mEmerald-GFP Mab reporter strain at an MOI of five. After 4 hours, infection media was removed and replaced with 4μg/mL Linezolid for three days. Then macrophages were washed with PBS and fixed with 4% paraformaldehyde. Infected library was then sorted using a BioRad S3e cell sorter to isolate macrophage populations expressing mEmerald^{hi} and mEmerald^{low} fluorescence. 2.5-3.5x10^7 cells were sorted into each bin from triplicate experiments. Genomic DNA was isolated from each sorted population using Qiagen DNeasy kits after reversing DNA crosslinks following a 55°C incubation overnight. Amplification of sgRNAs by PCR was performed as previously described

[39] using Illumina compatible primers from IDT and amplicons were sequenced on an Illumina NextSeq 500 at the Genomics Core at Michigan State University.

Sequenced reads were first trimmed to remove any adapter sequence and to adjust for the p5 primer stagger. We used model-based analysis of genome-wide CRISPR-Cas9 knockout (MAGeCK) to map reads to the sgRNA library index without allowing for any mismatch [40]. Subsequent sgRNA counts were median normalized to control sgRNAs in MAGeCK to account for variable sequencing depth. To test for sgRNA and gene enrichment, we used the "test" command in MAGeCK to compare the distribution of sgRNAs in the mEmerald^{hi} and mEmerald^{low} bins. The Gene Summary output from the MAGeCK software provided a ranked list of genes significantly underrepresented in the mEmerald^{hi} bin based on 4 independent sgRNAs that was used to curate the candidate gene list.

CRISPR-targeted knockouts.

Individual knockouts were made using specified ribonucleoproteins (RNPs) from Synthego. In short, assembled RNP complexes were combined with the appropriate quantity of suspended cells as instructed in the Synthego Protocol: *CRISPR Editing of Immortalized Cell Lines with RNPs using Nucleofection* (Synthego). Transfections were conducted using the Lonza 4D Nucleofector (Lonza Bioscience) as per manufacturer instructions. Following transfections, prewarmed cell culture media was added to the transfected cell suspension, then the mixture was transferred into 6-well tissue culture plates to allow for cell recovery and clonal expansion. Genomic DNA was isolated from clones and edited regions were amplified by PCR before being sent for Sanger Sequencing (Genewiz). The resultant ABI files were used for Synthego Interference of CRISPR Editing (ICE) analysis to assess the frequency and size of indels in each

population compared to control macrophages. All targeted cell lines selected for follow-up analysis had an editing efficiency >90%.

Bioinformatics analysis.

Using the robust rank aggregation (RRA), the top enriched positive regulators (2-fold change with at least 3 sgRNAs) were used as a "candidate list". Functional analysis and functional annotation analysis were completed using DAVID analysis, and top enriched pathways and protein families were identified.

Statistical analysis.

Statistical analysis and data visualization were performed using Prism version 10 (GraphPad Software) or Biorender, as indicated in figure legends. Data are presented, unless otherwise indicated, as the mean ± SD and individual data points are shown for each experiment. For parametric data, one-way or two-way ANOVA followed by Tukey's or Dunnett's multiple comparisons test were used to identify significant differences between multiple groups.

REFERENCES

1. Johansen, M.D., J.L. Herrmann, and L. Kremer, *Non-tuberculous mycobacteria and the rise of Mycobacterium abscessus.* Nat Rev Microbiol, 2020. **18**(7): p. 392-407.

2. Abdelaal, H.F.M., et al., *Mycobacterium abscessus: It's Complex.* Microorganisms, 2022. **10**(7).

3. De Rose, V., et al., *Airway Epithelium Dysfunction in Cystic Fibrosis and COPD.* Mediators Inflamm, 2018. **2018**: p. 1309746.

4. Antonio Oliver, L.M., Rafael Canton, Hector Escobar, Fernando Baquero, and Enrique Gomez-Mampaso, *Nontuberculous Mycobacteria in Patients with Cystic Fibrosis.* Clin Infect Dis, 2001. **32**(9): p. 1298-1303.

5. Harris, K.A. and D.T.D. Kenna, *Mycobacterium abscessus infection in cystic fibrosis: molecular typing and clinical outcomes.* J Med Microbiol, 2014. **63**(Pt 10): p. 1241-1246.

6. Jarand, J., et al., *Clinical and microbiologic outcomes in patients receiving treatment for Mycobacterium abscessus pulmonary disease.* Clin Infect Dis, 2011. **52**(5): p. 565-71.

7. Griffith, D.E. and C.L. Daley, *Treatment of Mycobacterium abscessus Pulmonary Disease.* Chest, 2022. **161**(1): p. 64-75.

8. Daley, C.L., et al., *Treatment of Nontuberculous Mycobacterial Pulmonary Disease: An Official ATS/ERS/ESCMID/IDSA Clinical Practice Guideline.* Clin Infect Dis, 2020. **71**(4): p. 905-913.

9. Haworth, C.S., et al., *British Thoracic Society guidelines for the management of non-tuberculous mycobacterial pulmonary disease (NTM-PD).* Thorax, 2017. **72**(Suppl 2): p. ii1-ii64.

10. Ubeda, C. and E.G. Pamer, *Antibiotics, microbiota, and immune defense.* Trends Immunol, 2012. **33**(9): p. 459-66.

11. Patangia, D.V., et al., *Impact of antibiotics on the human microbiome and consequences for host health.* Microbiologyopen, 2022. **11**(1): p. e1260.

12. Santucci, P., et al., *Intracellular localisation of Mycobacterium tuberculosis affects efficacy of the antibiotic pyrazinamide.* Nat Commun, 2021. **12**(1): p. 3816.

13. Kiritsy, M.C., et al., *Mitochondrial respiration contributes to the interferon gamma response in antigen-presenting cells.* Elife, 2021. **10**.

14. Shin, D.M., et al., *Mycobacterium abscessus activates the macrophage innate immune response via a physical and functional interaction between TLR2 and dectin-1.* Cell Microbiol, 2008. **10**(8): p. 1608-21.

15. Li, D. and M. Wu, *Pattern recognition receptors in health and diseases.* Signal Transduct Target Ther, 2021. **6**(1): p. 291.

16. Rougerie, P., V. Miskolci, and D. Cox, *Generation of membrane structures during phagocytosis and chemotaxis of macrophages: role and regulation of the actin cytoskeleton.* Immunol Rev, 2013. **256**(1): p. 222-39.

17. Kheir, W.A., et al., *A WAVE2-Abi1 complex mediates CSF-1-induced F-actin-rich membrane protrusions and migration in macrophages.* J Cell Sci, 2005. **118**(Pt 22): p. 5369-79.

18. Scott, C.C., et al., *Phosphatidylinositol-4,5-bisphosphate hydrolysis directs actin remodeling during phagocytosis.* J Cell Biol, 2005. **169**(1): p. 139-49.

19. Lee, H.J., et al., *Formation and Maturation of the Phagosome: A Key Mechanism in Innate Immunity against Intracellular Bacterial Infection.* Microorganisms, 2020. **8**(9).

20. Roux, A.L., et al., *The distinct fate of smooth and rough Mycobacterium abscessus variants inside macrophages.* Open Biol, 2016. **6**(11).

21. Roberts, E.A., et al., *Higher order Rab programming in phagolysosome biogenesis.* J Cell Biol, 2006. **174**(7): p. 923-9.

22. Lukacs, G.L., O.D. Rotstein, and S. Grinstein, *Phagosomal acidification is mediated by a vacuolar-type H(+)-ATPase in murine macrophages.* Journal of Biological Chemistry, 1990. **265**(34): p. 21099-21107.

23. Rosales, C. and E. Uribe-Querol, *Phagocytosis: A Fundamental Process in Immunity.* Biomed Res Int, 2017. **2017**: p. 9042851.

24. Laencina, L., et al., *Identification of genes required for Mycobacterium abscessus growth in vivo with a prominent role of the ESX-4 locus.* Proc Natl Acad Sci U S A, 2018. **115**(5): p. E1002-E1011.

25. Dubois, V., et al., *MmpL8(MAB) controls Mycobacterium abscessus virulence and production of a previously unknown glycolipid family.* Proc Natl Acad Sci U S A, 2018. **115**(43): p. E10147-E10156.

26. Gilliland HN., B.O., Olive AJ *A Genome-Wide Screen in Macrophages Defines Host Genes Regulating the Uptake of Mycobacteirum abscessus.* mSphere, 2023. **8**(2): p. e0066322.

27. Kiritsy, M.C., et al., *A genetic screen in macrophages identifies new regulators of IFNgamma-inducible MHCII that contribute to T cell activation.* Elife, 2021. **10**.

28. Fratti, R.A., et al., *Role of phosphatidylinositol 3-kinase and Rab5 effectors in phagosomal biogenesis and mycobacterial phagosome maturation arrest.* J Cell Biol, 2001. **154**(3): p. 631-44.

29. Poteryaev, D., et al., *Identification of the switch in early-to-late endosome transition.* Cell, 2010. **141**(3): p. 497-508.

30. Quan, H., Chung, H., Je, S., Hong, JJ., Kim, BJ., Na, YR., Seok, SH, *Pyruvate dehydrogenase kinase inhibitor dichloroacetate augments autophagy mediated constraining the replication of Mycobacteroides massiliense in macrophages.* Microbes Infect, 2023. **25**(7).

31. Guo, Q., et al., *Antimicrobial susceptibility profiles of Mycobacterium abscessus complex isolates from respiratory specimens in Shanghai, China.* J Glob Antimicrob Resist, 2021. **25**: p. 72-76.

32. Wallace, R.J., Jr., et al., *Activities of linezolid against rapidly growing mycobacteria.* Antimicrob Agents Chemother, 2001. **45**(3): p. 764-7.

33. Obregon-Henao, A., et al., *Susceptibility of Mycobacterium abscessus to antimycobacterial drugs in preclinical models.* Antimicrob Agents Chemother, 2015. **59**(11): p. 6904-12.

34. Bernut, A., et al., *In vivo assessment of drug efficacy against Mycobacterium abscessus using the embryonic zebrafish test system.* Antimicrob Agents Chemother, 2014. **58**(7): p. 4054-63.

35. Ordway, D., Henao-Tamayo, M., Smith, E., Shanley, C., Harton, M., Troudt, J., et al., *Animal model of Mycobacterium abscessus lung infection.* J. Leukoc. Biol., 2008. **83**: p. 1502-1511.

36. Fahy, J.V. and B.F. Dickey, *Airway mucus function and dysfunction.* N Engl J Med, 2010. **363**(23): p. 2233-47.

37. Kreda, S.M., C.W. Davis, and M.C. Rose, *CFTR, mucins, and mucus obstruction in cystic fibrosis.* Cold Spring Harb Perspect Med, 2012. **2**(9): p. a009589.

38. Liu, X., et al., *Legionella-Infected Macrophages Engage the Alveolar Epithelium to Metabolically Reprogram Myeloid Cells and Promote Antibacterial Inflammation.* Cell Host Microbe, 2020. **28**(5): p. 683-698 e6.

39. Doench, J.G., et al., *Optimized sgRNA design to maximize activity and minimize off-target effects of CRISPR-Cas9.* Nat Biotechnol, 2016. **34**(2): p. 184-191.

40. Li, W., Xu, H., Xiao, T., Cong, L., Love, MI., Zhang, F., Irizarry, RA., Liu, JS., Brown, M., Liu, XS, *MAGeCK enables robust identification of essential genes from genome-scale CRISPR/Cas9 knockout screens.* Genome Biology, 2014. **15**(554).